



Politecnico di Torino

Department of Environment, Land and Infrastructure Engineering (DIATI)
Master of Science in Petroleum and Mining Engineering (Mining Engineering Path)

Evaluation of the time course of the mechanical parameters of conditioned cohesionless soils

By

Nima Bahrami | S289085

Supervisor:

Professor Daniele Peila

Co-supervisors:

Ing. Andrea Carigi

Ing. Gerardo Sorrentino

Declaration

I hereby declare that, except where specific reference is made to the work of others, the contents and organization of this dissertation constitute my own original work and does not compromise in any way the rights of third parties, including those relating to the security of personal data. This dissertation is entirely the result of my own work and includes nothing which is the outcome of work done in collaboration. This dissertation contains less than 21,000 words and less than 320 figures.

Nima Bahrami
October 2023

A handwritten signature in black ink, appearing to be 'Nima Bahrami', written over the printed name and date.

I would like to dedicate this thesis to my lovely parents

Acknowledgment

First and foremost, I would like to express my sincere gratitude and appreciation to my supervisor, Professor Daniele Peila. His constant interest and enthusiasm for this research was a never-ending source of inspiration and motivation. I am profoundly honored for the opportunity he provided me to immerse myself in the specialized field of Earth Pressure Balance – Tunnel Boring Machine (EPB-TBM) and write this thesis under his supervision.

In this context, I feel incredibly fortunate to have been mentored by Ing. Andrea Carigi. His mentorship has nurtured in me the importance of thinking with an open mind and seeking deeper perspectives. This invaluable perspective, which I owe to his guidance, has significantly enriched my research experiences. I would like to extend my sincere appreciation for his dedicated time and support, especially during the demanding period when he was concluding his own PhD thesis. I am truly thankful for sparing your valuable time to offer feedback and guidance, despite your busy schedule.

I am deeply grateful to Ing. Gerardo Sorrentino for his invaluable technical expertise and practical outlook. His contributions and hand-on assistance have played a vital role in ensuring the accuracy and reliability of our experimental work. Working alongside him at the TUSC laboratory has been both enjoyable and enlightening. Additionally, a special thanks goes to Ing. Alfio Di Giovanni for his assistance in conducting one of the important tests essential to this research at the Raw Materials laboratory.

Last but certainly not least, my profound gratitude goes to my beloved parents for their persistent support, boundless love, and constant encouragement, despite being kilometers away. To my dear Monireh, your love has been a consistent source of motivation and support from the very beginning. You all have consistently been my pillar of support, and your unwavering faith in me has incessantly inspired my academic endeavors.

Abstract

In the domain of mechanized tunneling, a substantial portion of the market is occupied by Earth Pressure Balance-Tunnel Boring Machines (EPB-TBM). Over recent decades, this technology has gained popularity due to several constraints such as limited space on the surface, noise and vibration concerns, and safety requirements. Ensuring efficient EPB-TBM operation necessitates a radical alteration in the rheological characteristics of excavated soil, achieving through soil conditioning.

Soil conditioning is an indispensable aspect of EPB-TBM technology because it provides suitable soil for better pressure control within the bulk chamber and soil extraction with the screw conveyor. Furthermore, soil conditioning reduces both the internal friction angle and soil cohesion while enhancing material workability. This transformation is achieved by introducing additives, such as foam, at the excavation face and within the bulk chamber, thus altering the natural soil properties from solid-like to fluid-like with a pulpy consistency.

Currently, the conditioning set parameters are usually determined through a trial-and-error procedure. Therefore, a contribution to reduce the errors and understand their causes may be helpful to reduce both time and costs of conditioning assessments required for each job site.

The primary focus of this research is to evaluate how different foam generation methods influence the time-dependency of mechanical properties of conditioned soil. An essential aspect in characterization of soil conditioning involves evaluating the stability of both the conditioned soil and the foam used. Consequently, the core objective of the research is explored through the arrangement and implementation of various test campaigns, encompassing 2 half-life test campaigns, 2 preliminary test campaigns, and 17 main test campaigns.

The half-life test is employed to investigate the stability of generated foam. In the subsequent step, to assess the behavior and properties of the conditioned soil with different foam generation methods over time, a series of specific tests, including slump tests, density test, and vane shear test, were systematically conducted in time for distinct conditioning set parameters. These tests evaluate

key characteristics of the conditioned soil, such as workability, bulk density, and shear strength. Followingly, the potential variations between the abovementioned properties of conditioned soil with different foam generation methods can be detected.

In the final stage, semi-quantitative analyses of the results were performed, with the goal of gaining a more profound understanding of the potential correlations among distinct foam generation parameters, including foam generator flow rates, Foam Expansion Ratios (FER), and Foam Injection Ratios (FIR), and their influence on the time-dependency of mechanical properties of conditioned soil.

Table of Contents

Declaration	I
Acknowledgment.....	III
Abstract.....	IV
Table of Contents.....	VI
List of Figures.....	IX
List of Tables.....	XII
Introduction	1
1.1 Context.....	1
1.2 Problem statement.....	2
1.3 Objective of thesis	5
EPB-TBM technology.....	7
Soil Conditioning.....	12
3.1 General aspects	12
3.2 Conditioning agents	13
3.2.1 Water	13
3.2.2 Foam	13
3.2.3 Additives	15
3.3 Soil conditioning parameters	15
3.3.1 Flow rate	15
3.3.2 Foam Injection Ratio.....	16
3.3.3 Foam Expansion Ratio.....	16
3.3.4 Foaming agent Concentration	16
3.3.5 Total water content	17
3.3.6 Added water content.....	17
3.3.7 Half-life time.....	17

Materials	18
4.1 Soil characterization	18
4.2 Atterberg limits.....	21
4.3 Conditioning agents	21
Methods	22
5.1 Foam generator	22
5.2 Half-life test.....	24
5.3 Slump test	25
5.4 Density test	27
5.5 Vane shear test.....	27
5.6 Semi-quantitative analysis.....	29
Laboratory Tests	37
6.1 General overview.....	37
6.2 Optimal conditioning set parameters.....	37
6.3 Procedure description.....	38
6.4 Mathematical formulation.....	42
6.4.1 Half-life test.....	42
6.4.2 Slump test, Density test, and Vane shear test	42
Discussion on the results	44
7.1 Half-life test.....	44
7.2 Preliminary test campaigns.....	50
7.3 Main test campaigns.....	52
7.4 Semi-quantitative analysis	59
7.4.1 Slump test	59
7.4.2 Density test	62
7.4.3 Vane Shear test	64
Conclusions.....	68

Annexes.....	70
9.1 Test Campaign A.....	70
9.2 Test Campaign B.....	73
9.3 Test Campaign C.....	76
9.4 Test Campaign D.....	80
9.5 Test Campaign E.....	83
9.6 Test Campaign F.....	86
9.7 Test Campaign G.....	89
9.8 Test Campaign H.....	92
9.9 Test Campaign I.....	95
9.10 Test Campaign J.....	98
9.11 Test Campaign K.....	101
9.12 Test Campaign L.....	104
9.13 Test Campaign M.....	107
9.14 Test Campaign N.....	110
9.15 Test Campaign O.....	113
9.16 Test Campaign Q.....	116
References.....	117

List of Figures

Figure 1_1: Support pressure for EPB-TBM (Herrenknecht AG).....	3
Figure 2_1: Screw shield by Brunel (Herrenknecht et al., 2011)	8
Figure 2_2: EPB-TBM functional principle (Herrenknecht AG).....	9
Figure 2_3: EPB-TBM operating principle (Vinai, 2006)	10
Figure 2_4: Traditional area of application for EPB-TBM technology (Herrenknecht et al., 2011).....	11
Figure 2_5: EPB-TBM application field and necessary conditioning agents (Shin et al., 2021).....	11
Figure 3_1: Foam composition	14
Figure 3_2: Simplified two-dimensional model for foam-conditioned sand (Wang et al., 2022).....	15
Figure 4_1: Soil sample.....	18
Figure 4_2: Averaged grain size distribution curve	20
Figure 5_1: Foam generation process scheme (Peila et al., 2008)	23
Figure 5_2: Laboratory scale foam generator at TUSC laboratory	23
Figure 5_3: Half-life test apparatus scheme (Carigi et al., 2022)	24
Figure 5_4: Schematic representation of slump test (Martinelli, 2016).....	25
Figure 5_5: FIR and Water content correlation diagram (Peila et al., 2009)	26
Figure 5_6: Vane shear test principle (Gylland et al., 2016).....	28
Figure 5_7: Modified vane shear apparatus (Carigi et al., 2020).....	29
Figure 5_8: Gap in the empirical results – Slump test.....	31

Figure 5_9: Anomaly type I in a descending trend	31
Figure 5_10: Gap in the empirical results – Slump test.....	32
Figure 5_11: Anomaly type II in a descending trend	32
Figure 5_12: Gap in the empirical results – Vane shear test.....	33
Figure 5_13: Anomaly type I in an ascending trend	33
Figure 5_14: Gap in the empirical results – Vane shear test.....	34
Figure 5_15: Anomaly type II in an ascending trend	34
Figure 5_16: Dataset with 12 potential models	35
Figure 5_17: Optimal model with the minimum sum of squared differences	36
Figure 6_1: Grain size distribution curve.....	38
Figure 7_1: Cumulative weight vs. time for Q(min).....	45
Figure 7_2: Cumulative weight vs. time for Q(max).....	45
Figure 7_3: Adjusted determination coefficient ranges for Q(min)	46
Figure 7_4: Adjusted determination coefficient ranges for Q(max).....	46
Figure 7_5: Asymmetric sigmoid parameter “b” vs. FER for different foam generator flow rates.....	47
Figure 7_6: Asymmetric sigmoid parameter “c” vs. FER for different foam generator flow rates.....	47
Figure 7_7: Asymmetric sigmoid parameter “d” vs. FER for different foam generator flow rates.....	48
Figure 7_8: Asymmetric sigmoid parameter “m” vs. FER for different foam generator flow rates.....	48
Figure 7_9: Representation of asymmetric sigmoid parameter “a” and “d”	49

Figure 7_10: Half-life time vs. FER for different foam generator flow rates	49
Figure 7_11: Preliminary test campaigns results – Slump tests	51
Figure 7_12: Preliminary test campaigns results – Density tests	51
Figure 7_13: Preliminary test campaigns results – Vane shear tests	52
Figure 7_14: Slump test results for all test campaigns.....	54
Figure 7_15: Density test results for all test campaigns.....	55
Figure 7_16: Vane shear test results for all test campaigns.....	56
Figure 7_17: Optimal line parameter m_1 for slump test	60
Figure 7_18: Optimal line parameter q_1 for slump test.....	60
Figure 7_19: Optimal line parameter m_2 for slump tests.....	61
Figure 7_20: Optimal line parameter q_2 for slump tests	61
Figure 7_21: Optimal line parameter m_1 for density test.....	62
Figure 7_22: Optimal line parameter q_1 for density test.....	63
Figure 7_23: Optimal line parameter m_2 for density test.....	63
Figure 7_24: Optimal line parameter q_2 for density test.....	64
Figure 7_25: Optimal line parameter m_1 for vane shear test.....	65
Figure 7_26: Optimal line parameter q_1 for vane shear test	65
Figure 7_27: Optimal line parameter m_2 for vane shear test.....	66
Figure 7_28: Optimal line parameter q_2 for vane shear test.....	66

List of Tables

Table 4_1: Sieve analysis records	19
Table 4_2: Technical information of the foaming agent	21
Table 6_1: Summary of test campaigns conditioning set parameters	40
Table 6_2: Slump test procedure	41
Table 6_3: Density test procedure	41
Table 6_4: Vane shear test procedure	41
Table 9_1: Conditioning set parameters – Test campaign A	70
Table 9_2: Slump test results – Test campaign A	71
Table 9_3: Conditioning set parameters – Test campaign B	73
Table 9_4: Slump test results – Test campaign B	74
Table 9_5: Conditioning set parameters – Test campaign C	76
Table 9_6: Slump test results – Test campaign C	77
Table 9_7: Conditioning set parameters – Test campaign D	80
Table 9_8: Slump test results – Test campaign D	81
Table 9_9: Conditioning set parameters – Test campaign E	83
Table 9_10: Slump test results – Test campaign E	84
Table 9_11: Conditioning set parameters – Test campaign F.....	86
Table 9_12: Slump test results – Test campaign F.....	87
Table 9_13: Conditioning set parameters – Test campaign G.....	89
Table 9_14: Slump test results – Test campaign G.....	90

Table 9_15: Conditioning set parameters – Test campaign H.....	92
Table 9_16: Slump test results – Test campaign H.....	93
Table 9_17: Conditioning set parameters – Test campaign I	95
Table 9_18: Slump test results – Test campaign I	96
Table 9_19: Conditioning set parameters – Test campaign J.....	98
Table 9_20: Slump test results – Test campaign J	99
Table 9_21: Conditioning set parameters – Test campaign K	101
Table 9_22: Slump test results – Test campaign K	102
Table 9_23: Conditioning set parameters – Test campaign L.....	104
Table 9_24: Slump test results – Test campaign L.....	105
Table 9_25: Conditioning set parameters – Test campaign M.....	107
Table 9_26: Slump test results – Test campaign M.....	108
Table 9_27: Conditioning set parameters – Test campaign N.....	110
Table 9_28: Slump test results – Test campaign N.....	111
Table 9_29: Conditioning set parameters – Test campaign O.....	113
Table 9_30: Slump test results – Test campaign O.....	114
Table 9_31: Conditioning set parameters – Test campaign Q.....	116
Table 9_32: Slump test results – Test campaign Q.....	116

Introduction

1.1 Context

Tunneling is the process of creating underground passages or galleries for various purposes including transportation, infrastructure, mining, utilities, and exploration. By excavating through soil and rock masses a subsurface passage is created to support vital utilities, to provide access to resources and to increase the efficiency and safety of people and goods transportation.

From the ancient underground passages to modern-day engineering masterpieces, tunnels have played a vital role in meeting people's daily needs by improving connectivity, harnessing natural resources for various purposes such as hydropower generation, mining, water supply, and promoting environmental sustainability, hence shaping the world we live in. Thus, it can be said that the evolution of tunneling techniques and technologies mirrors the progress of human civilization and subsequently, the increasing necessity to overcome the challenges that arise in increasingly long and complex tunneling projects.

With respect to transportation, subway systems have emerged as efficient modes of transportation addressing the challenges of congestion and providing consistent connectivity for millions of commuters all around the world. The London Underground, New York City's Subway, and Tokyo's Metro are iconic examples of how tunnels revolutionized urban mobility, shaping the way people travel and work in crowded metropolises. On the other hand, construction of distinguished tunnels like the Gotthard Base Tunnel, the Ahmed Hamdi Tunnel (Tunnel under the Suez Canal), and the Channel Tunnel is also facilitating faster and more efficient transportation of people and goods across vast distances between countries and continents.

Beyond transportation and urban connectivity, tunnels have played a crucial role in harnessing natural resources. Mining operations rely on tunnels to access valuable minerals and ores buried deep within the Earth's crust. Tunnels have facilitated the exploration and extraction of oil and gas reserves, mineral deposits,

and secured nuclear waste disposal, thus fulfilling the energy demands of society and safeguarding future generations from potential hazards.

Also, water supply and wastewater management systems, underground laboratories, storage facilities and underground electrical transmission lines all rely on underground structures and tunnels to ensure the consistent delivery of essential services. Having these tunnels beneath the surface enable cities to function efficiently, protect public health, and promote environmental sustainability.

The significance of various infrastructure elements, including tunnels, became increasingly evident with the rapid urbanization of cities. According to the United Nations Department of Economic and Social Affairs, in a momentous shift, 2007 marked the first time in human history when the urban population surpassed that of rural areas (UN-DESA WPP, 2022). This transformation signaled the profound impact of urbanization on population distribution and highlighted the need for novel, efficient and sustainable urban infrastructure. As projections indicate that by 2050, an estimated 75% of the global population will reside in cities (UN-DESA WPP, 2022), the importance of innovative urban planning, including the strategic implementation of tunnels, has become ever more crucial in creating resilient urban environments for future generations.

1.2 Problem statement

Earth Pressure Balance Tunnel Boring Machines (EPB-TBMs) have gained extensive popularity in the field of tunneling due to their efficiency, versatility, and ability to overcome challenging ground conditions. EPB-TBMs have been known as a preferred choice for tunnel excavation in urban areas where, differently from Cut-and-Cover method, surface disruptions are avoided, and socio-environmental impacts are minimized. The EPB-TBM technology has revolutionized tunneling practices, making it possible to construct tunnels through various soil types, including cohesive and cohesionless soils, with enhanced safety and productivity.

These machines are designed to operate in pressurized environments to counterbalance the earth and groundwater pressures encountered during tunnel

excavation (Figure 1_1). The pressure inside the excavation chamber (plenum) is maintained to balance the pressure exerted by the surrounding ground, thereby preventing the tunnel from collapsing during excavation. This balance is kept by regulating the volume of excavated material (muck) present in the plenum by adjusting its extraction rate through the screw conveyor.

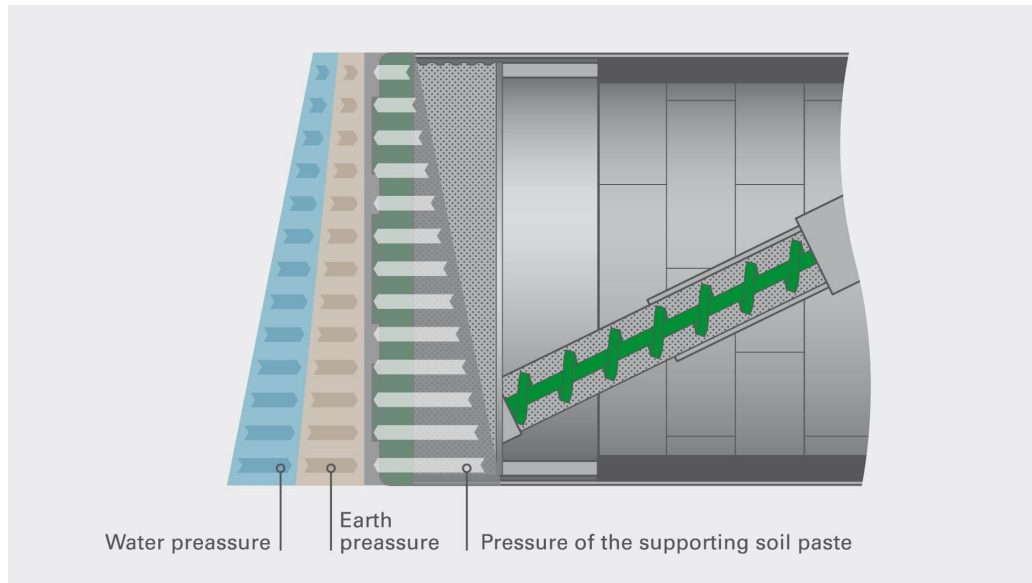


Figure 1_1: Support pressure for EPB-TBM (Herrenknecht AG)

Without a proper conditioning, in cohesionless soils, the excavated soil cannot be transported smoothly due to poor flow plasticity, which could lead to various problems, including aggregate segregation in the excavation chamber, locking of cutterhead, and increase in thrust force and cutterhead torque (Xu et al., 2020). To address these issues and optimize tunneling performance, correct assessment of the conditioning quantity and conditioning products is essential to transform the soil originally excavated by the cutterhead into a plastic paste with a pulpy consistency, that is highly compressible and less permeable (Thewes et al., 2012; Todaro, 2016). Moreover, this process aids in minimizing wear on the mechanical parts of machine (Peila et al., 2008; Salazar et al., 2016; Salazar et al., 2018; Baghali et al., 2020), and permitting easy handling of muck during transport (Peila et al., 2008). Numerous studies have been carried out on soil conditioning, emphasizing the importance of identifying optimum soil conditioning for various soil types through laboratory tests. This emphasis is crucial for accomplishing correct soil management. Continuously, achieving optimal soil conditioning is necessary to

facilitate a homogenous flow of material within the pressure chamber and along the screw conveyor, to apply stabilizing counter-pressure to the excavation face, and to waterproof the pressure chamber (Carigi et al., 2020). Conditioning agents, such as foam, polymer, or bentonite are often used to modify the mechanical behavior of soil into a homogenous, low permeable, plastic, and pulpy paste in order to achieve several objectives (Zheng et al., 2021). From a geo-mechanical perspective, soil conditioning aims to reduce both the internal friction angle and cohesion of the soil (Martinelli et al., 2017), and to increase the workability of the material (Carigi et al., 2022). From a tunnel excavation perspective, in addition to the abovementioned purposes, correct conditioning is necessary to waterproof the screw conveyor, reduce wear, control water flow, and permit easy handling of the muck during transport. (Peila et al., 2009; Salazar et al., 2016; Carigi et al., 2022).

In recent years, the feasibility of conducting large-scale laboratory screw conveyor tests has gained attention within the context of EPB-TBM tunneling, due to its potential to directly measure key parameters associated with EPB-TBM excavation process (Mair et al., 2003; Merritt & Mair, 2006; Peila et al., 2007; Vinai et al., 2007). Although this type of test appears to be the best tool for conditioning design, its execution requires a large volume of soil to be handled. Hence, systematic comparison of various conditioning sets of different types of products is significantly limited (Peila et al., 2009). The application of foam in EPB-TBM soil conditioning has evolved over five decades and it is still largely based on empirical knowledge. Despite this, the application of foam lacks standardized guidelines, particularly in terms of the injection strategy. One possible reason for this variability could be the limited understanding of foam-soil interaction (Zheng et al., 2022). Bringing these two aspects together highlights the core of the present issue. The properties of the conditioned soil and the influence of time on its mechanical behavior should be evaluated using laboratory tests. These tests offer insights into determining the correct amount of conditioning agents and provide an easy control of the conditioning quality during excavation (Peila et al., 2008). Consequently, addressing this issue offers the prospect of not only enhancing the tunnel excavation process but also contributing to a more knowledgeable and efficient methodology with informed insights and practical advancements.

1.3 Objective of thesis

Soil conditioning is a critical process in EPB-TBM tunneling, as it influences the behavior of the excavated soil, consequently influencing the efficiency of tunnel construction. Among various conditioning agents, foam is the most important additive, with multiple benefits including the temporary increase of void index and compressibility, as well as decreasing the shear stress and the permeability of soils (Bezuijen et al., 1999; Psomas, 2001; Thewes et al., 2012). For the characterization of the soil conditioning, a key aspect is the stability of the conditioned soil and, as its important constituent element, the stability of foam itself (Carigi et al., 2022). Additionally, the interaction with solid particles strongly influences the stability of foam (Horozov, 2008; Fameau et al., 2014; Al Yousef et al., 2018). Consequently, the stability of foam is measured through the half-life test. The decay rate is essential to estimate, in order to know the time duration for which the soil conditioning agent will remain effective in enhancing the properties of soil. The test has to be conducted following the EFNARC standard (EFNARC, 2005), which involves measuring the time (t_{50}) needed for an 80-grams foam sample to drain half of its weight due to drainage.

Thus, the half-life test, according to the methodology detailed in Chapter 5.2, was conducted on samples produced with a commercial foaming agent, with a single foaming agent concentration (c_f) and several Foam Expansion Ratios (FER). The study was carried out to assess the influence of two different foam generator flow rates (Q_{min} and Q_{max}) on the stability of the generated foam, covering the FER range of 5 to 30. Then, the two foam generator flow rates were used also to produce foam for soil conditioning and the resulting material was studied to understand how different foam generation methods influence the time-dependency of mechanical properties of the conditioned soil.

Hence, preliminary test campaigns were performed, utilizing the same foam generator flow rates with a consistent foaming agent concentration (c_f). The aim was to evaluate potential differences in the outcomes related to characterization of conditioned soil, specifically workability, bulk density, and shear strength of the conditioned soil, when subjected to two different types of generated foam. The assessment of these soil characteristics over time was performed through the implementation of specific tests, including slump test, density test, and vane shear

test. The importance of time-dependency of mechanical properties of the conditioned soil arises from the excavation cycle. The material excavated by the cutterhead spends a variable amount of time inside bulk chamber before being extracted by the screw conveyor. This duration can vary from the stoppage time due to the ring assembling, which takes around one hour, to potentially several hours in cases where unforeseen excavation issues occur (Peila et al., 2008). Moreover, a critical characteristic of foam-conditioned soil is its stability, which refers to its ability to maintain the engineering properties, throughout the residency time. This period encompasses the time of injection at the cutterhead, through the mixing process in the excavation chamber, and into the screw conveyor for transport to the belt conveyor, and depending on factors such as diameter of TBM, depth of excavation chamber, and advance rate it ranges between 30 to 90 minutes (Wu et al., 2020). Thus, gaining a deeper understanding of how foam properties influence the stability of conditioned soil could have significant impact on the job site management.

Chapter 2

EPB-TBM technology

There are several methods employed for tunnel construction, depending on the specific geological conditions, tunnel length, purpose, budget, and project requirements. The main methods include: conventional method, Cut-and-Cover, Drill and Blast, and mechanized tunneling.

In particular, mechanized tunneling is a modern tunnel construction method that relies on advanced machinery (Tunnel Boring Machines, TBM) and equipment to carry out the excavation and support installation processes efficiently and with a higher degree of automation which significantly reduces the need for extensive manual labor. These specialized machines are designed to handle various geological conditions and operate in confined spaces, ensuring precision and accuracy during the excavation process. The main advantage of mechanized tunneling is its speed and efficiency. Compared to conventional methods, mechanized tunneling can significantly reduce the construction time, making it ideal for projects with tight schedules, or in densely populated urban areas where minimizing disruptions is crucial. Additionally, another important advantage of this technology is improved safety, as it shortens the need for direct human involvement in dangerous excavation tasks.

Tunnel Boring Machines (TBM) are an advanced tunneling technology that incorporate a combination of excavation, support, and muck removal systems within a single unit. The origins of current process technology for shielded machines goes back to Sir Marc Isambard Brunel, who developed the principle of shield tunnelling as long ago as 1806 (Figure 2_1). His design intended that the soil at the face would be excavated by a screw shield and the lining of the tunnel would take place simultaneously (Herrenknecht et al., 2011).

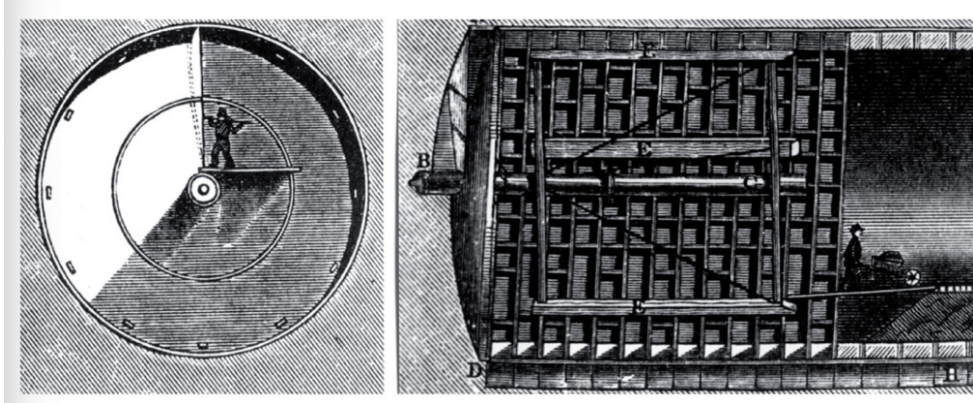


Figure 2_1: Screw shield by Brunel (Herrenknecht et al., 2011)

Earth Pressure Balance (EPB) was first introduced in Japan in the 1970 and since then, due to their unique characteristics in soil conditioning, excavation, and spoil removal, EPB-TBMs have been widely used in various construction projects worldwide. In densely populated cities, this technology is preferred because the tunnel excavation can be performed with minimal disturbance to the surrounding environment. Advancements in EPB-TBM technology, particularly in soil conditioning, have led to enhanced tunneling efficiency and expanded the range of applications for EPB-TBMs. These advancements allow them to adapt to various geological conditions and project specifications, resulting in numerous successful tunneling projects worldwide. For instance, in 2010, the Gotthard Base Tunnel in Switzerland was completed using an EPB-TBM, resulting in the world's longest railway tunnel with a length of 57.09 km and a total of 151.84 of tunnels, shafts and passages. Similarly, in 2019, tunnel boring phase of the West Gate Tunnel Project in Australia was completed using an EPB-TBM, which involved the construction of twin tunnels totaling 9 km in length which give Melbourne a second freeway link between the west and the city. It is notable that currently, over 90% of the shield machines worldwide incorporate active face supports as earth pressure shields, covering wide spectrum of soils, including hard rock, and also transitional areas with mixed face conditions (Herrenknecht et al., 2011).

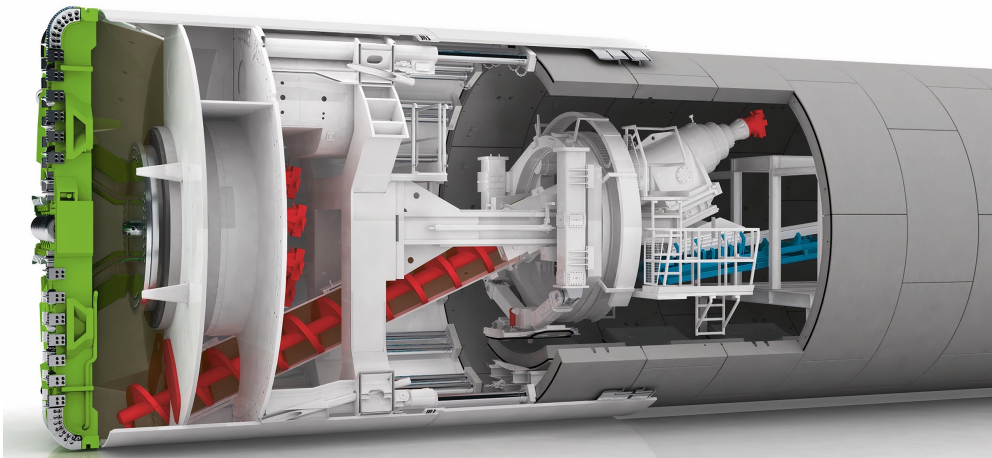


Figure 2_2: EPB-TBM functional principle (Herrenknecht AG)

In EPB-TBM machine, the face support is achieved by maintenance of pressure within excavation chamber (plenum) using excavated soil. This is accomplished by a combination of the advancement rate and the volume rate removal of the material, which provides a stabilizing action at the tunnel face to counteract the underground water and soil pressure (Maidl et al., 1995; Anagnostou & Kovari, 1996; Guglielmetti et al., 2007). The removal of the material is performed through a screw conveyor system that continuously removes spoil from excavation chamber into the area of the machine under atmospheric pressure (Herrenknecht et al., 2011). The conditioned soil within the screw conveyor forms an impermeable plug that ensures that there is no loss of pressure in the bulk chamber, and that no water enters (Yoshikawa, 1996). Notably, pressure control is enabled by adjustment in both its rotation speed and transportation capacity. By regulating rotation speed, the flow rate of conditioned soil can be controlled. This regulation is critical to achieve the optimal balance between the external earth pressure and the internal chamber pressure, preventing excessive pressure that could lead to soil instability or insufficient support. Furthermore, this operational system contributes to efficient transport of excavated material, reducing risk of blockage and allowing for consistent tunneling process. Thus, by maintaining this balance, EPB-TBM ensures the stability of the tunnel face through preventing entry of soil and groundwater to excavation chamber, while facilitating efficient excavation and spoil removal (Figure 2_3).

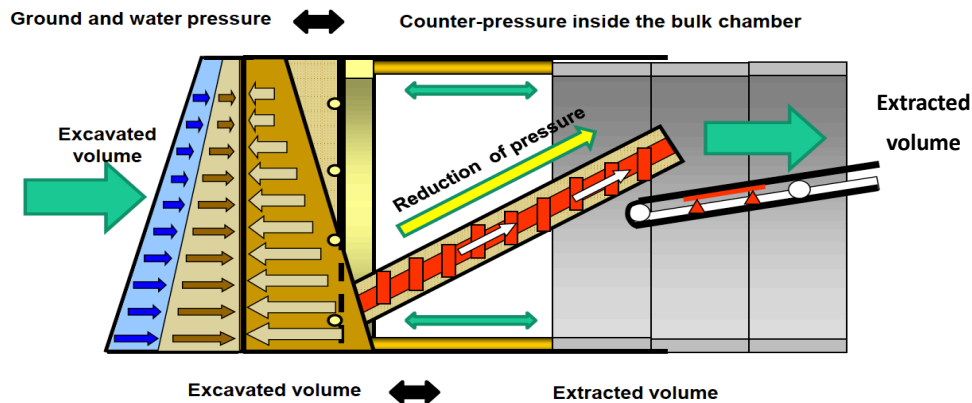


Figure 2_3: EPB-TBM operating principle (Vinai, 2006)

One of the most critical concerns in EPB-TBM tunneling is dealing with mixed and changing ground conditions, where the possibility arises that excavation cannot be carried out in a safe, efficient, and economical way. Therefore, instead of costly modifications and adaptation of the machine, it is generally simpler to treat the ground in order to provide appropriate properties that the machine can effectively manage working in (EFNARC, 2005). Consequently, adaptability to varying geological conditions can be achieved through the proper selection of soil conditioning parameters. With that being said, soil conditioning involves the injection of additives such as water, foam, or polymer into the excavated soil to modify its properties, in order to achieve some desirable properties such as high fluidity, certain compressibility, low frictional strength, and low permeability. Hence, a more uniform pressure distribution within the excavation chamber can be achieved, making the conditioned soil suitable for applying counter-pressure at the excavation face. Moreover, it is strongly recommended to select the type and dosage of soil conditioning agents based on the geotechnical properties of the encountered soil and project requirements, by conducting laboratory test (Martinelli et al., 2015).

Accordingly, a percentage of passing at the sieve 0.075 mm at least of 30% was considered as the minimum value in order to guarantee a suitable functioning of machine (Herrenknecht et al., 2011). Generally, the permeability of the ground has to be as low as possible, in order to prevent the free flow of the water in the excavating chamber, to avoid fluctuation on the water table level that could lead to induced subsidence and destabilizing forces, which act on the front and may cause flows through the machine itself. A permeability value equal to $10^{-5} m/s$ is indicated as limit for EPB-TBM operations (Herrenknecht et al., 1994).

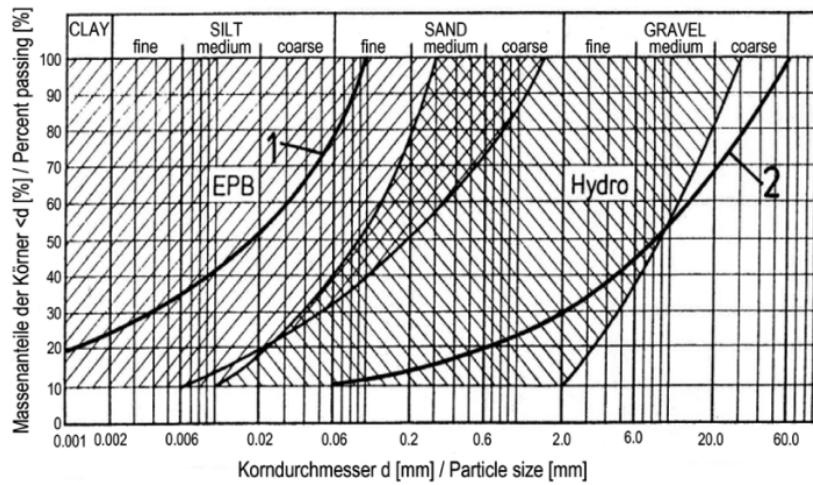


Figure 2_4: Traditional area of application for EPB-TBM technology (Herrenknecht et al., 2011)

Thanks to the effect of soil conditioning, the range of application of EPB-TBM technology has been extended to encompass sand, gravel, and even rock formations. However, achieving this expansion requires the accomplishment of several key features, all of which are attained through effective soil conditioning. Figure 2_5 provides valuable insights of EPB-TBM application considering variations in grain size distribution and required soil conditioning agents. It is notable that, grain size distribution plays a vital role in determining the behavior of excavated soil, influencing factors such as cohesion, permeability, and compressibility. Consequently, the choice of an appropriate soil conditioning agent significantly influences EPB-TBM tunneling performance.

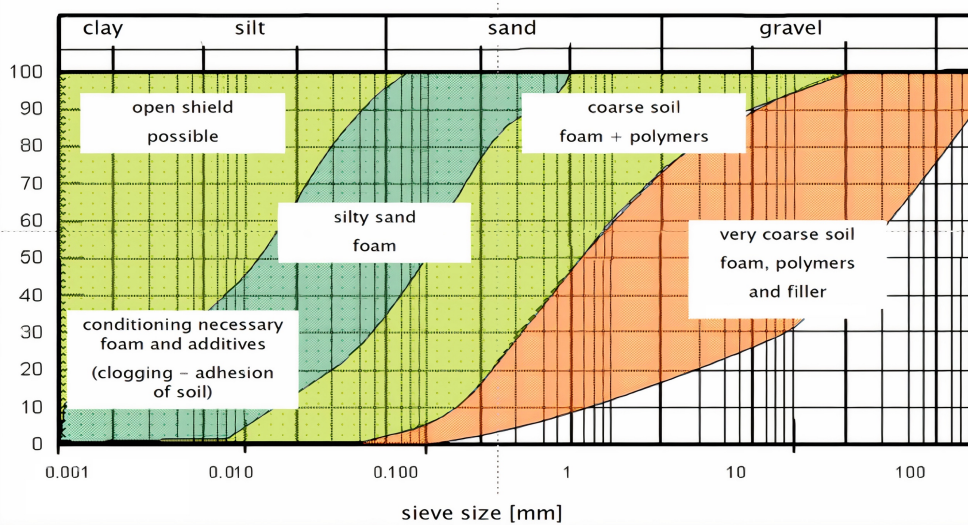


Figure 2_5: EPB-TBM application field and necessary conditioning agents (Shin et al., 2021)

Soil Conditioning

Soil conditioning is a crucial aspect of the excavation process with EPB-TBMs that involves the modification of soil properties. The use of soil conditioning agents can lead to several benefits, such as reducing wear of mechanical part in contact with soil, improving uniformity of pressure distribution in excavation chamber, reducing friction forces in excavation chamber, reducing permeability and so on (Vinai et al., 2008; Thewes et al., 2012). Hence, proper assessment of the conditioned soil is essential to ensure optimal performance of EPB-TBM tunneling.

The selection of type and amount of soil conditioning agents depends on characteristics of soil and specific project requirements. The soil conditioning process affects the properties of soil, such as its strength, permeability, and compressibility. Thus, additives can be injected in several points in machine, such as ahead of cutting head, within excavation chamber, and along screw conveyor (Gharahbagh et al., 2014). The challenges could be more significant and could make the process of selecting conditioning agents more difficult due to variability of soil characteristics across various geological formations.

3.1 General aspects

The key aspect of the design is therefore the correct assessment of the conditioning quantity and conditioning products in order to make the original soil, excavated by the cutterhead, fluid, highly compressible, less permeable (Thewes et al., 2012; Martinelli et al., 2019; Peila et al., 2016; Todaro, 2016; Carigi et al., 2020), and homogeneous plastic paste to correctly apply the support pressure onto the tunnel face (Anagnostou & Kovari, 1996; Peila et al., 2009; Borio & Peila, 2011; Thewes et al., 2012; Elbaz et al., 2018; Liu et al., 2018; Zhang et al., 2020). Furthermore, to reduce wear on the mechanical parts of the machine (Salazar et al., 2016; Salazar et al., 2018), and it is also beneficial in reducing the torque of the cutting head (Pellet & Kastner, 1998).

Selection of suitable soil conditioning agents and parameters requires a comprehensive understanding of the differences in soil behavior. For instance, in

cohesionless soils, the ultimate role of soil conditioning is to maintain proper pressure within excavation chamber while facilitating efficient excavation and soil removal.

Moreover, a correct soil conditioning is needed for EPB-TBM tunneling can be mentioned as (Thewes et al., 2012):

- Reduction of wear for all mechanical parts of machine in contact with soil;
- Better uniformity of pressure distribution in excavation chamber;
- Control of the flow of excavated material through cutter head;
- Reduction of friction forces in excavation chamber;
- Reduction of permeability with consequent better control of water inflow;
- Smoother flow of material along screw conveyor;
- Easier spoil handling.

3.2 Conditioning agents

Successful soil conditioning is in direct relation with proper selection of conditioning set parameters and conditioning agents. The most used additives for soil conditioning are water, foam, long chain polymers, anti-clogging agents (only in cohesive soils), lubricating agents, dispersing agents, abrasion-preventers, bentonite slurry, and fillers.

3.2.1 Water

Water is one of the most commonly used conditioning agent in EPB-TBM soil conditioning, and plays a vital role in maintaining the desired pressure within excavation chamber. Water can be used to regulate consistency and flowability of excavated soil.

3.2.2 Foam

Foam is the key conditioning additive in EPB-TBM tunneling, which normally contains a large amount of air in the form of air-filled surfactant bubbles (Zhao et al., 2018). In order to generate foam, water and foaming agent are mixed in the given proportions to make a foaming solution. The foaming solution is supplied together with a stream of compressed air through a foam generator that contains turbulators. The whirling and turbulent flow through the turbulators causes the

foaming solution to foam (Thewes et al., 2012), as shown in Figure 3_1. The typical composition of a commonly used foam includes approximately 0.5% to 3% of foaming agent, 5% to 10% of water, and 90% to 95% of air. If enhanced foam stability is required, a small fraction, less than 0.1% of polymer can also be added to the composition.

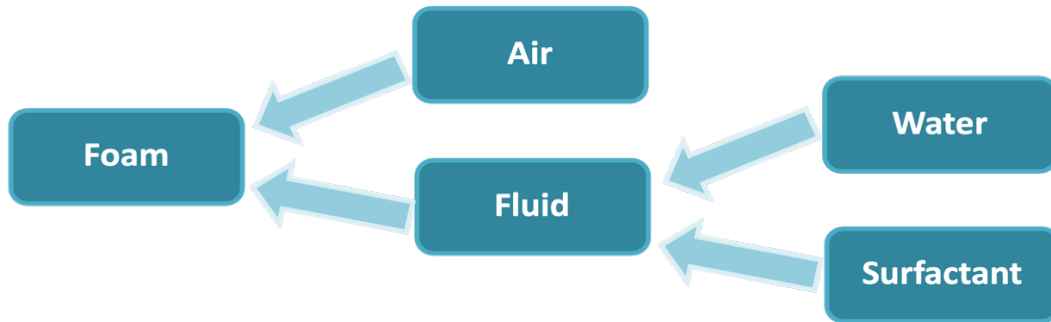


Figure 3_1: Foam composition

One of the advantages of foam is its ability to enhance the properties of conditioned soil, especially in cohesionless soil. It is notable that, proper control over foam's characteristics is essential to achieve optimal results. An excessive amount of foam could lead to over-conditioning situation, resulting in difficulties in managing and transporting the excavated soil. Additionally, to be able to determine what foam and how much foam has to be injected for different soils, it is necessary to know the mechanical parameters of the foam-water-soil mixture (Hajjalilu-Bonab et al., 2014). With respect to quality of foam, at present, there is no standardized method for determining the quality of foam for EPB-shields neither on shield machines nor in laboratories. For foams to be used with an EPB-shield, the following requirements can be defined. The foam should have the following properties (Thewes et al., 2012):

- constant and uniform density, which means that liquid and air are completely mixed and that all parts of the produced foam have the same properties;
- Stability for the duration of stay in the excavation chamber;
- homogenous structure of bubble size.

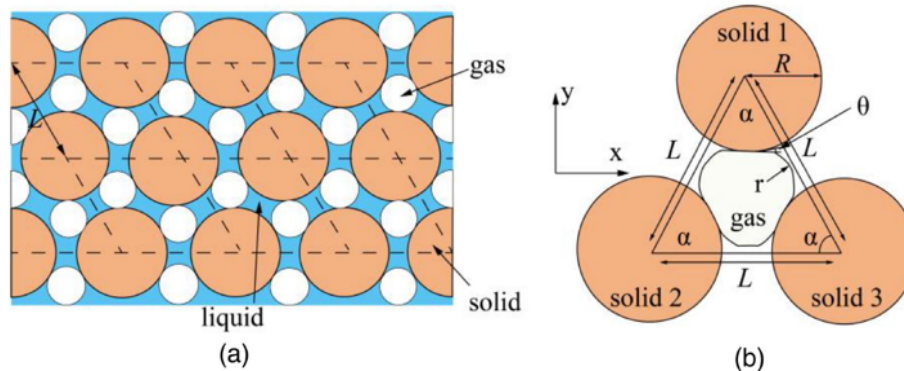


Figure 3_2: Simplified two-dimensional model for foam-conditioned sand (Wang et al., 2022)

3.2.3 Additives

Additives play a crucial role in soil conditioning for EPB-Tunneling. Polymers, which are long-chain man-made chemicals with high molecular weight, modify soil behavior, enhancing cohesion and stability, especially in cohesive grounds. With respect to bentonite, it can be mixed with water to create a slurry that stabilizes and improves flowability, benefiting cohesionless soils and preventing water entry. Additionally, anti-clogging and lubricating agents are special additives used to address clogging and friction issues, maintaining steady excavation rates, reducing wear, and preventing the need for repetitive stoppage to clear clogs.

3.3 Soil conditioning parameters

Study of soil conditioning parameters is significantly important to be carried out, as the ultimate purpose is to determine the optimal and most effective conditioning set parameters particularly for project's specification.

3.3.1 Flow rate

Flow rate of the foam generator determines the amount of foam solution produced per unit time and may have significant impact on effectiveness of foam conditioning system, as it influences the quality of generated foam.

3.3.2 Foam Injection Ratio

Foam Injection Ratio (FIR) represents the ratio between the volume of foam added and the volume of soil. This ratio has a direct impact on the properties of the conditioned soil, and subsequently influences the efficiency and effectiveness of the tunneling operation. FIR is typically expressed as a percentage, and globally provides quantitative representation of the amount of foam induced into the soil (Todaro et al., 2021).

$$FIR (\%) = \frac{V_{foam}}{V_{soil}} \cdot 100$$

A wide range of FIR can be observed in real tunnel excavations, encompassing percentages from 10% to 80%, with a common range of 30% to 60% (EFNARC, 2005).

3.3.3 Foam Expansion Ratio

Foam Expansion Ratio (FER) represents the ratio between the volume of foam and the volume of liquid generator. This ratio can vary depending on the specific foam generator and foaming agent used. FER is a dimensional parameter, and generally serves as the indicator of foam quality.

$$FER (-) = \frac{V_{foam}}{V_{liquid\ generator}}$$

Lower FER values describe wet foam, often utilized in clayey soil conditions. Conversely, high FER values, typically higher than 10, correspond to dry foam, commonly employed in sand and gravel conditions (Todaro et al., 2021). Moreover, FER values must fall within the range of 5 to 30 (EFNARC, 2005), and typical values for FER are found to be between 10 and 25 (Thewes et al., 2012).

3.3.4 Foaming agent Concentration

Foaming agent concentration (c_f) is the proportion of the foaming agent added to the foaming solution. The concentration of the foaming agent influences the quality and characteristics of generated foam. This value is usually expressed as a

percentage, and it is commonly used within the range of 0.5% to 5.0% (EFNARC, 2005) in EPB-TBM tunneling.

$$c_f(\%) = \frac{V_{conditioning\ agent}}{V_{liquid\ generator}} \cdot 100$$

3.3.5 Total water content

Total water content (w_{total}) represents the ratio between the mass of free water and the mass of dry material. This ratio is typically expressed as a percentage.

$$w_{total}(\%) = \frac{M_w}{M_s} \cdot 100$$

3.3.6 Added water content

Added water content ($w_{water\ added}$) represents the differences between total water content (w_{total}) and natural water content ($w_{natural}$). This ratio is typically expressed as a percentage.

$$w_{water\ added}(\%) = w_{total} - w_{natural}$$

3.3.7 Half-life time

Half-life time of foam is the time required for a foam sample of 80 g to drain half of its weight (EFNARC, 2005). In EPB-TBM soil conditioning, half-life time is an important parameter that indicates stability and longevity of generated foam. Hence, it is evaluated to get information on stability and drainage performance of foam (Wu et al., 2018; Wang et al., 2022). A longer half-life time indicates that the foam will remain stable and effective for a longer duration within the excavation process. It is notable that, the foam stability time is a function of the bubble size, which, in turn, is related to FER, uniformity of the bubbles, and strength of the bubble wall, influenced by the conditioning agent type (Hajjalilu-Bonab et al., 2014).

Materials

4.1 Soil characterization

Grain size distribution is a fundamental characteristic of soil which refers to distribution of different particle sizes present in a soil sample. In this research, the soil coming from alluvial and moraine formations is used as the reference soil (Figure 4_1). The grain size distribution of the samples was determined using a set of sieves with various mesh sizes. According to ASTM D6913, each sample was weighed and subsequently sieved, starting with the largest mesh size, and progressing downwards. The weight of each soil particle retained on each sieve was recorded, and the percentage weight of each particle size was then computed and plotted on a graph to visualize the grain size distribution of each sample.



Figure 4_1: Soil sample

The sieve mesh sizes employed in the test included 16, 8, 6.3, 4, 2, 1, 0.5, 0.25, 0.125, and 0.075 mm. Having sieved all the samples in the laboratory with mechanical sieve shaker, the data are given in Table 4_1.

Table 4_1: Sieve analysis records

Particle Diameter	Percent Finer					
	Sample 1	Sample 2	Sample 3	Sample 4	Sample 5	Sample 6
[mm]	[%]	[%]	[%]	[%]	[%]	[%]
31.5	100.0	100.0	100.0	100.0	100.0	100.0
16	95.6	92.9	96.0	96.9	97.7	97.1
8	76.6	67.2	78.2	76.9	78.4	83.9
6.3	71.9	61.7	72.6	71.2	72.5	78.7
4	62.7	52.8	64.3	61.6	61.0	70.6
2	51.1	42.9	55.4	48.7	52.2	55.4
1	38.1	38.4	43.0	41.9	38.0	45.2
0.5	26.6	28.6	33.1	30.6	25.4	27.9
0.25	15.5	19.2	22.6	19.4	14.9	16.2
0.125	8.4	12.4	14.7	10.8	8.8	9.5
0.075	4.3	8.4	9.1	6.3	5.5	5.9

Consequently, the averaged grain size distribution curve for the all six samples is provided in Figure 4_2.

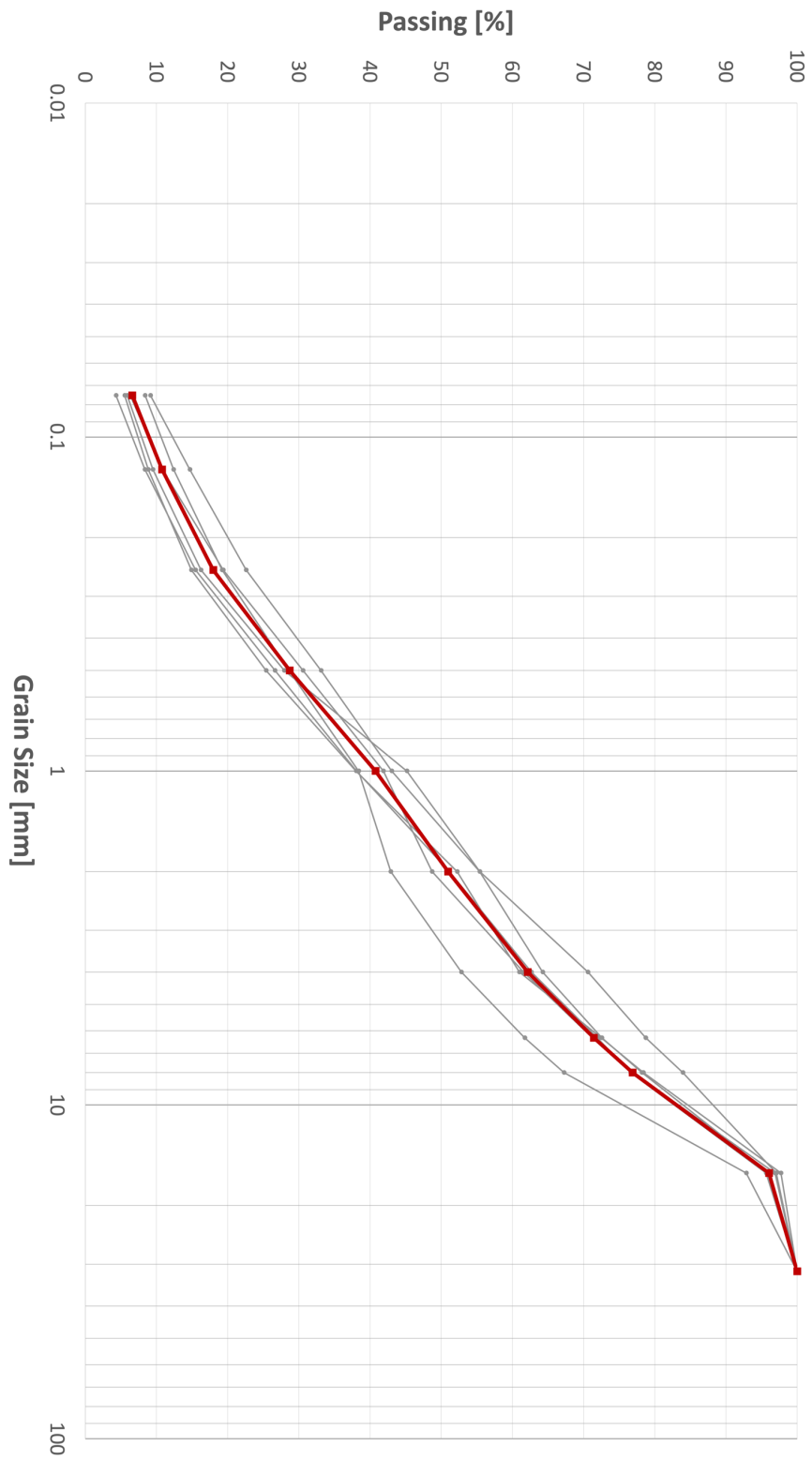


Figure 4_2: Averaged grain size distribution curve

4.2 Atterberg limits

Atterberg limits are important physical properties of soil that describe its behavior under different conditions. The tests are performed according to the ASTM D4318 standard.

For this research, it was not possible to perform the Atterberg limits test. This outcome means that the reference soil is not plastic.

4.3 Conditioning agents

In this research, the selected foaming agent is specifically designed for the conditioning of soils excavated with a shielded TBM. Technical information of the foaming agent is indicated in the Table 4_2.

Table 4_2: Technical information of the foaming agent

Parameter	Value
Form	Liquid, Viscous
Color	No color, light yellow
Density (at 20°C)	1035 – 1045 kg/m^3
pH value (1:1 water solution) (at 20°C)	6.5 – 7.5
Total water solubility	Total
Viscosity (Brookfield LV 30 Needle 3)	100 mPa. s

Chapter 5

Methods

To perform the characterization of the conditioned soil, a variety of tests can be employed to investigate its changing behavior over time. Among these, slump test is the most commonly used test, as it allows evaluation of the conditioned soil rheology, and was originally applied to cohesionless soils such as silt, sand, and gravel (Peila et al., 2009; Thewes et al., 2012). This test provides insights into the changes in workability of soil as a result of different conditioning test parameters. Another important test is the evaluation of density that is performed to assess the change in the physical characteristics of soil with both different conditioning set parameters and in various periods of time. Regarding vane shear test, it introduces a different perspective, focusing on shear strength measurement of conditioned soil. For the conditioned soil due to the very low shear strength, a modified apparatus was used, and it will be described in the following. The results help in understanding how the conditioned soil would behave when subjected to various conditioning set parameters, and in different periods of time, using distinct foam generation methods.

Illustrating and comparing the results of all the mentioned tests across different test campaigns performed with different conditioning parameters, valuable insights into the behavior of conditioned soil in time can be obtained. These insights contribute to the understanding of the effect of foam generator flow rate on essential soil conditioning parameters, such as workability, bulk density, and shear strength. Thus, an investigation into the comparison of how different foam generation methods influence the time-dependency of mechanical properties of the conditioned soil can be pursued. Accordingly, the detailed proposed tests and the test procedures are shortly described in the following.

5.1 Foam generator

A critical component in foam production for EPB-TBM soil conditioning is foam generator. Its role is creating foam mixture by adjusting water flow, air pressure

and foaming agent, which is subsequently added to sample soil to alter its properties. In EPB-TBM machine, foam generator is responsible for producing a consistent and well-structured foam that meets the specific requirements of the tunneling operation. The foam generator consists of two lines, one for the foaming solution and another for pressurized air that. These lines converge into a mixing column that through turbulence generation produces foam.

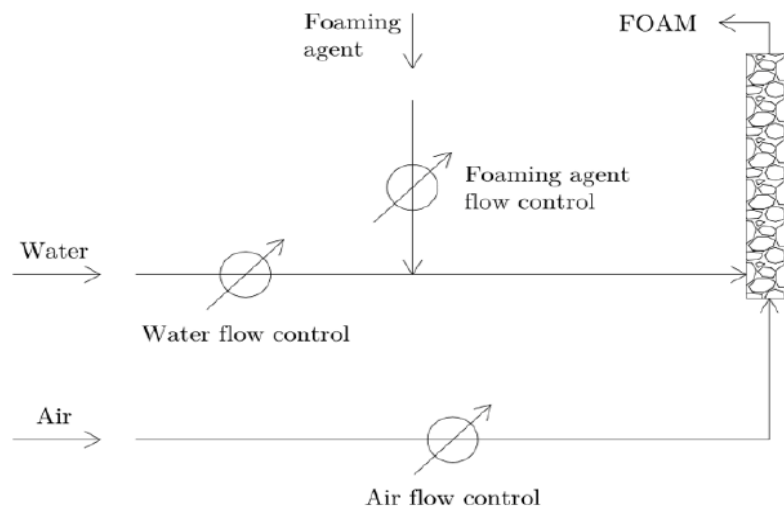


Figure 5_1: Foam generation process scheme (Peila et al., 2008)

The design and performance of foam generators can vary based on different manufacturers and project specifications. The foam generator adopted in this research is produced by SpoilMaster Limited (Figure 5_2), with following properties of foam injection control unit such as maximum water flow rate of 15 l/min, maximum pressure of 6 bar, additive dosing of 300 ml/min (Martinelli, 2016).



Figure 5_2: Laboratory scale foam generator at TUSC laboratory

5.2 Half-life test

Half-life time test is a crucial laboratory evaluation in assessing the stability and decay rate of produced foam as soil conditioning agents in the EPB-TBM tunneling. The decay rate is essential to estimate, in order to know the time duration for which the soil conditioning agent will remain effective in enhancing the properties of soil. The test has to be conducted following to the EFNARC standard (EFNARC, 2005), which involves measuring the time (t_{50}) needed for an 80-grams foam sample to drain half of its weight.

Several authors have previously focused on this kind of test for evaluating foam stability. Relationships between surfactant concentration, viscosity of the liquid generator, and foam stability have been identified. The viscosity of the liquid generator strongly influences the stability of the foam, but no reference, in positive or in negative, has been made on the possibility that the concentration of the surfactant could influence the viscosity of the liquid generator (Moll et al., 2019). Furthermore, it was demonstrated that adding starch to the liquid generator increases both the viscosity of the liquid generator and the stability of the foam (Zhang et al., 2015).

In this research, a novel and dedicated apparatus is used to better study the evolution of degradation of foam in time. In greater detail, this apparatus consists of three funnels positioned above three recipients. Each funnel is equipped with a porous stone to prevent the foam from falling in the recipient. All the funnels and the recipients are connected to load cells with a maximum load capacity of 1000 grams. All six load cells are connected to an Arduino Mega 2560 processor equipped with an LCD screen and a micro-SD data logger (Carigi et al., 2022).

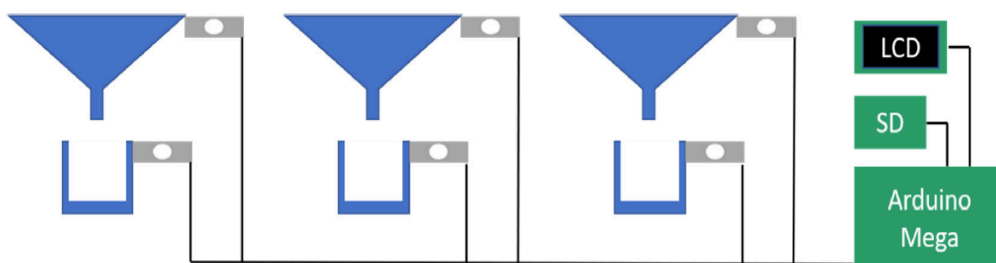


Figure 5_3: Half-life test apparatus scheme (Carigi et al., 2022)

The apparatus allows operators to perform three half-life tests at the same time and to sample the drained weight with a frequency of 10 Hz and a precision of 0.01 gram. After the production of foam, it is collected in a known volume recipient and, by measuring the net weight, the FER is calculated. Then, 80 g of foam is poured directly into each funnel. The data acquisition starts at the moment foam has been placed in the funnel and stops when 65 g of liquid is drained through the porous stone. This threshold corresponds to 80% of the total mass and was arbitrarily set taking into account both the extremely long time required to investigate the drainage of the last 20% of the mass and that the extreme dryness of the remaining foam is completely incompatible with the concept of soil conditioning, hence of scarce interest in this research (Carigi et al., 2022).

5.3 Slump test

Slump cone test is a widely used test within the construction industry for evaluating the consistency and workability of fresh concrete. This test is also used in EPB-TBM tunneling to ensure the quality of conditioned soil. It must be performed following either the ASTM C143 standard or the British & European slump test standard (BS EN 12350-2). The slump cone is a frustum-shaped cone made of steel, with a top diameter of 100 mm, bottom diameter of 200 mm and a height of 300 mm (Figure 5_4). The cone is placed on a smooth, flat surface and filled with material to be tested. Having filled the cone, it must be lifted vertically. Next, the slump or drop of the material due to effect of gravity is measured from the original height of the cone to the highest point of the material.

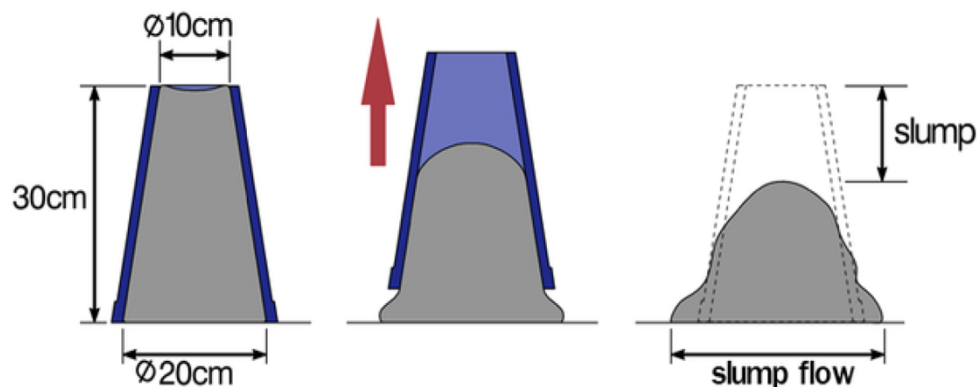


Figure 5_4: Schematic representation of slump test (Martinelli, 2016)

By adjusting both FIR and water content, it becomes possible to classify the conditioned soil into five general behaviors, as illustrated in Figure 5_5. These behaviors provide an instant answer for the efficiency of the conditioning process. According to the plastic behavior of the material as well as the presence or absence of free liquid around the cone, the quality of the mix can be defined as Suitable, Borderline, or Not suitable. Continuously, three main behavior fields can be introduced, such as too stiff and dry behavior due to insufficient water or foam content, too fluid and wet behavior due to excessive water or foam content, and suitable behavior of the mix where the ground behaves plastically.

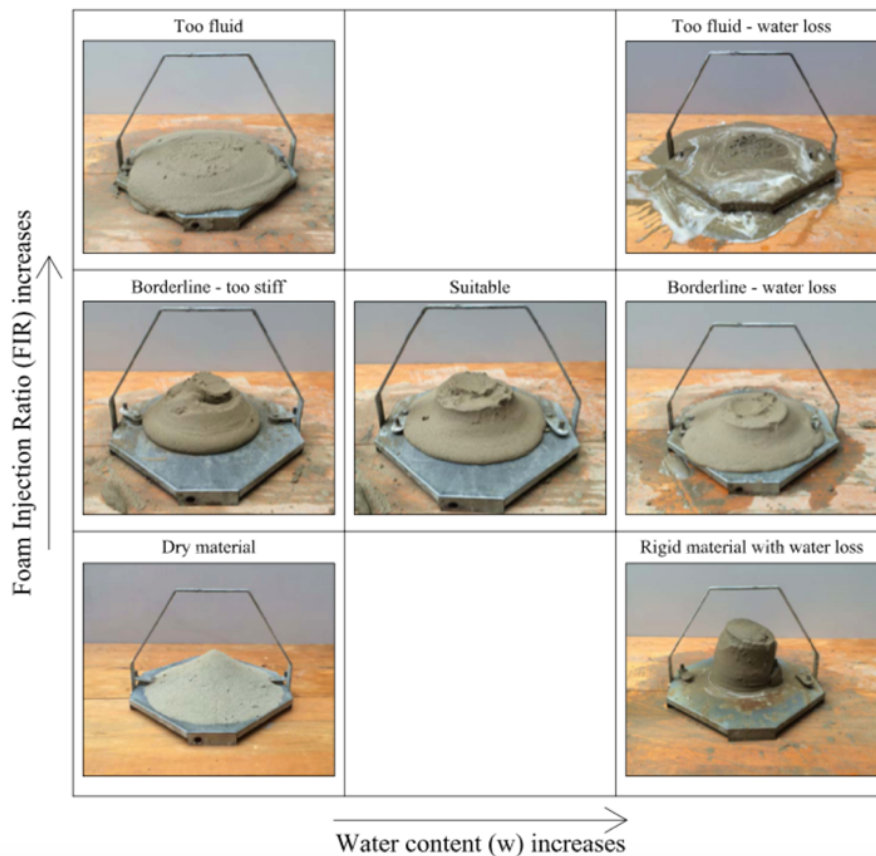


Figure 5_5: FIR and Water content correlation diagram (Peila et al., 2009)

The results of the slump cone test can be used to evaluate the stability and flowability of the conditioned soil. A higher slump indicates a more fluid mixture, while a shorter slump indicates a more stable mixture. If the slump is too high, it may lead to segregation and bleeding, which can affect the performance of the

conditioned soil at excavation face. On the other hand, if the slump is too low, it may cause blockages and difficulties in injecting the soil conditioning agent. The drop of the cone and its shape are outcomes of test. A value below 100 mm is usually considered too low while above 250 mm the mix is considered too fluid (Peila et al., 2019). The suggested value of slump varies in different research studies. Other authors suggested to have values in the range of 200–250 mm (Williamson et al., 1999; Jancsecz et al., 1999) and 80-100 mm (Boone et al., 2005).

It is worthy to note that the slump value is used as an important indicator to evaluate the performance of foam-conditioned soil (Tao et al., 2019), and it has the advantage of being simple to perform and of giving an overall index of the behavior of the conditioned material (Vinai et al., 2008; Zhao et al., 2018). Conversely, the slump value alone is not sufficiently accurate to evaluate the workability of conditioned soil, and the current slump testing method still involves some subjective factors. For example, it requires engineers to observe whether water and foam drain out of the test soil. The inclusion of these subjective descriptions has been a barrier to developing standardized and automatic soil-conditioning evaluation methods (Wang et al., 2022).

5.4 Density test

Density test is one of the important laboratory procedures performed in EPB-TBM soil conditioning to analyze changes in physical characteristics of soil after addition of conditioning agents. The procedure consists of weighting a bucket with a known volume filled with soil. This process is repeated three times, and an average value is calculated to represent the bulk density of the soil sample.

5.5 Vane shear test

The undrained shear strength of the soil affects the wear and tear of the machine's moving parts and cutting tools. If the soil's shearing resistance at the face is decreased, this reduces wear and tear because the cutting resistance is reduced. Thus, low shear strength decreases power consumption and reduces wear and tear throughout the tunneling process (Hajjalilu-Bonab et al., 2014).

Vane shear test is one of the crucial laboratory procedures conducted in EPB-TBM soil conditioning to assess shear strength and resistance of soil. The test has

to be performed according to the ASTM D2573 standard. It is an easy and well-known test to obtain the torque and shear strength properties of soil. This test is based on the field vane test in saturated clay and silt soils for determination of undrained shear strength (ASTM 2015a) and on the miniature vane test in very soft to stiff saturated fine-grained clayey soils (ASTM 2016; Pamukcu & Suhayda, 1988). The miniature vane shear test is carried out by inserting a four-bladed vane in a sample of soil and rotating it at a constant speed to determine the torque required to induce shearing along a cylindrical surface by the apparatus. This torque is subsequently converted into a unit shearing resistance of the cylindrical surface area.

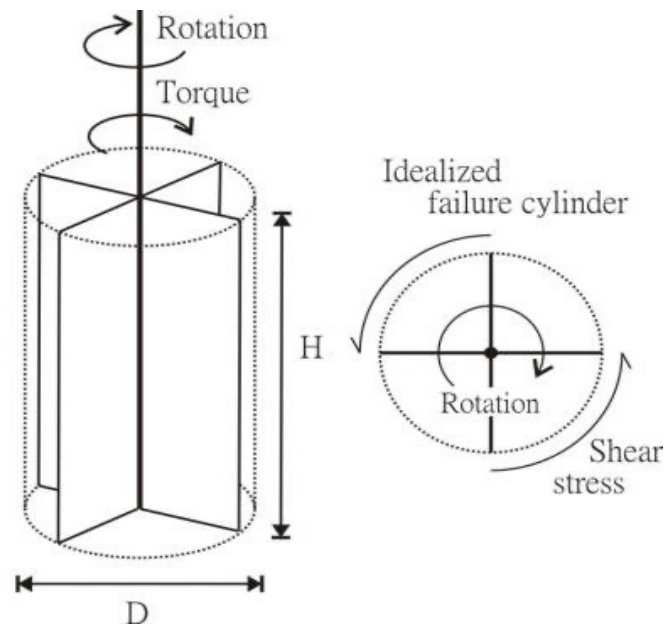


Figure 5_6: Vane shear test principle (Gylland et al., 2016)

Particularly for this research, a modification was made on the test apparatus due to very low mechanical resistance of conditioned soil. The vane dimension has been increased to a diameter of 54 mm and a height of 109 mm to have more sensibility for the measurement when coarse-grained materials are present (Figure 5_7). Being the behavior of the conditioned soil different from the one of the soils for which the test was developed, the ratio between the torque necessary to create a cylindrical failure surface and the area of the surface itself is named Scissometric Index, symbolized as I_{sc} (Carigi et al., 2020). It is critical to emphasize that, owing to the maximum capacity of the vane shear apparatus, there is a

limitation at 5.23 kPa, and values exceeding this limit in all tests are considered as “out of scale”. The test is repeated three times, and an average value is calculated.



Figure 5_7: Modified vane shear apparatus (Carigi et al., 2020)

5.6 Semi-quantitative analysis

Segmented Regression Analysis is employed to perform a semi-quantitative analysis of the collected data from slump test, density test, and vane shear test throughout all the test campaigns. The assessment is performed on investigating potential correlations among the outcomes in relation to distinct foam generator flow rates, Foam Expansion Ratios (FER), and Foam Injection Ratios (FIR). Segmented Regression Analysis, also known as piecewise regression or broken-stick regression, is a statistical technique used to model relationships between variables when there are different breakpoints or segments in the data.

The initial step is Data Splitting, where the obtained results from the test campaigns are separated into two series denoted as “Set i ” and “Set j ”. A predetermined breakpoint, defined as $n = 3$, is chosen to split the set of data with N observations. Continuously, the first three data points are assigned to “Set i ”, while the remaining data points from 4 to N belong to “Set j ”. Proceeding to Model Specification, a linear model is established for each segment. For “Set i ”, the model is represented as $S_i^* = m_1 t_i + q_1$, where S_i^* denotes the estimated

value, m_1 corresponds to the slope, q_1 stands for the intercept, and t signifies the time interval between the initial and current tests. Similarly, regarding "Set j ", the model is expressed as $S_j^* = m_2 t_j + q_2$, where m_2 and q_2 represent the slope and intercept, respectively.

Advancing to the Parameter Estimation, the values of slope and intercept for each set are separately estimated using optimization technique, called the method of least squares. Specifically, the objective is to minimize the sum of squared differences between the observed values and the predictions generated by the respective linear models. The optimization process is aimed at finding the optimal values for lines parameters, denoted as m_1 , q_1 , m_2 , and q_2 to minimize the following expression:

$$\left[\sum_{i=1}^n (S_i - (m_1 t_i + q_1))^2 + \sum_{j=n+1}^N (S_j - (m_2 t_j + q_2))^2 \right]$$

Having successfully minimized the abovementioned expression, the associated line parameters are preserved. Subsequently the next step is initiated, with an increase of one in the value of n , and a repetition of the same procedure. The objective is always same which is minimization of the sum through the optimization process to derive new parameters for "Set i " and "Set j ", representing the best fit for the encompassing data points. This procedure is iteratively performed until n reaches $n = N - 3$. In the final iteration, the last three data points are allocated to "Set j ", while the remaining data points, from 1 to $n = N - 3$, are assigned to "Set i ". The final step involves identifying the minimum sum of squared differences among all the estimated values. This step is crucial in determining the best-fitting model for the empirical data, revealing the optimal model to describe the behavior of the given dataset. With respect to the final step, it is critical to emphasize that certain constraints need to be satisfied to confirm the suitability of the chosen fitting lines as the most appropriate model. It is notable that constraints differ depending on the type of test including slump test, density test, and vane shear test.

Due to logistic limitations in laboratory operations, it is not feasible to conduct tests continuously at consistent intervals over a 24-hour period. These limitations are the primary reason for the existence of gaps in the empirical results of the earlier mentioned tests. Consequently, performing the mathematical analysis for

these data, anomalies may arise in assessments where the specified constraints are not satisfied. In such instances, it becomes challenging to maintain continuity for preventing the occurrence of unacceptable values of m_1 and m_2 .

Regarding slump test, the general trend is in a downward direction, which may result in potential modeling anomalies as illustrated in Figure 5_9 and Figure 5_11.

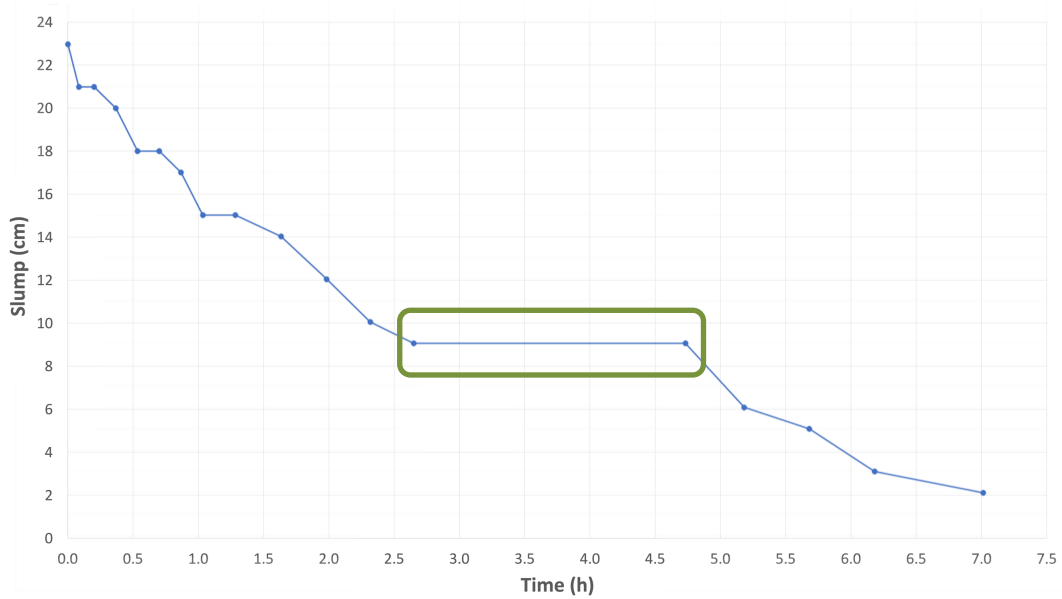


Figure 5_8: Gap in the empirical results – Slump test

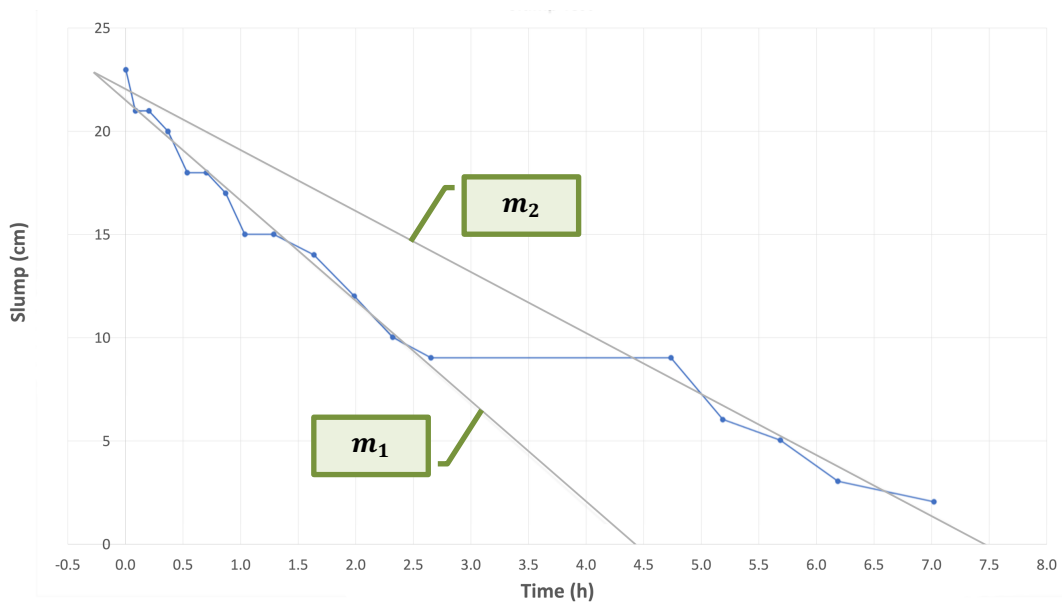


Figure 5_9: Anomaly type I in a descending trend

In Figure 5_9, an instance of modeling anomaly is depicted, where two constraints are violated. Firstly, the interception of two lines is not permitted for $t < 0$. Additionally, having $m_2 > m_1$ cannot be considered as acceptable. The highlighted gap, in Figure 5_8, creates a situation where the mathematical approach could become inefficient.

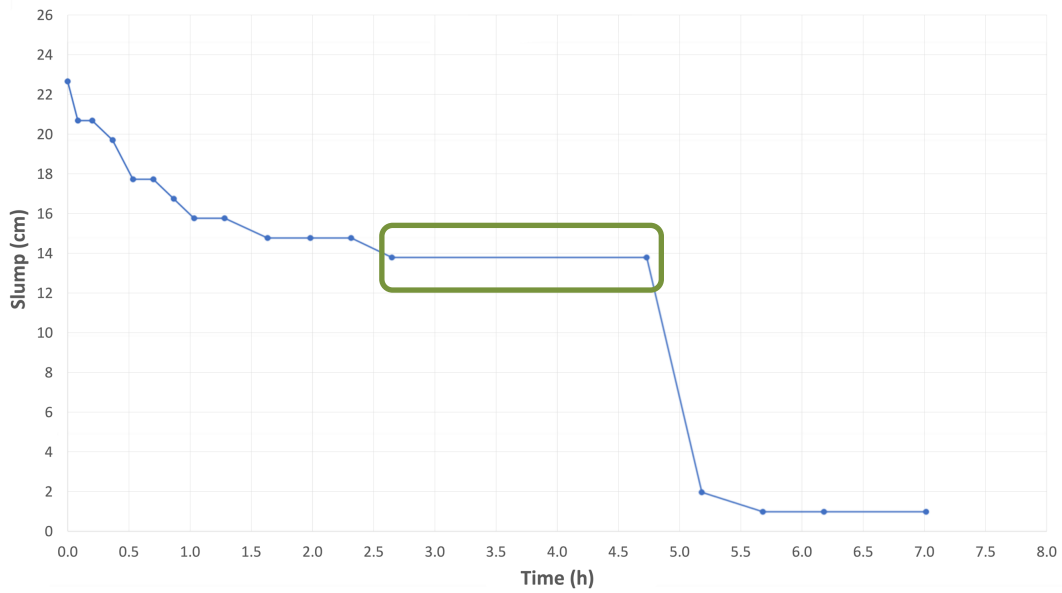


Figure 5_10: Gap in the empirical results – Slump test

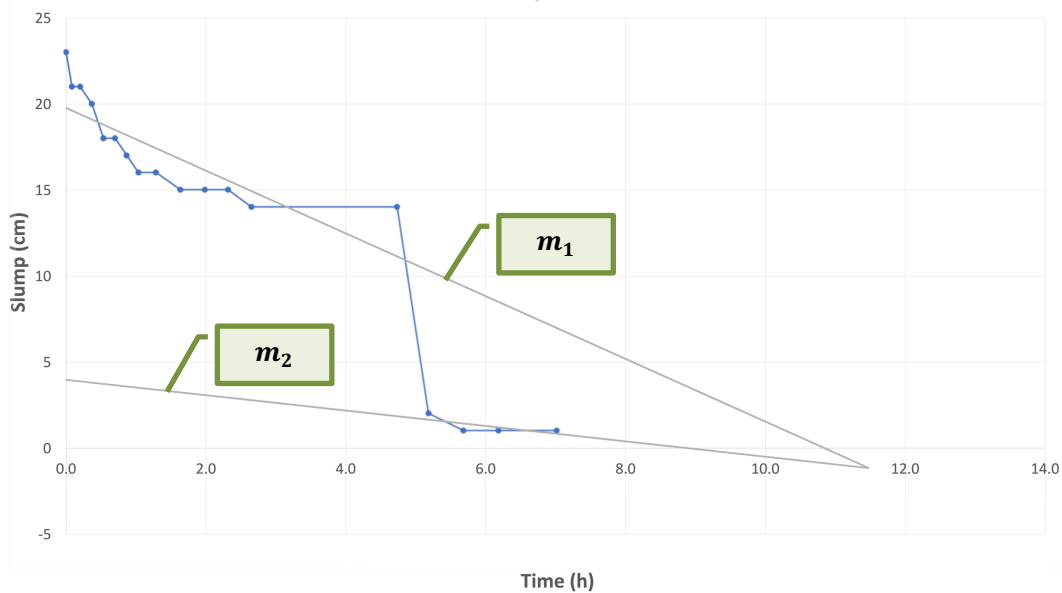


Figure 5_11: Anomaly type II in a descending trend

In Figure 5_11, another type of modeling anomaly is illustrated, where having $m_2 > m_1$ cannot be considered as acceptable. The highlighted gap, in Figure 5_10, creates a situation where the mathematical approach may become inefficient.

Regarding density and vane shear tests, the typical trend is in an upward direction, which different modeling anomalies can be faced as depicted in Figure 5_13 and Figure 5_15.

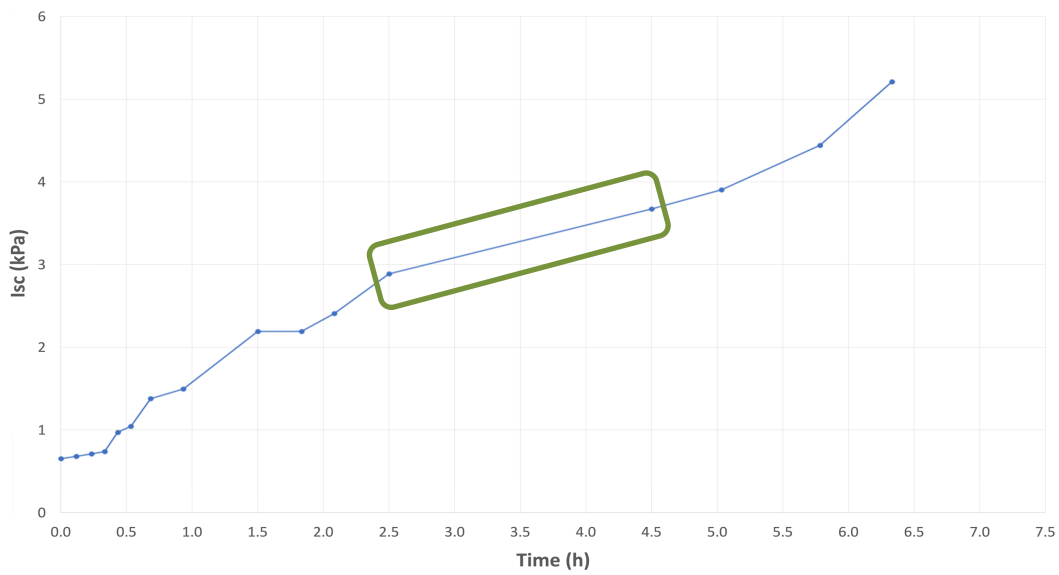


Figure 5_12: Gap in the empirical results – Vane shear test

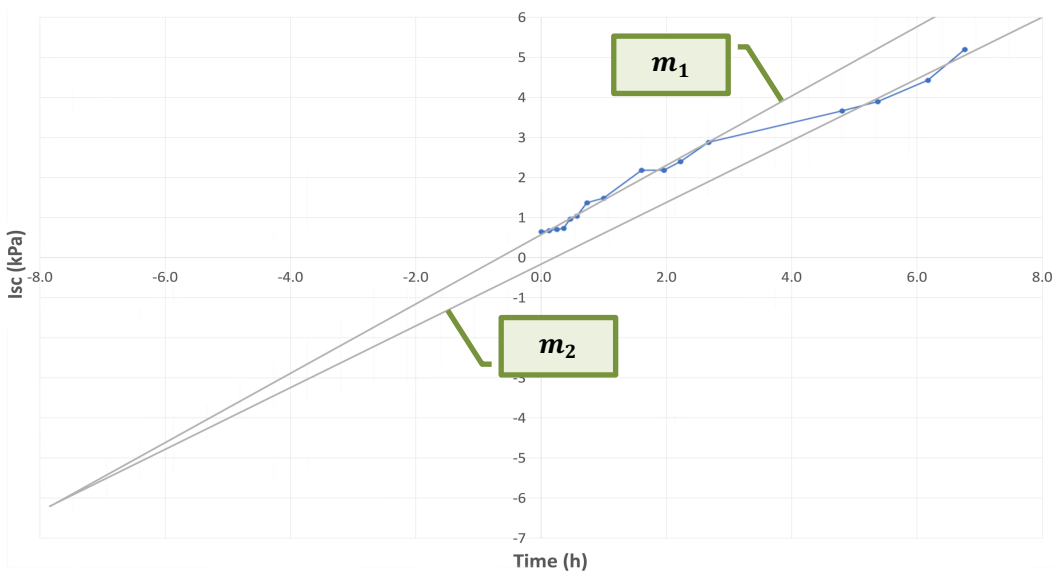


Figure 5_13: Anomaly type I in an ascending trend

In Figure 5_13, an example of modeling anomaly is illustrated, where two constraints are found to be violated. Initially, the interception of two lines is not allowed for $t < 0$. Moreover, having $m_2 > m_1$ is considered as unacceptable. The highlighted gap, in Figure 5_12, leads to a situation where the mathematical approach may lose its efficiency.

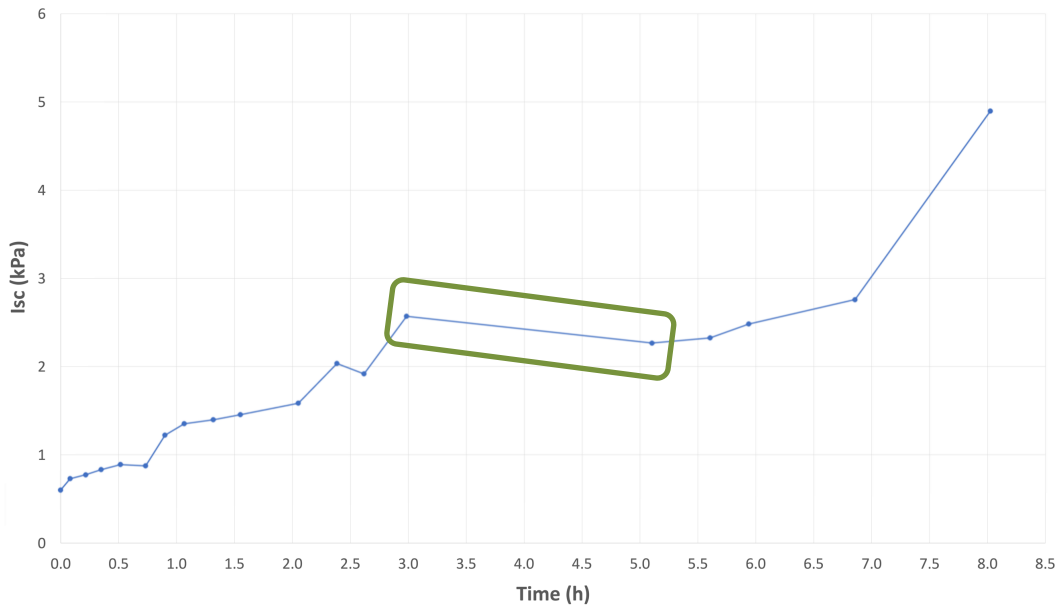


Figure 5_14: Gap in the empirical results – Vane shear test

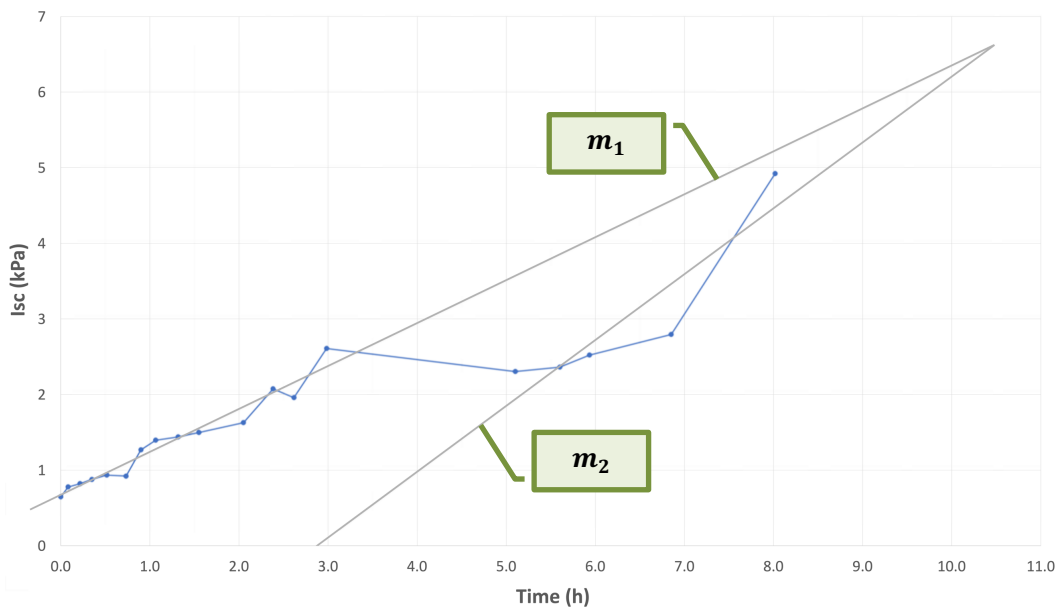


Figure 5_15: Anomaly type II in an ascending trend

In Figure 5_15, another type of modeling anomaly is presented, where the condition of $m_2 > m_1$ is not acceptable. The highlighted gap, in Figure 5_14, leads to a situation where the mathematical approach may fail.

Addressing these potential modeling anomalies, the priority is shifted to selecting the most appropriate fitting alternative. This was performed by adjusting the lines parameters to corresponding values that would result in the sum closest to the minimum, aiming to achieve the highest level of alignment with the empirical data.

Figure 5_16 highlights the outcomes of finding the optimization for a test encompassing 17 data points. Notably, in the diagram all 12 potential models are presented in gray. In scenarios like this instance, where no anomalies are detected, the minimum sum of squared differences among all the estimated values would represent the best-fitting model for the given dataset. In Figure 5_17, the optimal model is visually highlighted in red, demonstrating an acceptable correlation with the data points.

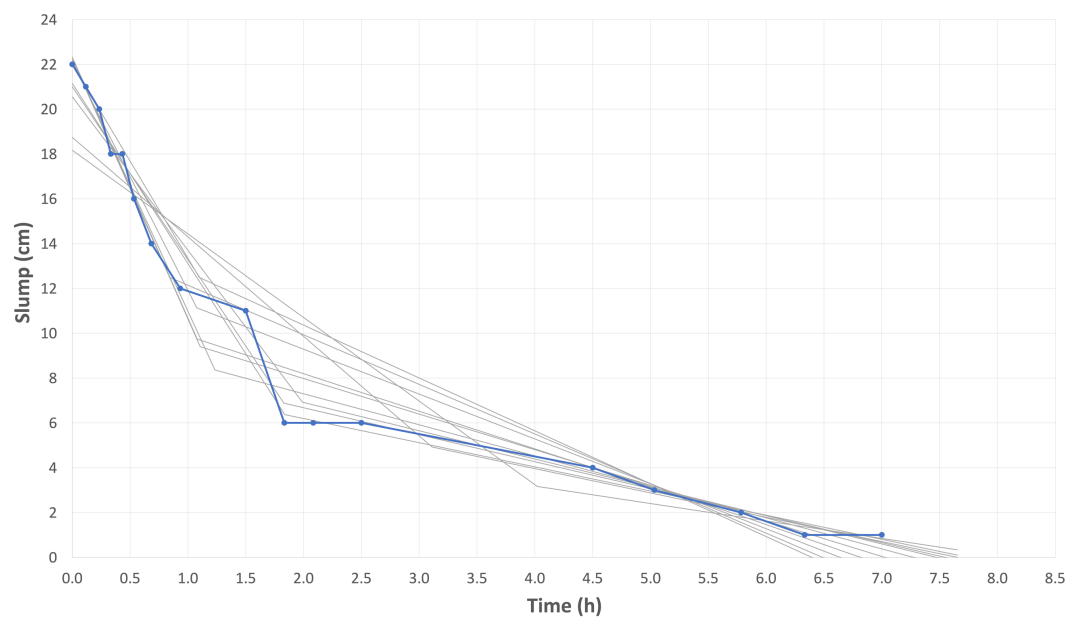


Figure 5_16: Dataset with 12 potential models

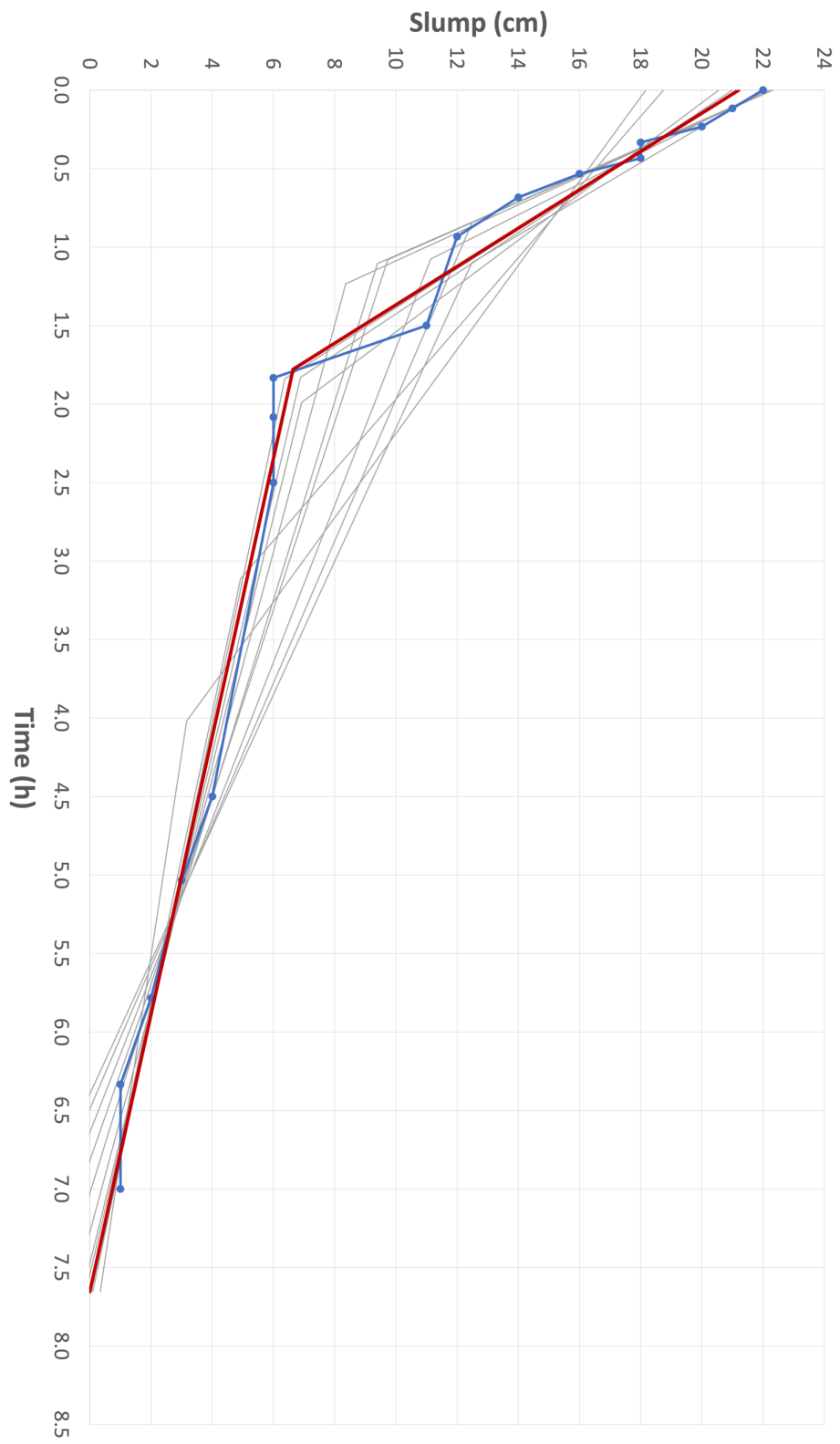


Figure 5_17: Optimal model with the minimum sum of squared differences

Laboratory Tests

6.1 General overview

The objective of this research is investigating the effect of flow rate in foam generator on various mechanical properties of conditioned soil such as workability, bulk density, and shear strength during time. This objective has arisen from the results of half-life test, where the same foaming agent concentration was utilized with two distinct foam generator flow rates, leading to variation in the stability of the generated foam. Hence, by employing two different foam generator flow rates, specifically denoted as the maximum foam generator flow rate ($Q_{max} = 10 \text{ l/min}$) and the minimum foam generator flow rate ($Q_{min} = 2.8 \text{ l/min}$), with the foaming agent concentration (c_f) of 2.0%, in combination with two values of Foam Expansion Ratios (FER) of 8 and 15, and a relatively wide range of Foam Injection Ratios (FIR) encompassing 20%, 30%, 40%, and 50%, a comprehensive examination of various scenarios was conducted. This involved performing 19 test campaigns, which provided valuable insights into the influence of various methods for foam generation on the behavior and mechanical characteristics of conditioned soil.

Continuously, by correlating foam generator flow rate, FIR, and FER with the outcomes of various tests such as slump test, density test, and vane shear test across all test campaigns, variations can be identified and described. Additionally, by performing a semi-quantitative evaluation on the mentioned tests, connections between the conditioning set parameters and engineering properties of the conditioned soil are investigated.

6.2 Optimal conditioning set parameters

The grain size distribution of the soil utilized for the research is reported in Figure 6_1. The soil exhibited a density of 1.91 kg/l, and its natural water content ($w_{natural}$) was 4.44%. However, for enhanced accuracy and precision of the

results, the water content for each campaign was estimated according to ASTM D2216 standard. Subsequently, the ascertained value was employed in the testing procedure.

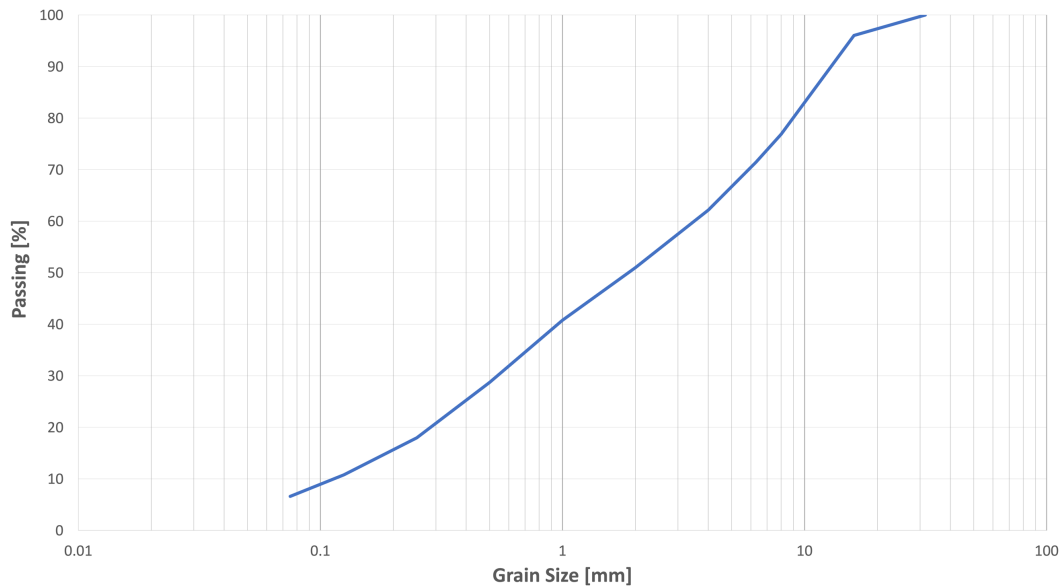


Figure 6_1: Grain size distribution curve

According to the preliminary tests and visual observations of the conditioned soil, a total water content of 9% was chosen as the reference value for all test campaigns. Therefore, prior to the introduction of foam to the soil sample, water content was configured to the total water content value (w_{total}) by adding water to the soil sample, and mixing it in the mixing tank. Continuously, based on the specific parameter values associated with each test campaign, the remaining conditioning set parameters are chosen to initiate the soil conditioning process and begin the subsequent test procedures. The testing conditions and parameters are detailed in Table 6_1.

6.3 Procedure description

To study the evolution of conditioned soil properties, the first step is investigation to assess foam stability itself. The half-life test proposed by EFNARC standard (EFNARC, 2005) is described in Chapter 5.2. Furthermore, for engineering application, a Foam Expansion Ratio (FER) in the range of 5 to 30 is suggested by the standard. Consequently, the same FER range was deliberately chosen for the

purpose of studying how the half-life test behaves under the influence of various foam generator flow rates.

The half-life test using the foaming agent with a consistent foaming agent concentration (c_f) was performed, covering the FER range of 5 to 30. The observed variation in the test results suggests that the utilized Minimum flow rate (Q_{min}) and Maximum flow rate (Q_{max}) in the foam generator, highlight differences in the stability of the generated foam. Consequently, the idea of comparing how different foam generation methods influence the time-dependency of mechanical properties of the conditioned soil has become the core objective of this research.

In the context of this research, the available soil mass (434 kg) allowed the execution of a total of 19 planned tests on 20 kg samples, encompassing 2 preliminary test campaigns and 17 main test campaigns. It is critical to note that, two preliminary test campaigns were carried out, revealing potential differences in the abovementioned characteristics of conditioned soil to identical conditioning set parameters but with foam produced using two different foam generator flow rates. Consequently, the detected variation in the outcome of the slump test, density test, and vane shear test, prompted the arrangement and implementation of comprehensive main test campaigns, that constitutes the main part of this research. The conditioning set parameters of each test campaign are presented in Table 6_1.

Table 6_1: Summary of test campaigns conditioning set parameters

Test Campaign	C_f	Q	FIR	FER
	[%]	[l/min]	[%]	[-]
A	2.0	10	50	15
B	2.0	2.8	50	15
C	2.0	10	50	8
D	2.0	2.8	50	8
E	2.0	10	40	15
F	2.0	2.8	40	15
G	2.0	10	40	8
H	2.0	2.8	40	8
I	2.0	10	30	15
J	2.0	2.8	30	15
K	2.0	10	30	8
L	2.0	2.8	30	8
M	2.0	10	20	15
N	2.0	2.8	20	15
O	2.0	10	20	8
P	2.0	2.8	20	8
Q	-	-	0	-

As mentioned earlier, to investigate the mechanical characteristics of the conditioned soil over time, various tests such as slump test, density test, and vane shear test were performed. The detailed description of these tests can be found in Chapter 5.3, 5.4, and 5.5, respectively. Additionally, Tables 6_2, 6_3, and 6_4 provide the step-by-step test procedures employed in this research. It is notable that, the present studies were performed at atmospheric pressure.

Table 6_2: Slump test procedure

Step	Operation
1	Clean the cone and base plate
2	Place the cone on the base plate, ensuring it is locked
3	Fill the cone and ensure proper compaction by tapping the sides gently
4	Strike off the excess of material ensuring it is completely filled (not overfilled)
5	Carefully lift the cone vertically upward with low constant speed
6	Measure the maximum vertical distance between them using tamping rod

Table 6_3: Density test procedure

Step	Operation
1	Fill a bucket of known volume and ensure proper compaction by jolting gently
2	Strike off the excess of material ensuring it is completely filled (not overfilled)
3	Measure the net weight of soil filling the bucket
4	Empty the bucket
5	Repeat the same process for two more times
6	Take the average of measured values and compute the bulk density

Table 6_4: Vane shear test procedure

Step	Operation
1	Fill the bucket and ensure proper compaction by jolting gently
2	Strike off the excess of material ensuring it is completely filled (not overfilled)
3	Insert the vane blade into the soil
4	Rotate the vane shear apparatus at a continuous constant rate
5	Measure the maximum vane value from apparatus
6	Empty the bucket
7	Repeat the same process for two more times
8	Take the average of measured values and compute the Scissometric Index (I_{sc})

In the final step, to investigate the properties of the conditioned soil with various conditioning set parameters, all graphs associated with each individual test such as slump test, density test, and vane shear test across all main test campaigns are plotted into a single figure. Hence, the discussion on the observed variations and trends is facilitated, simplifying the process of visual comparison.

6.4 Mathematical formulation

6.4.1 Half-life test

In this section, a mathematical formulation is applied on the obtained results from half-life test campaigns using an asymmetric sigmoid function (Carigi et al., 2020). This function is characterized by five parameters and is expressed by the following formulation:

$$w_d = d + \frac{a - d}{\left(1 + \frac{t^b}{c}\right)^m}$$

Where w_d represents the weight of drained liquid, expressed in grams, and t indicates the time from the start of test, expressed in seconds. Continuously, for all the half-life results, the five parameters were determined through an optimization process. The primary goal of optimization procedure was minimizing the least squared error, which serves as a fundamental criterion for fitting the asymmetric sigmoid function to the obtained results. Subsequently, to evaluate the goodness of the fit for multi-coefficient regression formulation, the adjusted determination coefficient (R_{adj}^2) was used. In the final step, graphs are illustrated plotting asymmetric sigmoid parameters versus FER, and also Half-life time versus FER, to examine any potential correlations.

6.4.2 Slump test, Density test, and Vane shear test

In this part, a semi-quantitative analysis is performed on the obtained results from slump test, density test, and vane shear test across all main test campaigns using Segmented Regression Analysis. The objective of the optimization process was minimizing the sum of squared differences between the observed values and the predictions generated by the respective linear models, with the aim of determining the optimal values for fitting lines parameters. Moreover, the

detailed description of the analysis, and potential modeling anomalies along with the way of addressing them are presented in Chapter 5.6. In the final stage, graphs are depicted plotting lines parameters of the best-fitting model versus Foam Injection Ratios (FIR) for distinct foam generator flow rates and Foam Expansion Ratios (FER), to explore any potential correlations.

Discussion on the results

7.1 Half-life test

Approximately 50 half-life tests were conducted across two test campaigns, following the methodology outlined in Chapter 5.2. The foam was generated using an identical foaming agent and consistent foaming agent concentration (c_f) at 2.0%. These tests involved monitoring the drainage of liquid until it reached 80% of the foam's weight. The relationship between cumulative weight and time exhibited a highly accurate fit with an asymmetrical sigmoid curve, which is a well-defined five parameter mathematical formulation (Carigi et al., 2022). It is critical to note that, the determined values of adjusted determination coefficient (R_{adj}^2) were always higher than 0.99 for all conducted tests.

The experimental results confirm the well-known relation between the stability of the foam and Foam Expansion Ratio (FER). As FER increases, there is an observed improvement in foam stability along with a corresponding reduction in water content (Zhou & Yang, 2020). This phenomenon can be attributed to the fact that, a greater amount of liquid is present in foams generated with lower FER, resulting in accelerated bubble growth compared to foams generated with higher FER, which can be characterize as drier foam (Magrabi et al., 1999; Wu et al., 2018). It is critical to note that, this relationship remains correct for both foam generator flow rates within the context of this study, as depicted in Figure 7_1 and Figure 7_2.

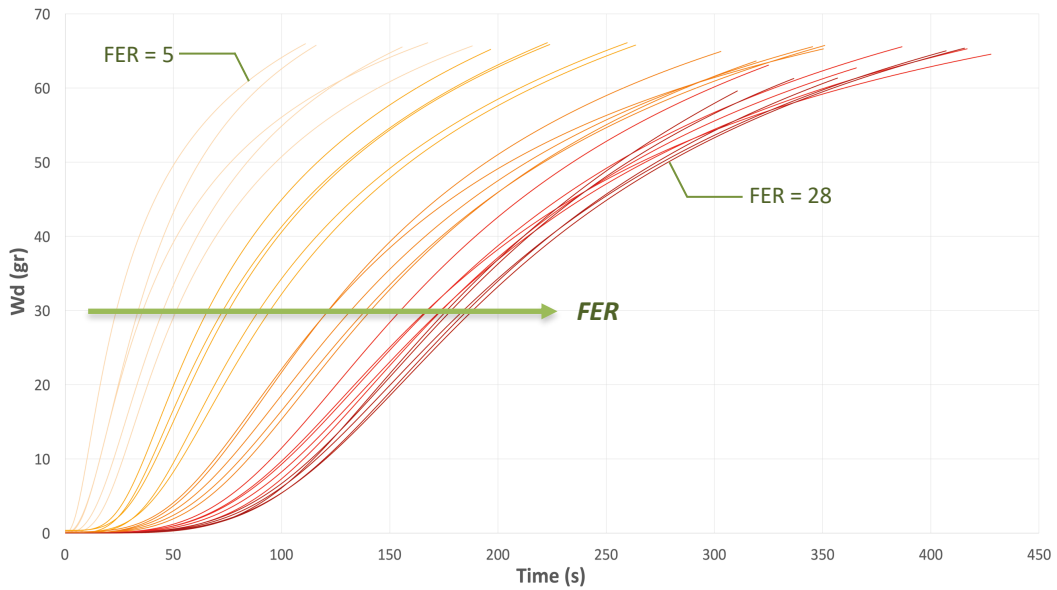


Figure 7_1: Cumulative weight vs. time for Q(min)

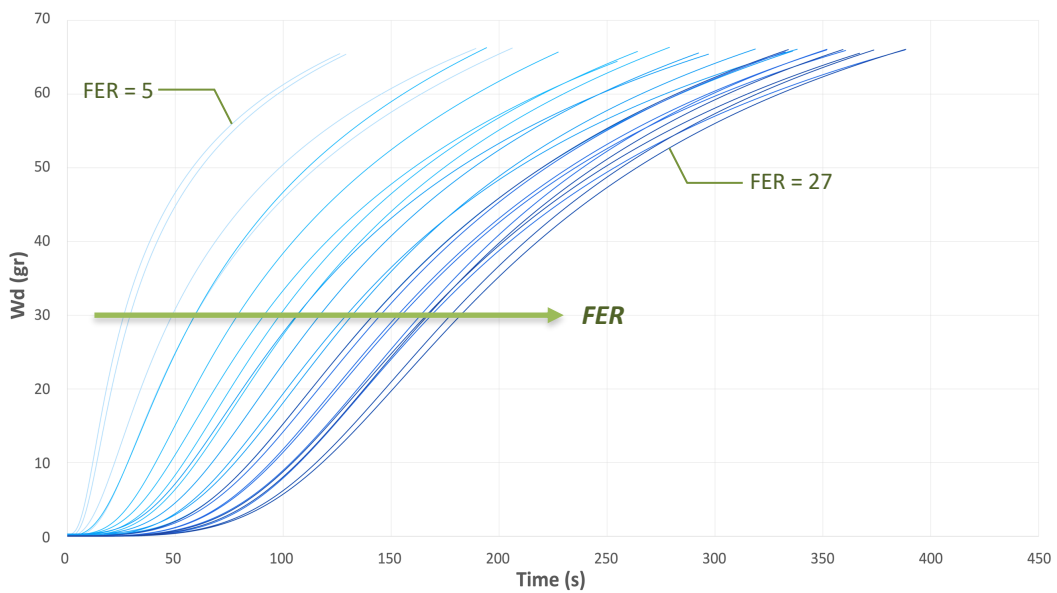


Figure 7_2: Cumulative weight vs. time for Q(max)

In the assessment of the fit quality for the multi-coefficient regression formulation, the adjusted determination coefficient (R_{adj}^2) was employed. Discussing the outcomes of these evaluations, with respect to minimum foam generator flow rate ($2.8 \text{ l}/\text{min}$), the R_{adj}^2 values were found to range between 1.000 and 0.9999 for 44% of tests, between 0.9999 and 0.999 for 24% of tests, and higher than 0.99 for the remaining 32%, as illustrated in Figure 7_3.

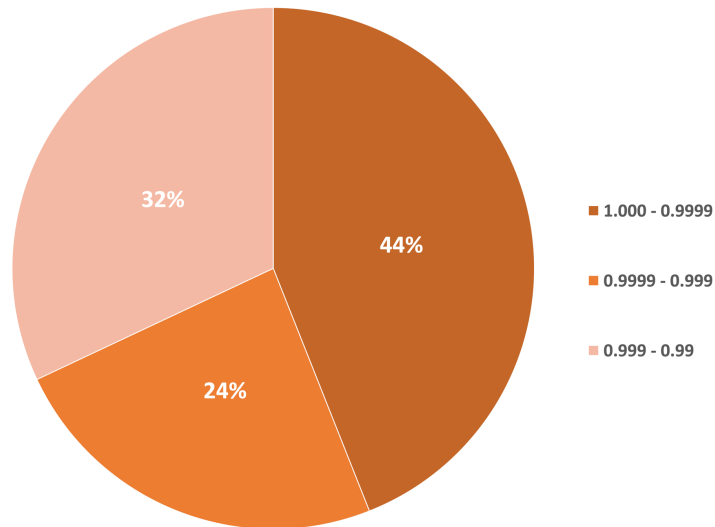


Figure 7_3: Adjusted determination coefficient ranges for Q(min)

Regarding the maximum foam generator flow rate ($10 \text{ l}/\text{min}$), the R_{adj}^2 values were observed in a range of between 1.000 and 0.9999 for 67% of tests, between 0.9999 and 0.999 for 25% of tests, and higher than 0.99 for the remaining 8%, as presented in Figure 7_4.

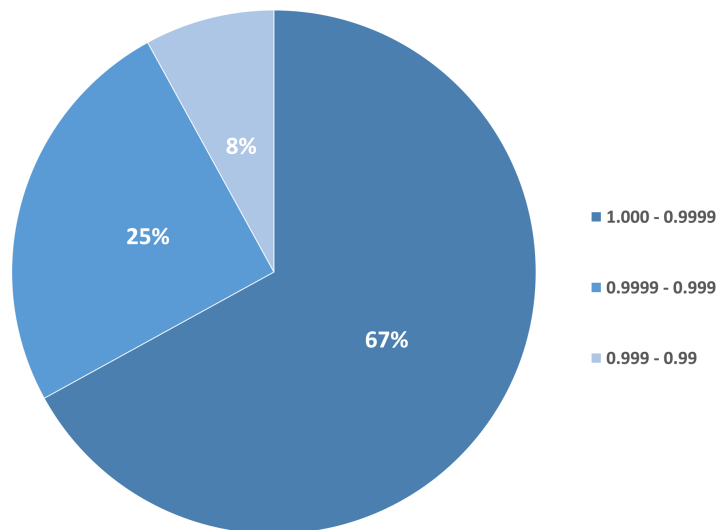


Figure 7_4: Adjusted determination coefficient ranges for Q(max)

Hence, for both test campaigns, the formulation is suitable to accurately describe the tests. Following this, the obtained results from mathematical formulation, show no strong correlation between FER and the parameters of

asymmetric sigmoid function across distinct foam generator flow rates, as depicted in Figures 7_5, 7_6, 7_7, and 7_8.

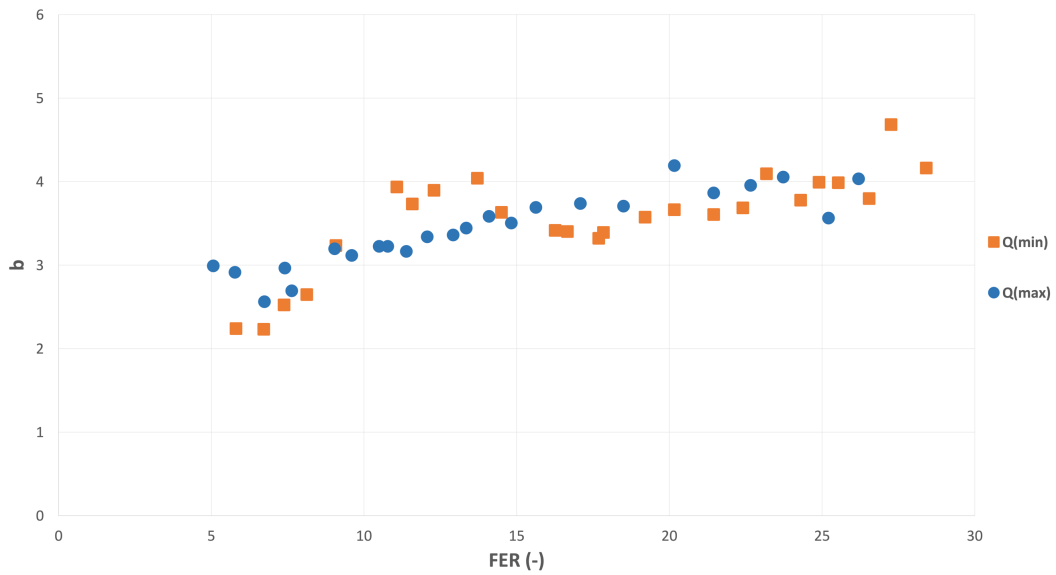


Figure 7_5: Asymmetric sigmoid parameter “b” vs. FER for different foam generator flow rates

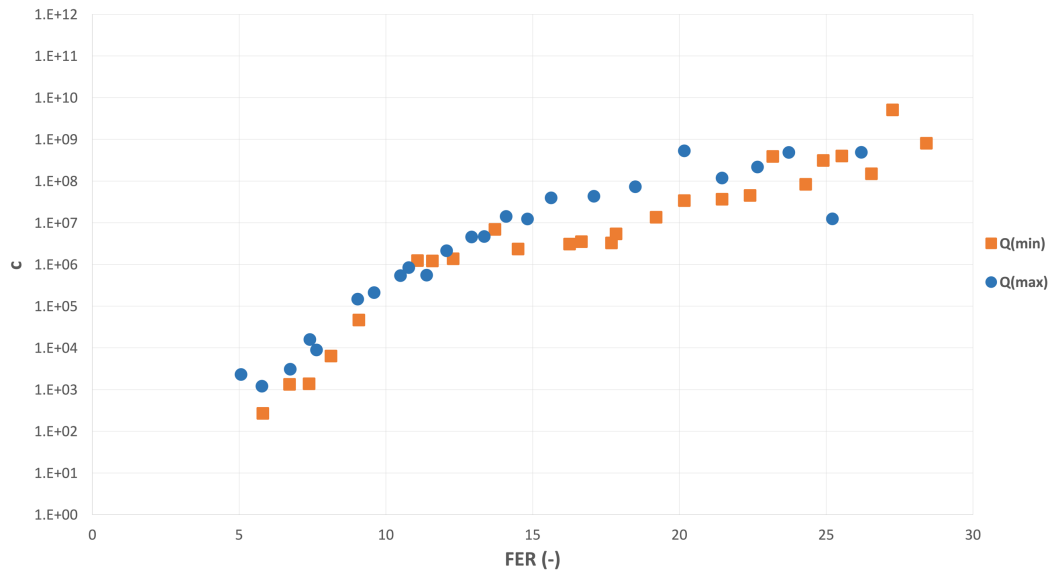


Figure 7_6: Asymmetric sigmoid parameter “c” vs. FER for different foam generator flow rates

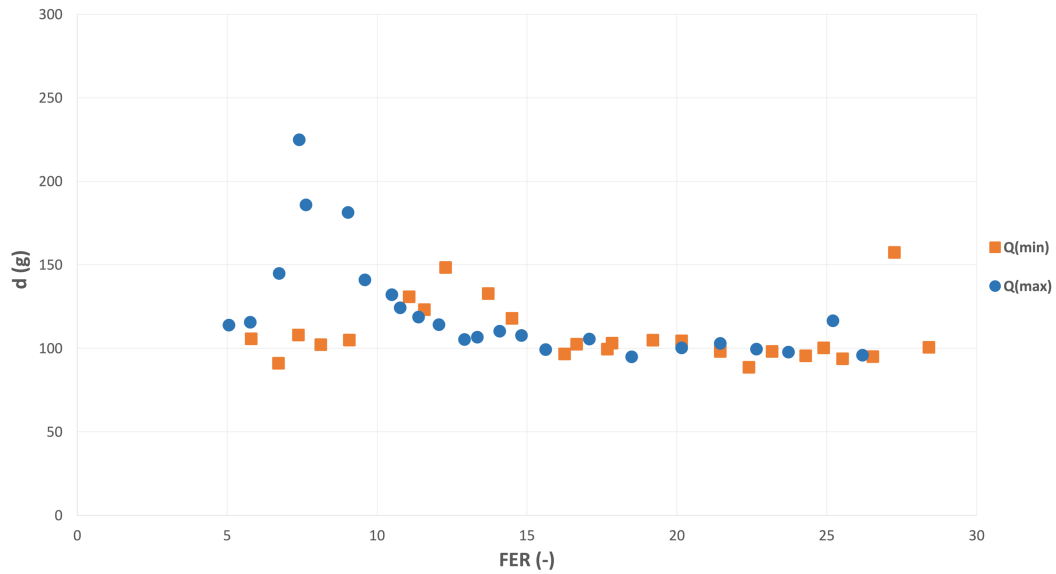


Figure 7_7: Asymmetric sigmoid parameter “d” vs. FER for different foam generator flow rates

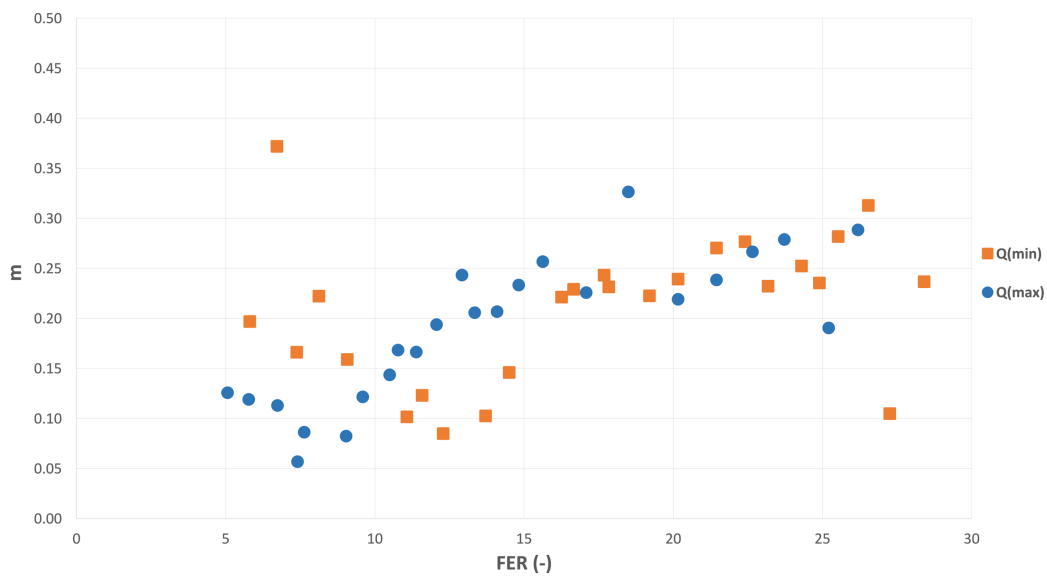


Figure 7_8: Asymmetric sigmoid parameter “m” vs. FER for different foam generator flow rates

In Figure 7_9, the representation of asymmetric sigmoid parameters “a” and “d” is presented. Notably, parameter “a” denotes the height of left asymmetric sigmoid parameter, and parameter “d” signifies the height of right asymmetric sigmoid parameter. Across all conducted tests, parameter “a” exhibited variations ranging from 0 and 0.37 for the minimum foam generator flow rate (Q_{\min}), and from 0 to 0.35 for the maximum foam generator flow rate (Q_{\max}). Although these variations were low and negligible, calibration was performed on this parameter,

and it reached nearly zero for the majority of cases. Nonetheless, in a few remaining instances, small deviations may be attributed to numerical issues.

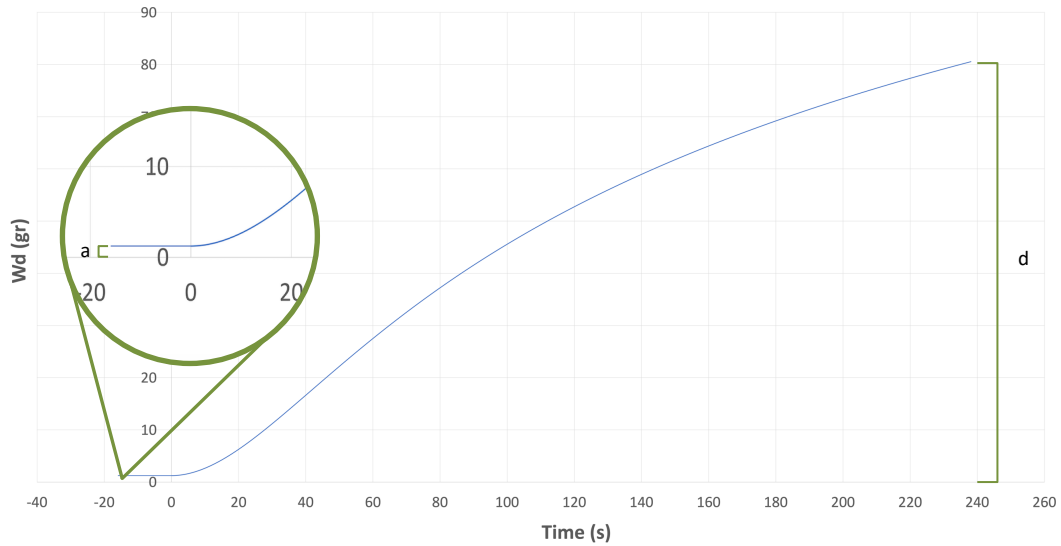


Figure 7_9: Representation of asymmetric sigmoid parameter “a” and “d”

Continuously, the result of the value of half-life time, as defined by EFNARC (EFNARC, 2005) standard, is presented in Figure 7_10. Accordingly, as previously stated, the correlation between Foam Expansion Ratio (FER) is verified and further relation with the foam generator flow rates can be investigated.

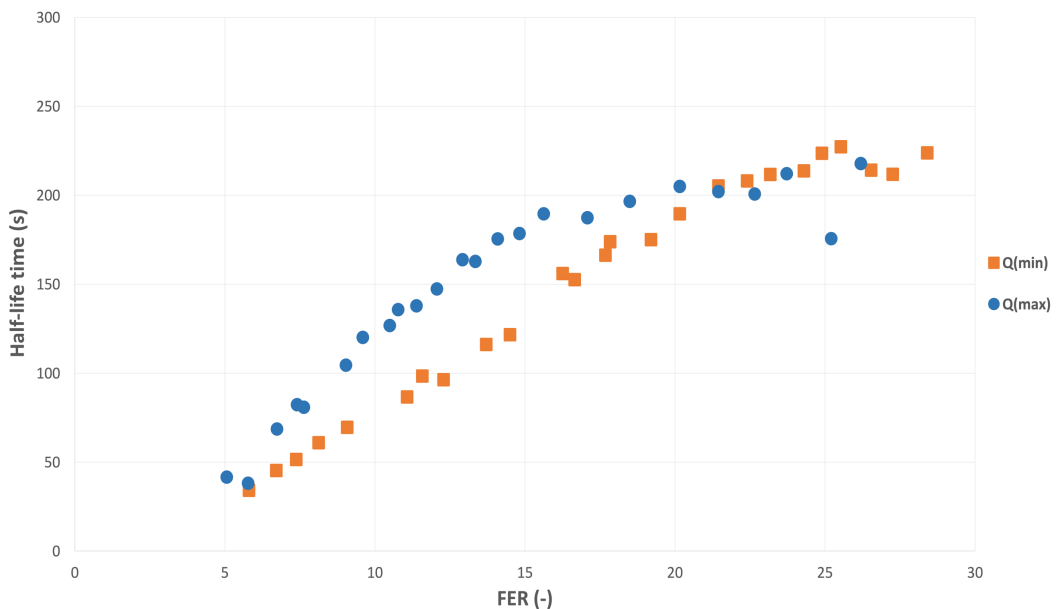


Figure 7_10: Half-life time vs. FER for different foam generator flow rates

Thus, it is evident that the foam generated with high foam generator flow rate (Q_{max}) appears to be more stable than the foam generated with low foam generator flow rate (Q_{min}). This difference is particularly pronounced within the Foam Expansion Ratio (FER) range of 8 to 20. However, beyond the FER of 20, the influence of foam generator flow rate diminishes, and the half-life times of the generated foams converge to nearly identical values. This phenomenon can be attributed to the fact that as the foam generator flow rate increases, smaller bubbles are generated. According to Wu et al. (2018), when foam bubbles are smaller exhibit greater uniformity, resulting in a notably slower growth in bubble size over time. Regarding the foam degradation mechanisms, foam bubbles with uniform sizes are more stable due to less gas diffusion between bubbles. Another plausible explanation is that smaller bubbles require more time for liquid drainage due to their increased surface area, resulting in longer liquid drainage travel pathways within smaller bubbles (Wu et al., 2018; Mooney et al., 2018).

In conclusion, the stability of foam-conditioned soil is of significant importance, representing the sustained persistence of desired engineering properties. Within the context of EPB-TBM tunneling, foam must maintain its desired engineering properties across various stages, starting from its injection at the cutterhead, continuing through the mixing process within the excavation chamber, and proceeding through its transport through the screw conveyor to the belt conveyor (Wu et al., 2020). Therefore, the outcome of half-life test campaigns directly aligns with the core objective of this research, which is to compare how different foam generation methods influence the time-dependency of mechanical properties of the conditioned soil.

7.2 Preliminary test campaigns

To comprehensively investigate the influence of foam generator flow rate on soil conditioning with foam, preliminary test campaigns were performed, utilizing the same and distinct foam generator flow rates with a consistent foaming agent concentration. The primary objective was to examine potential variations in the outcomes of the particular tests such as slump test, density test, and vane shear test, by following the step-by-step procedure detailed in Tables 6_2, 6_3, and 6_4, respectively. Consequently, Figures 7_11, 7_12, and 7_13 provide the outcomes of abovementioned tests.

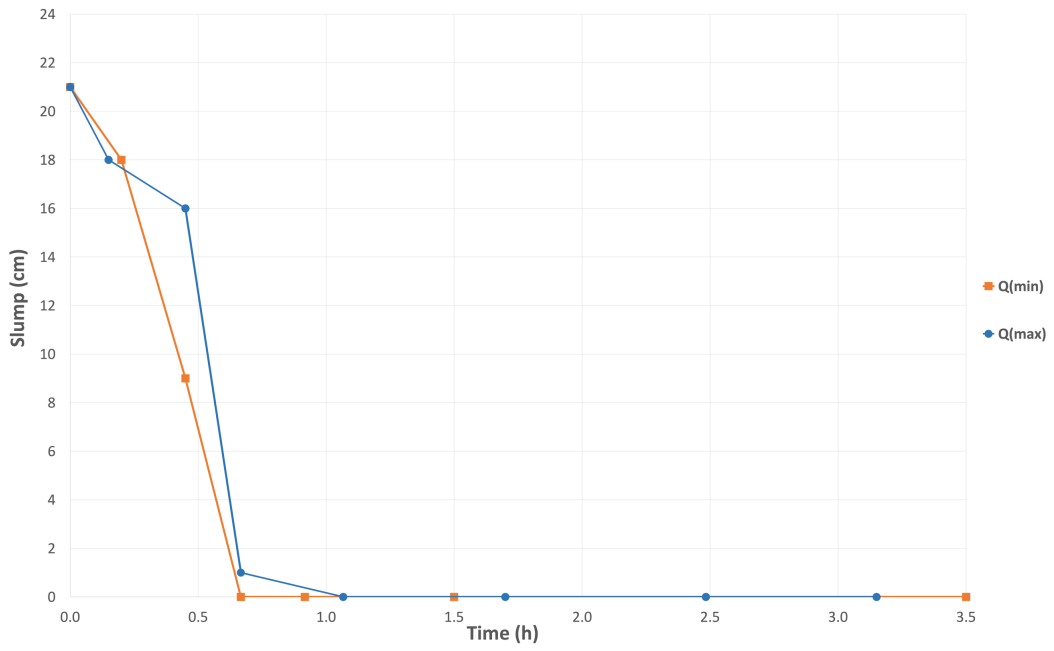


Figure 7_11: Preliminary test campaigns results – Slump tests

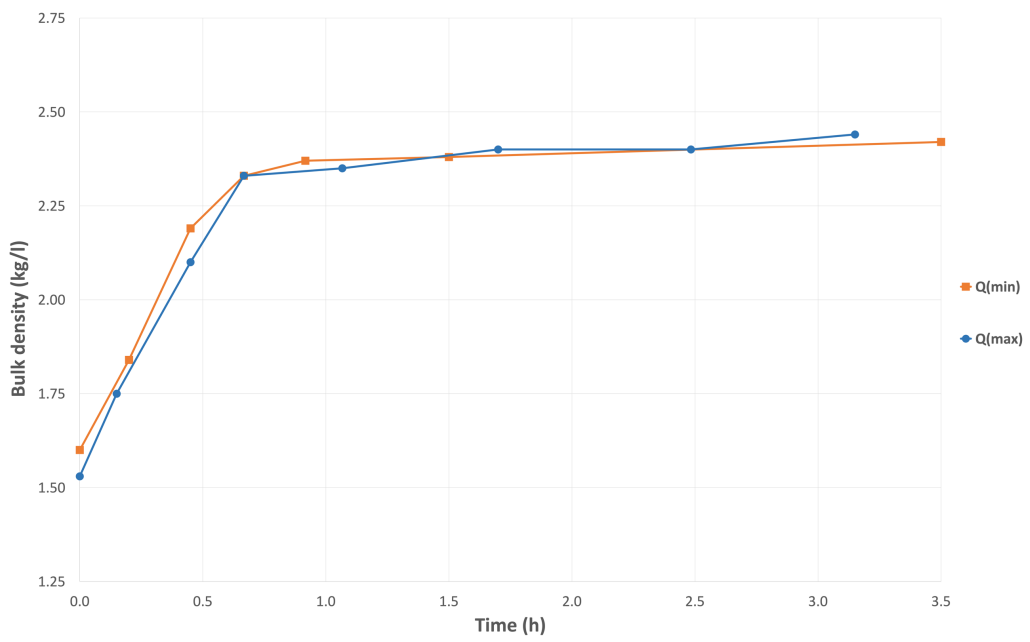


Figure 7_12: Preliminary test campaigns results – Density tests

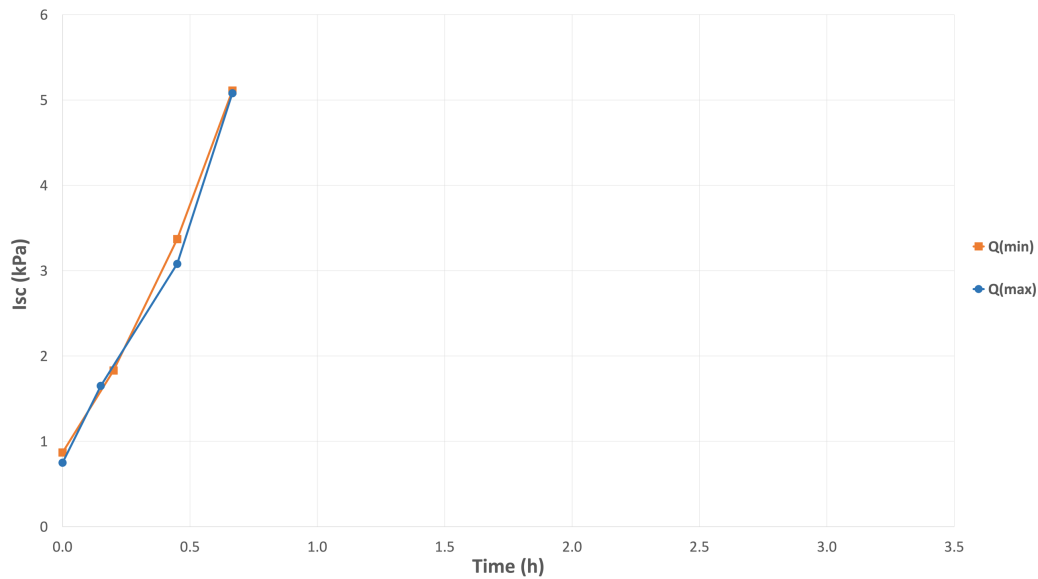


Figure 7_13: Preliminary test campaigns results – Vane shear tests

With the primary purpose on the study being the examination various foam generation methods and their influence on the time-dependent mechanical properties of conditioned soil, two kinds of foam were generated using the same conditioning set parameters but with different foam generator flow rates. Consequently, it can be observed that some differences exist in the preliminary test results. The variations are more evident within the first half-hour after initiating the test campaigns before reaching the results start to converge. Additionally, the test outcomes highlight more pronounced differences in the workability of the conditioned soil when subjected to two distinct generated foam.

7.3 Main test campaigns

The observed variation in the outcome of conducted tests, prompted the arrangement and implementation of a comprehensive test campaigns, to further investigate the influence of different foam generation methods. The following test campaigns, as it can be found in Table 6_1, are in total 17 distinct main test campaigns with a consistent foaming agent concentration (c_f), two distinct FER values, covering a range of FIR values between 20% to 50%, with systematically changing the values of foam generator flow rates between two different maximum and minimum values, as outlined in detail in Chapter 6.1.

Additionally, to establish the reference line, a dedicated test campaign was carried out under water-only condition, using a FIR value of 0%. During this test campaign, no foam was introduced to the soil sample, and the desired water content was achieved solely through the addition of water. This reference line is visually represented on the resulting figures, denoted by green dash-dot-dot line. Hence, the outcomes of the performed tests are illustrated in Figures 7_14, 7_15, and 7_16.

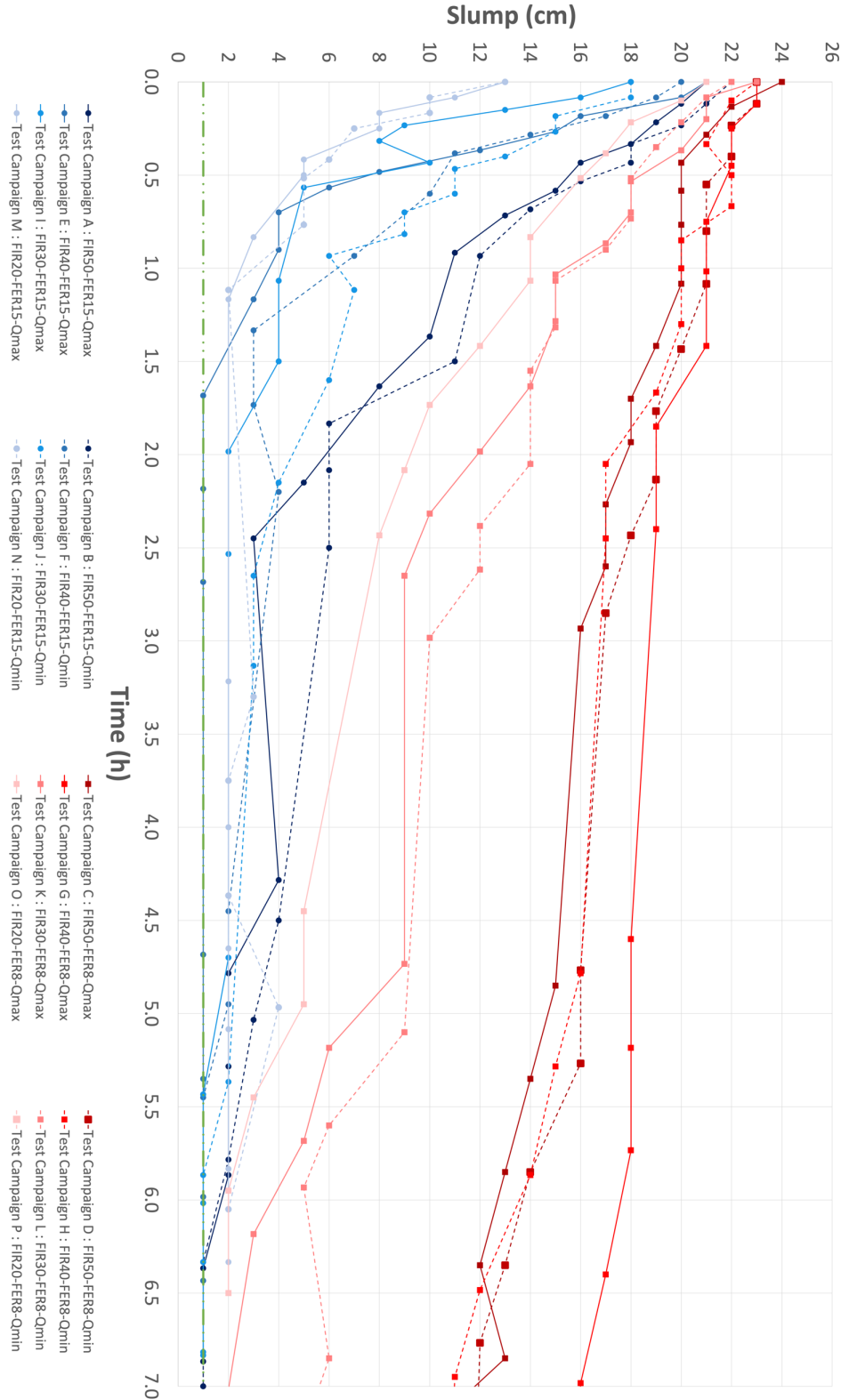


Figure 7_14: Slump test results for all test campaigns

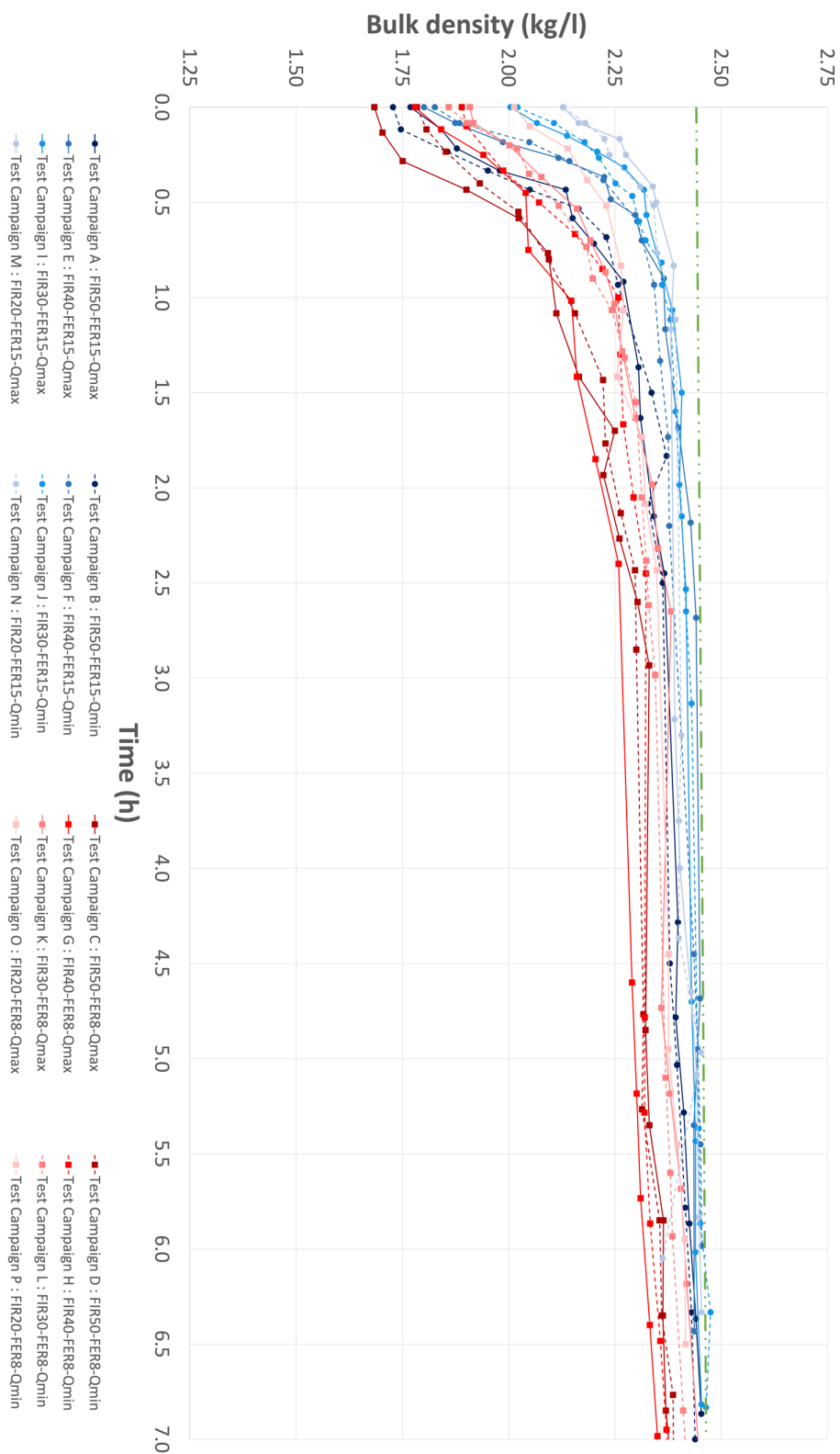


Figure 7_15: Density test results for all test campaigns

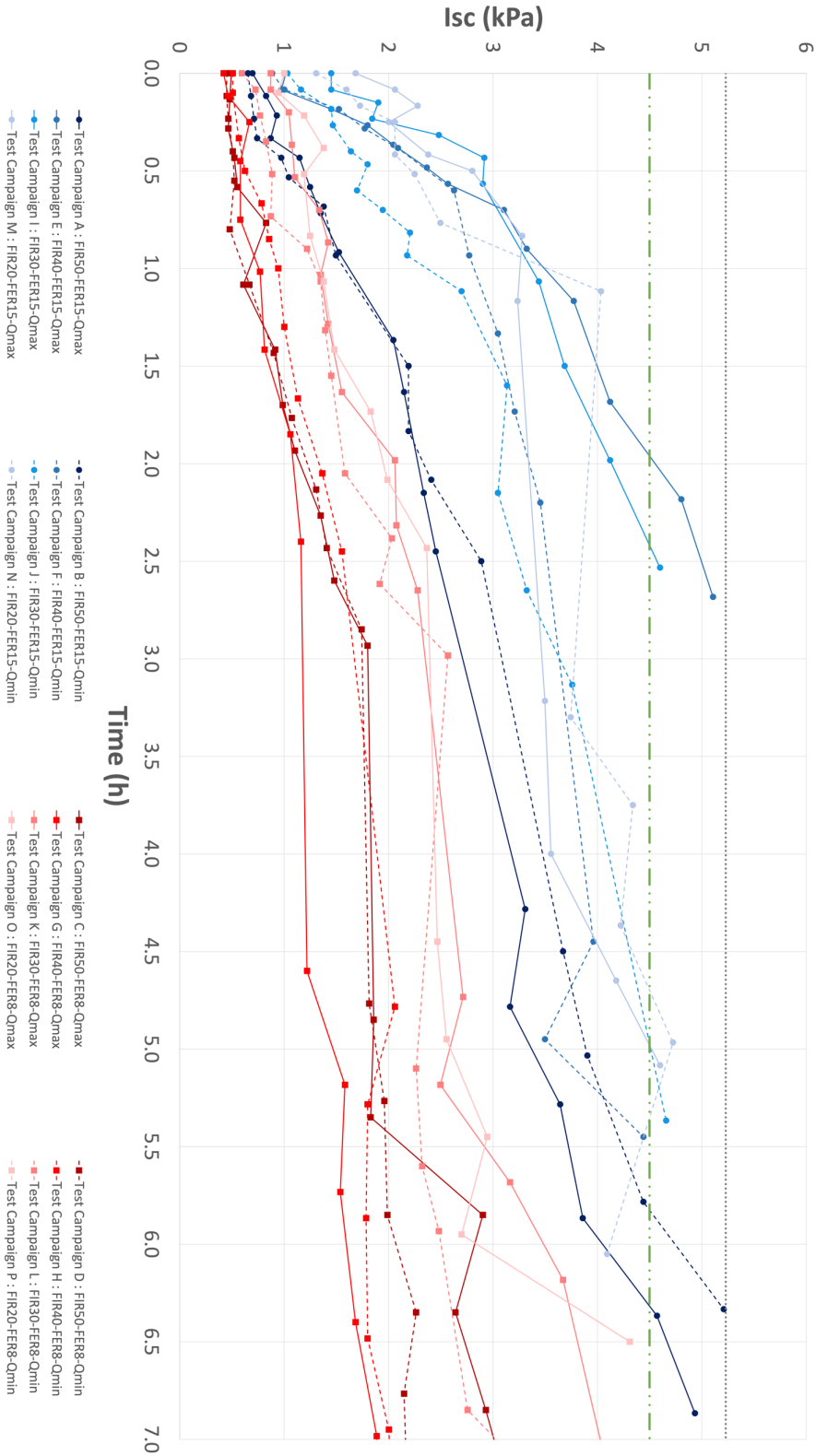


Figure 7_16: Vane shear test results for all test campaigns

On the basis of the slump test results from all test campaigns, considering Figure 7_14, following comments can be made:

- Regarding Foam Expansion Ratios, it is observed that the conditioned soil with a lower Foam Expansion Ratio (FER) exhibits higher stability in comparison with a higher Foam Expansion Ratio (FER). The distinction is clearly observable as FER 8 is indicated in red and FER 15 depicted in blue.
- With respect to foam generator flow rates, generally it is evident that for an identical Foam Expansion Ratio (FER), the conditioned soil with foam generated at minimum foam generator flow rate (Q_{min}), represented by dashed lines, demonstrates greater stability than the conditioned soil with foam generated at maximum foam generator flow rate (Q_{max}), depicted by solid lines.
- Comparing these findings with the results of half-life tests, where generated foam at higher foam generator flow rate (Q_{max}) exhibits greater stability, highlights a notable discrepancy between these two cases. These variations could be attributed to the complex characteristics of the interaction between soil and foam during preparation and execution of the slump tests.
- Furthermore, it is crucial to acknowledge that foam is not designed to exist in isolation, its primary purpose is within soil conditioning (Wu et al., 2020). Hence, making comparisons with the outcome of half-life tests may not be entirely representative of the situation encountered on the job site.
- Additionally, another potential reason could be related to the point underscored by Thewes et al. (2012). Although smaller bubble size leads to a longer drainage time and consequently enhanced foam stability, there is a critical lower limit for bubble dimensions. Beyond this limit, excessively small bubbles may potentially migrate through the pores, potentially affecting the stability of foam-conditioned soil.
- In reference to the results discussed, there is one exception that presents an anomaly, specifically within the pair of tests denoted as “Test Campaign G: FIR40-FER8- Q_{max} ” and “Test Campaign H: FIR40-FER8- Q_{min} ”. In these particular instances, the conditioned soil with foam using maximum foam generator flow rate (Q_{max}) is more stable than the counterpart with foam using minimum foam generator flow rate (Q_{min}). The reasons of this anomaly are not yet clear.

- With regards to Foam Injection Ratios, it is evident that as the Foam Injection Ratio (FIR) decreases, the stability of the conditioned soil also decreases. This trend is visually illustrated by color shading, with more saturated colors signifying higher percentage of Foam Injection Ratio (FIR) and lighter color representing lower percentage of Foam Injection Ratio (FIR).
- Considering the impact of foam, it can be noted that, foam is more stable when mixed with soil than by itself, indicating that soil particles play a role in stabilizing foam bubbles (Wu et al., 2020). However, for bubbles pressing against each other in the void space, bubble size tends to increase over time. The general mechanism of particles stabilizing foam is that soil particles create a steric barrier to bubble coalescence and coarsening (Wu et al., 2020), where the films between bubbles rupture and bubbles merge together to form larger bubbles (Schramm & Wassmuth, 1994). Continuously, bubbles become bigger and foam becomes less uniform in bubble size over time (Wu et al., 2018).

In accordance with the density test outcomes across all test campaigns, as depicted in Figure 7_15, the following comments can be drawn:

- Regarding Foam Expansion Ratios, it is evident that the conditioned soil with a lower Foam Expansion Ratio (FER) demonstrates lower bulk density when compared to a conditioned soil with a higher Foam Expansion Ratio (FER). The discrepancy is clearly visible through utilization of distinct colors, as FER 8 is denoted is red and FER 15 is represented in blue.
- With respect to foam generator flow rates, the observed differences are not significant, and no definitive conclusion can be drawn when comparing the conditioned soil with foam generated at the minimum foam generator flow rate (Q_{min}), represented by dashed lines, and the conditioned soil with foam generated at maximum foam generator flow rate (Q_{max}), depicted by solid lines.
- Concerning Foam Injection Ratios, it is evident that a reduction in the Foam Injection Ratio (FIR) correlates with an increase in the bulk density of the conditioned soil. This pattern is visually depicted through color shading, with more saturated colors signifying higher percentage of Foam Injection Ratio (FIR) and lighter color representing lower percentage of Foam Injection Ratio (FIR).

Considering the vane shear test results from all test campaigns, as illustrated in Figure 7_16, the following comments can be drawn:

- With respect to Foam Expansion Ratios, it is clear that the conditioned soil with a lower Foam Expansion Ratio (FER) exhibits lower shear strength when compared to a conditioned soil with a higher Foam Expansion Ratio (FER). The difference is visually apparent through the use of different colors, with FER 8 represented in red and FER 15 represented in blue.
- Concerning foam generator flow rates, the observed variations do not demonstrate a substantial correlation, and no conclusive conclusion can be reached when comparing the conditioned soil with foam generated at the minimum foam generator flow rate (Q_{min}), represented by dashed lines, and the conditioned soil with foam generated at maximum foam generator flow rate (Q_{max}), depicted by solid lines.
- Regarding Foam Injection Ratios, it is evident that a reduction in the Foam Injection Ratio (FIR) correlates with an increase in the vane shear of the conditioned soil. This pattern is visually depicted through color shading, with more saturated colors signifying higher percentage of Foam Injection Ratio (FIR) and lighter color representing lower percentage of Foam Injection Ratio (FIR).

7.4 Semi-quantitative analysis

All collected outcomes were subjected to a semi-quantitative analysis, with a specific emphasis on exploring potential correlations among the results linked to various foam generator flow rates, Foam Expansion Ratios (FER), and Foam Injection Ratios (FIR), as outlined in detail in Chapter 6.1. This analytical approach was utilized to transition from empirical observations to a semi-quantitative analysis, with the goal of achieving a deeper understanding of the relationships between foam characteristics and conditioned soil behavior.

7.4.1 Slump test

With respect to the semi-quantitative analysis outcomes for slump test, after identifying the best-fitting lines, graphs illustrating relationships between lines parameters versus Foam Injection Ratios (FIR) are provided. These illustrations encompass two values of Foam Expansion Ratios (FER) and two foam generator

flow rates values. Figure 7_17 and Figure 7_18 present the correlation of line parameters with respect to the *Set i*, while Figure 7_19 and Figure 7_20 provide the correlation of line parameters with regards to the *Set j*.

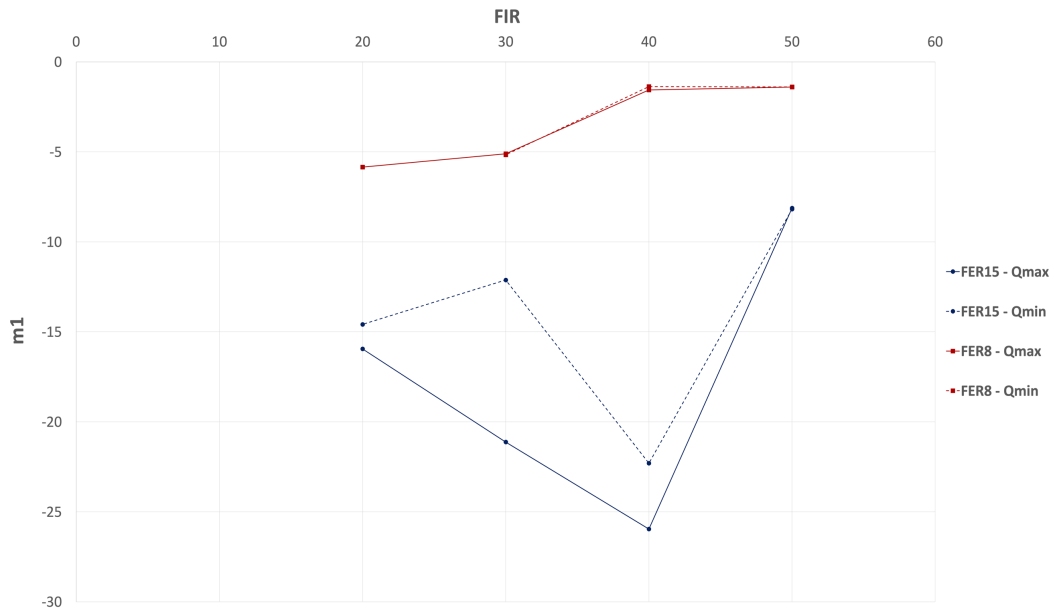


Figure 7_17: Optimal line parameter m_1 for slump test

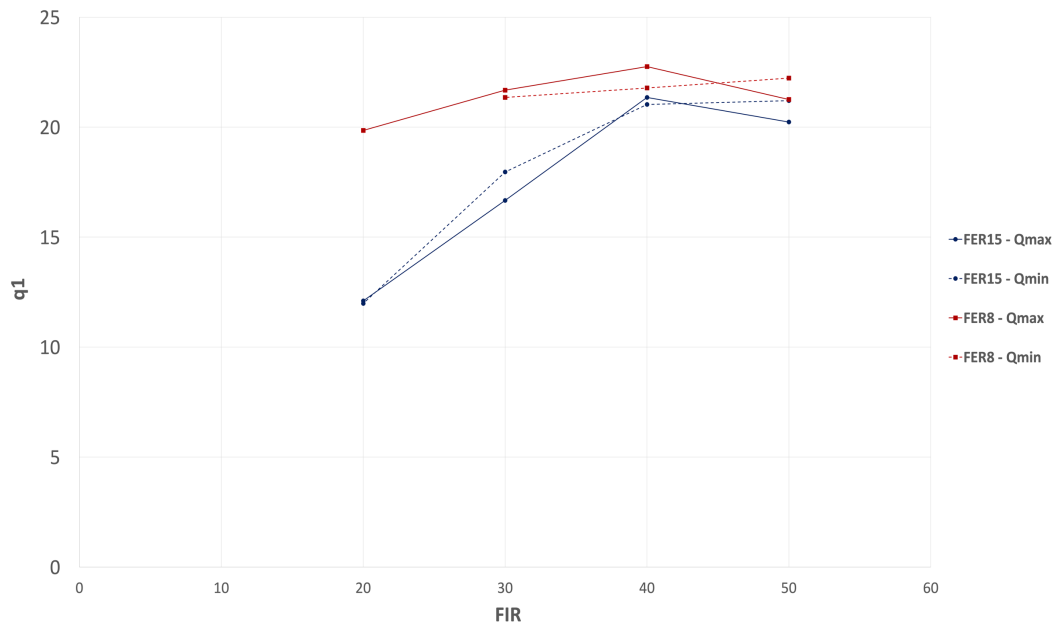


Figure 7_18: Optimal line parameter q_1 for slump test

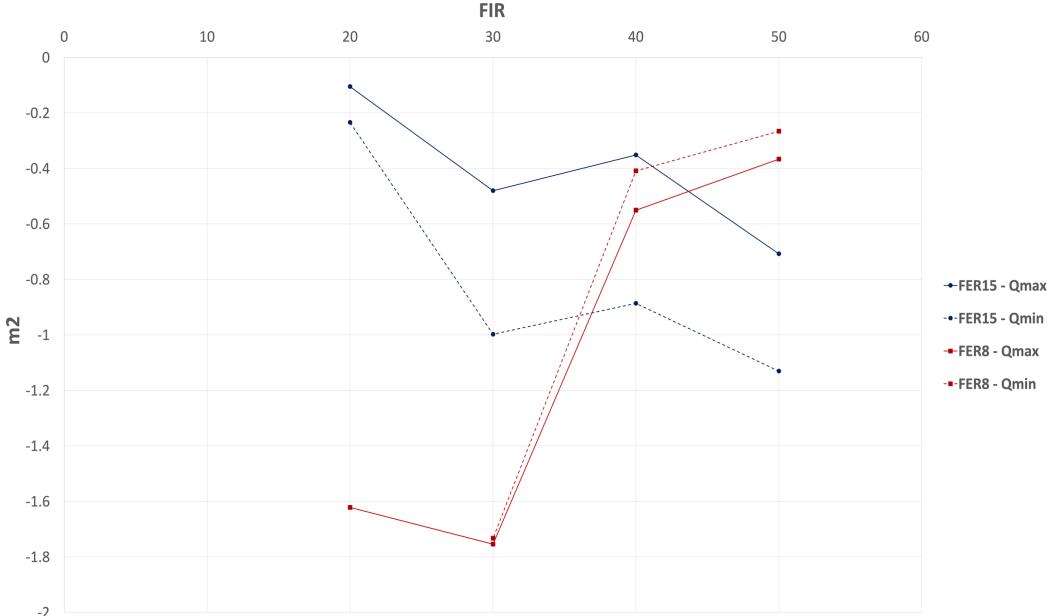


Figure 7_19: Optimal line parameter m_2 for slump tests

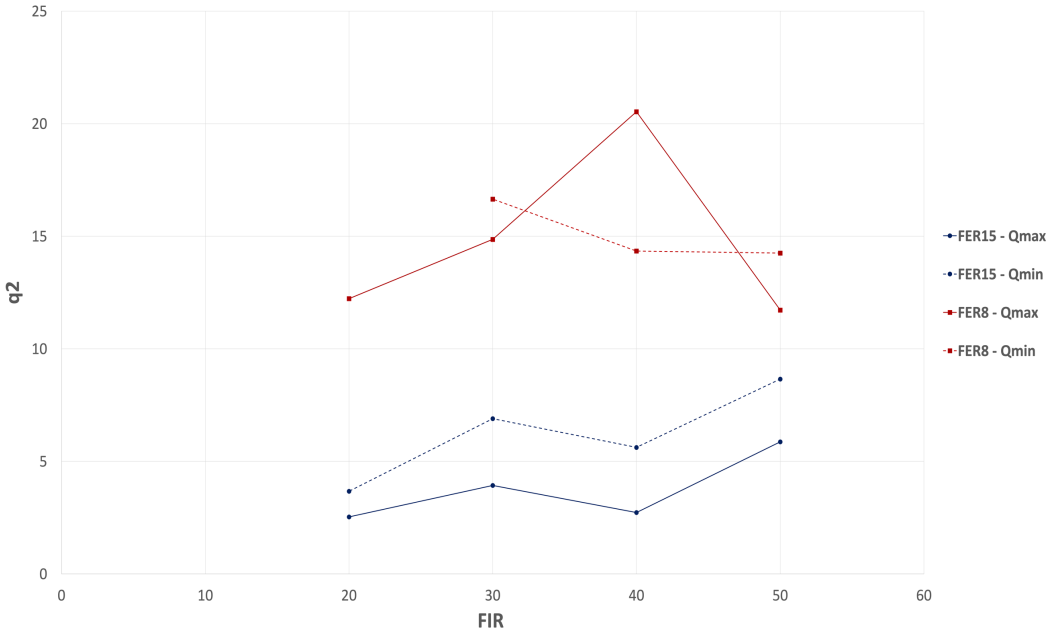


Figure 7_20: Optimal line parameter q_2 for slump tests

Based on the outcomes derived from the mathematical formulation for all test campaigns, the following comments can be noted:

- Regarding Figure 7_18, the trend of q_1 for distinct Foam Injection Ratios (FIR) and foam generator flow rates shows a regular increment of the intercept point with FIR. It means that the value of slump would be higher, mainly due to addition of higher amount of foam to the soil.
- With respect to Figures 7_19 and 7_20, the trends of m_2 and q_2 illustrate a more complex behaviors, which has more complex interpretation and may be affected by the uncertainties due to the already mentioned temporal gap in the tests.

7.4.2 Density test

With regards to the semi-quantitative analysis results for density test, having identified the best-fitting lines, graphs depicting correlations between lines parameters versus Foam Injection Ratios (FIR) are presented. These illustrations encompass two values of Foam Expansion Ratios (FER) and two foam generator flow rates values. Figure 7_21 and Figure 7_22 present the relationship of line parameters with respect to the *Set i*, whereas Figure 7_23 and Figure 7_24 provide the correlation of line parameters with regards to the *Set j*.

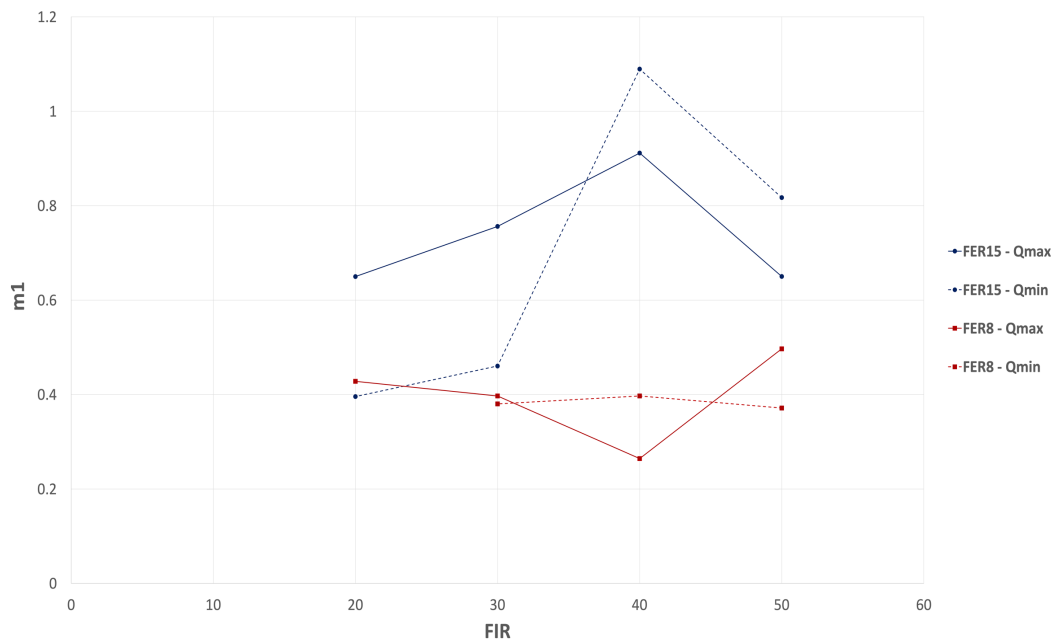


Figure 7_21: Optimal line parameter m_1 for density test

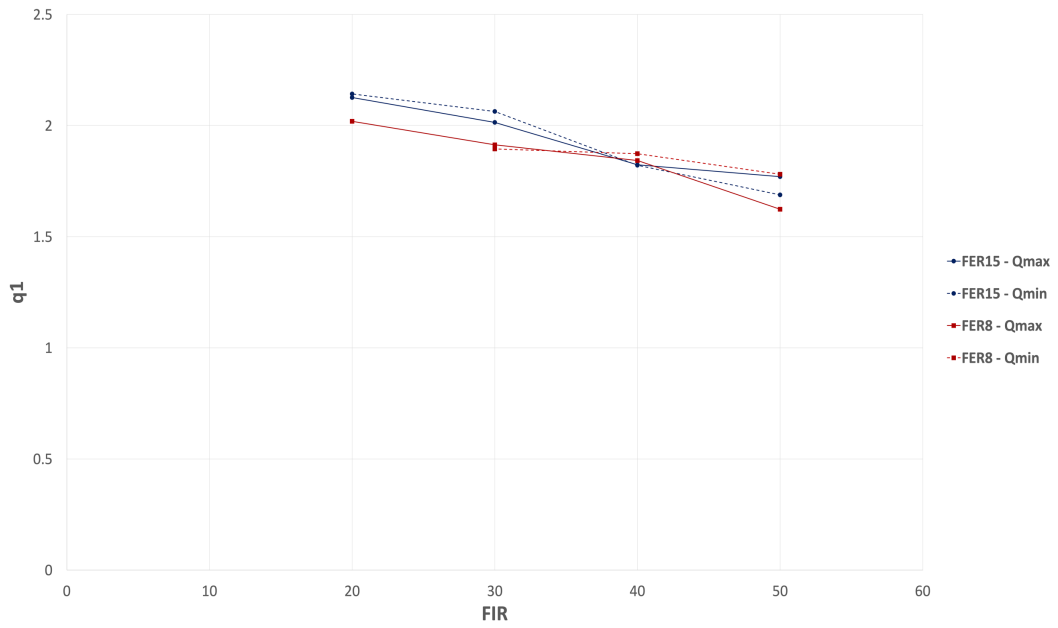


Figure 7_22: Optimal line parameter q_1 for density test

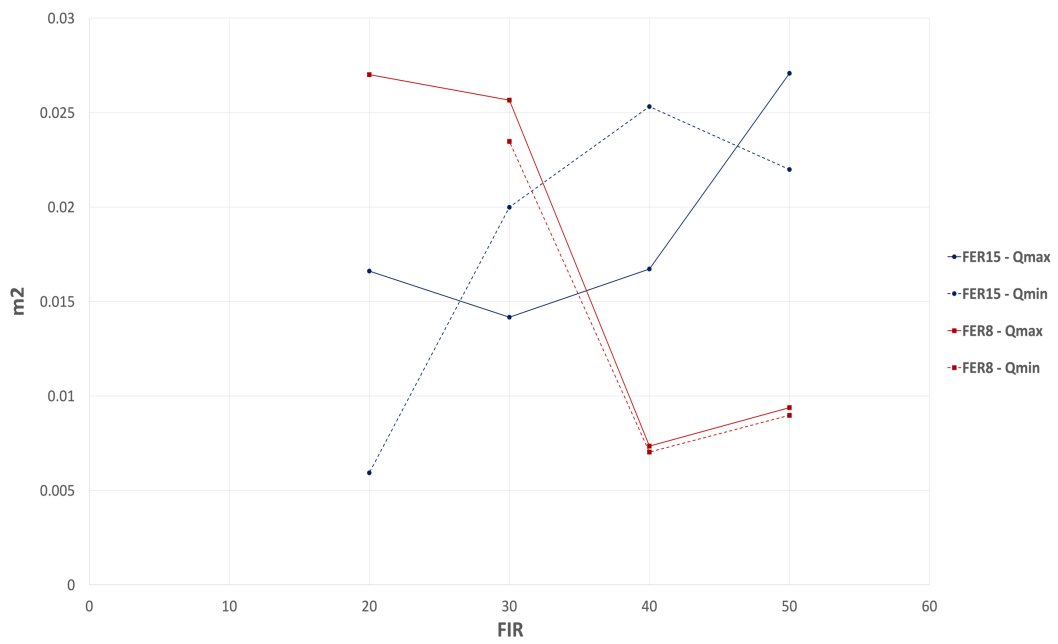


Figure 7_23: Optimal line parameter m_2 for density test

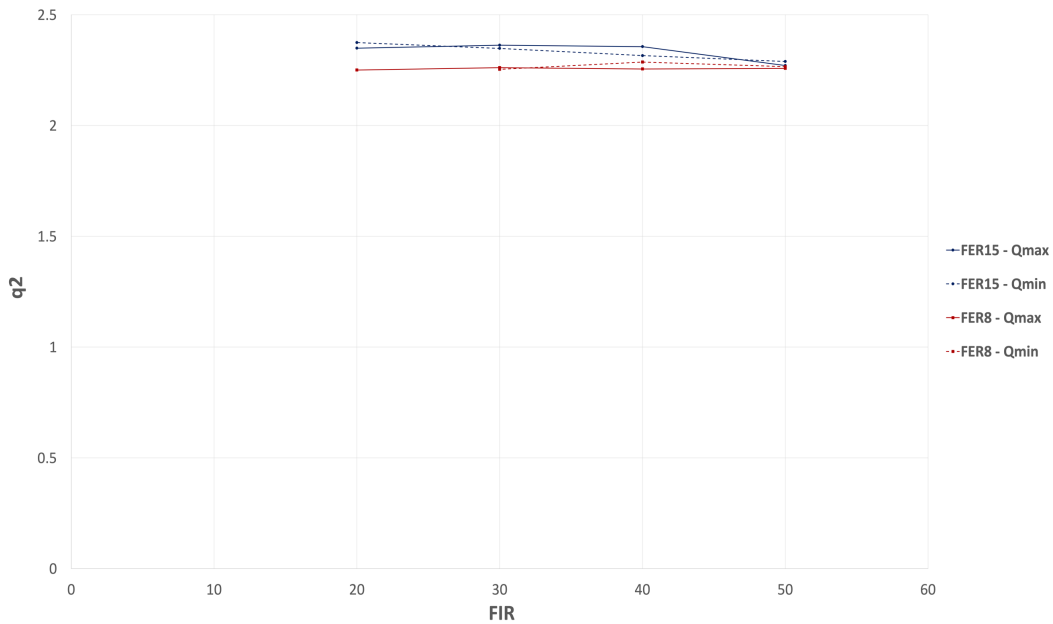


Figure 7_24: Optimal line parameter q_2 for density test

Considering the results obtained from the mathematical formulation across all test campaigns, the following remarks are noticeable:

- Regarding Figure 7_22, the trend of q_1 for various Foam Injection Ratios (FIR) and foam generator flow rates reveals an interesting pattern. It indicates that as the Foam Injection Ratio percentage increases, the intercept point decreases. This is mainly because the higher amount of foam is introduced to the soil, leading to reduced bulk density.
- With respect to Figures 7_23, the trend of m_2 shows a more complex behavior, which has more complex interpretation and may be affected by the uncertainties due to the already mentioned temporal gap in the tests.
- Conversely, in Figure 7_24, the similar scenario as mentioned in the first comment is observed for the behavior of q_2 , which exhibits an almost steady behavior despite variations in Foam Injection Ratios (FIR).

7.4.3 Vane Shear test

Regarding the outcomes of semi-quantitative analysis for vane shear test, once the optimal fitting lines are determined, graphs presenting correlations between

lines parameters versus Foam Injection Ratios (FIR) are provided. These illustrations encompass two values of Foam Expansion Ratios (FER) and two foam generator flow rates values. Figure 7_25 and Figure 7_26 present the relationship of line parameters with respect to the *Set i*, while Figure 7_27 and Figure 7_28 provides the correlation of line parameters with regards to the *Set j*.

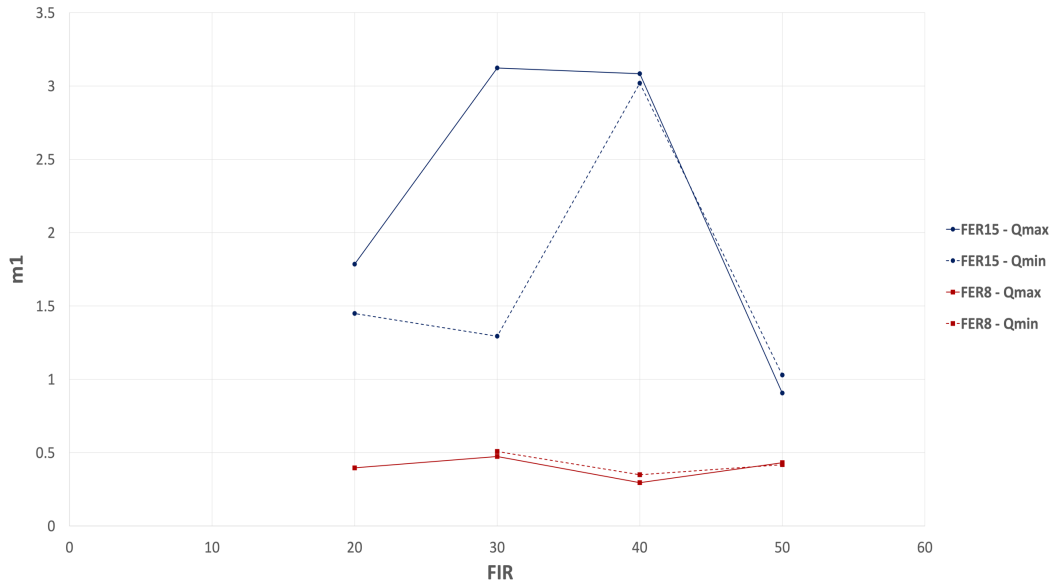


Figure 7_25: Optimal line parameter m_1 for vane shear test

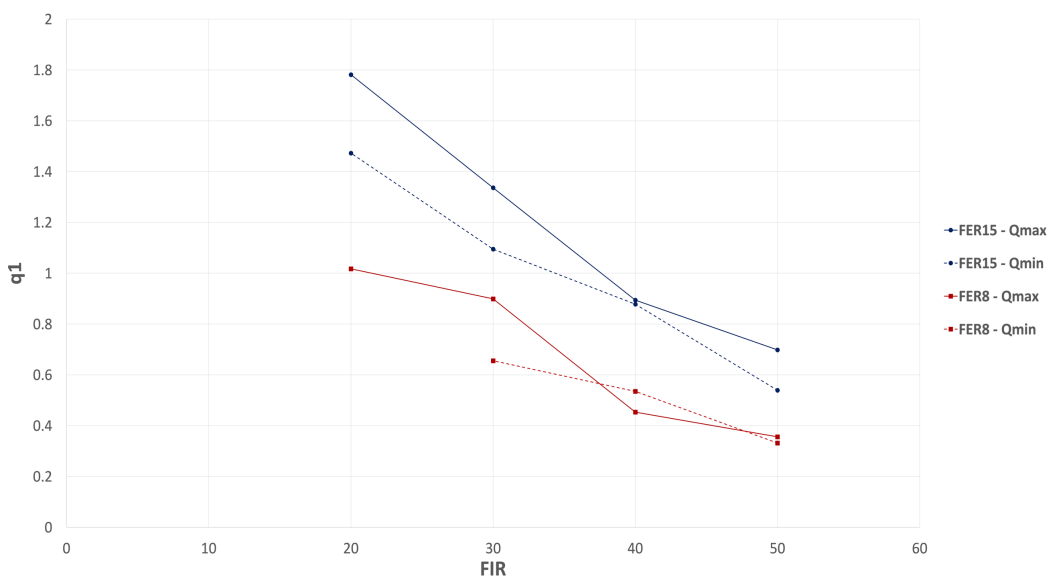


Figure 7_26: Optimal line parameter q_1 for vane shear test

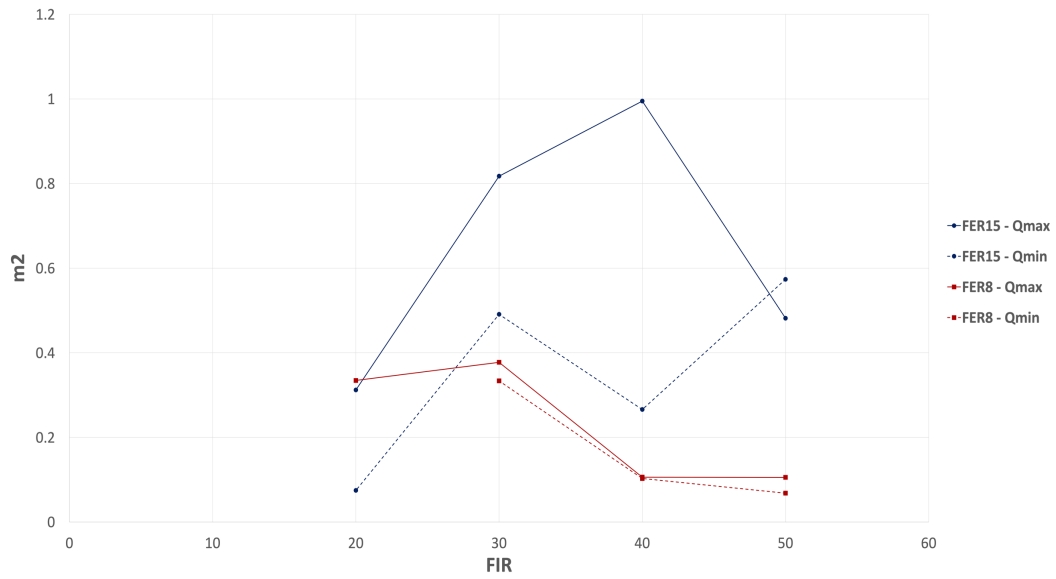


Figure 7_27: Optimal line parameter m_2 for vane shear test

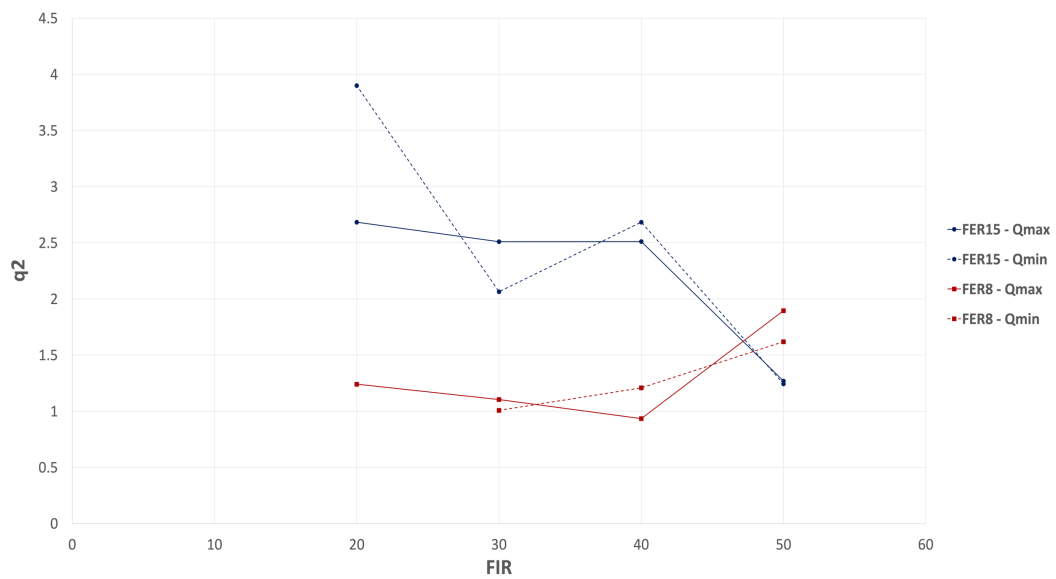


Figure 7_28: Optimal line parameter q_2 for vane shear test

From the findings generated through mathematical formulation for all test campaigns, the following conclusions can be drawn:

- With respect to Figure 7_26, the trend of q_1 for various Foam Injection Ratios (FIR) and foam generator flow rates shows an encouraging pattern. It suggests that as the Foam Injection Ratio percentage increases, the intercept point

significantly decreases. This occurs primarily because the increased foam content in the soil results in lower shear strength.

- Regarding Figures 7_27 and 7_28, the trends of m_2 and q_2 show a more complex behaviors, which has more complex interpretation and may be affected by the uncertainties due to the already mentioned temporal gap in the tests.

In conclusion, despite some promising results, the semi-quantitative analysis did not provide clear and understandable results and may need to be performed on a larger dataset to be effective.

Conclusions

Given the importance of optimization in conditioning set parameters for EPB-TBM technology, research to investigate the effect of various conditioning factors on the characteristics of conditioned soil was carried out. In particular, the study compared how different foam generator flow rates in foam generation influence the time-dependency of mechanical properties of the conditioned soil. A series of test campaigns were arranged. These test campaigns encompassed a wide range of conditioning set parameters and featured several specific tests, such as slump test, density test, and vane test. Ultimately, the results shown differences in the test outcomes, confirming that different foam generation method can have an effect on the properties of conditioned soil.

In particular, the research stems from the concept that the half-life of foams generated with different conditions may be different. Hence, some tests have been carried out and confirmed that in the investigated case foam generated at high foam generator flow rate (Q_{max}) has greater stability compared to foam generated at low foam generator flow rate (Q_{min}). This variation was particularly consistent up to Foam Expansion Ratio (FER) of 20.

The following tests conducted on conditioned soil shown variations in the mechanical properties of conditioned soil. Notably, these differences are more pronounced in the outcome of slump tests, while remaining relatively slight in terms of density and vane shear tests. Considering the influence of workability on soil conditioning assessment, it is remarkable that, under identical conditioning set parameters (water content, type of conditioning agent, concentration, FER, and FIR) but varying foam generator flow rates the results are different. Consequently, in the particular conditions investigated conditioned soil with foam generated at lower foam generator flow rate (Q_{min}) seems to have greater stability.

Additionally, a potential correlation between various conditioning set parameters through semi-quantitative analyses was searched for. However, these results do not provide definitive conclusions, necessitating further research for validation and verification.

In closing, this research underscores the need to include conditioning set parameters that were not previously considered in EPB-TBM conditioning assessment. Hence, future studies are recommended to further understand the effect of foam generator flow rate in foam generation on the behavior of conditioned soil.

Chapter 9










Annexes




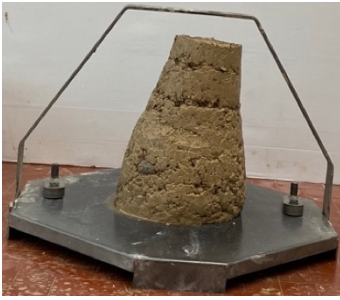


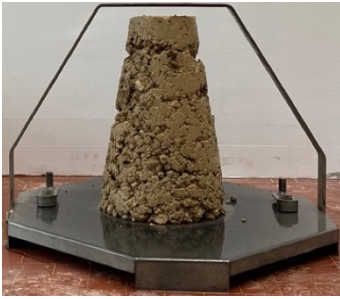
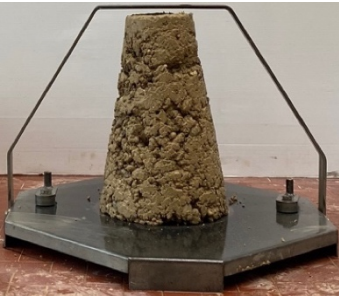
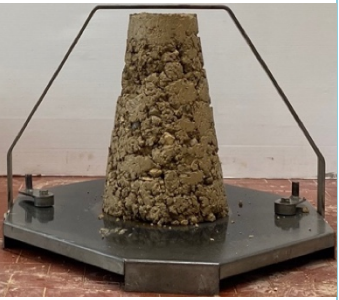
9.1 Test Campaign A

Table 9_1: Conditioning set parameters – Test campaign A

Conditioning Set Parameters		
Parameter	Value	Unit
Q	10	l/min
C_f	2.0	%
FIR	50	%
FER	15	-
w_{total}	9	%
$w_{natural}$	4	%
γ_s	1.912	kg/l
γ_{lg}	1	kg/l
W_s	20000	g
W_{dry}	19230.77	g
$W_{water\ added}$	961.54	g
W_{foam}	348.68	g
T_{water}	17.70	°C
T_{room}	26.80	°C
Humidity	70.80	%

Table 9_2: Slump test results – Test campaign A

Test Campaign A								
No.	Time (h)	Slump (cm)	No.	Time (h)	Slump (cm)	No.	Time (h)	Slump (cm)
1	0.00	21	2	0.12	20	3	0.22	19
								
No.	Time (h)	Slump (cm)	No.	Time (h)	Slump (cm)	No.	Time (h)	Slump (cm)
4	0.33	18	5	0.43	16	6	0.58	15
								
No.	Time (h)	Slump (cm)	No.	Time (h)	Slump (cm)	No.	Time (h)	Slump (cm)
7	0.72	13	8	0.92	11	9	1.37	10
								




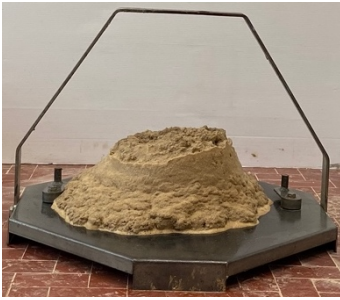





No.	Time (h)	Slump (cm)	No.	Time (h)	Slump (cm)	No.	Time (h)	Slump (cm)
10	1.63	8	11	2.15	5	12	2.45	3
								
No.	Time (h)	Slump (cm)	No.	Time (h)	Slump (cm)	No.	Time (h)	Slump (cm)
13	4.28	4	14	4.78	2	15	5.28	2
								
No.	Time (h)	Slump (cm)	No.	Time (h)	Slump (cm)	No.	Time (h)	Slump (cm)
16	5.87	2	17	6.37	1	18	6.87	1
								



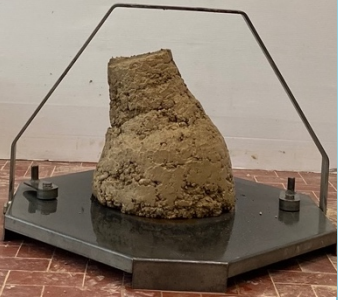





9.2 Test Campaign B

Table 9_3: Conditioning set parameters – Test campaign B

Conditioning Set Parameters		
Parameter	Value	Unit
Q	2.8	l/min
C_f	2.0	%
FIR	50	%
FER	15	-
w_{total}	9	%
$w_{natural}$	3.8	%
γ_s	1.912	kg/l
γ_{lg}	1	kg/l
W_s	20000	g
W_{dry}	19267.82	g
$W_{water\ added}$	1001.93	g
W_{foam}	348.68	g
T_{water}	19.00	$^{\circ}C$
T_{room}	29.10	$^{\circ}C$
Humidity	65	%

Table 9_4: Slump test results – Test campaign B

Test Campaign B								
No.	Time (h)	Slump (cm)	No.	Time (h)	Slump (cm)	No.	Time (h)	Slump (cm)
1	0.00	22	2	0.12	21	3	0.23	20
								
No.	Time (h)	Slump (cm)	No.	Time (h)	Slump (cm)	No.	Time (h)	Slump (cm)
4	0.33	18	5	0.43	18	6	0.53	16
								
No.	Time (h)	Slump (cm)	No.	Time (h)	Slump (cm)	No.	Time (h)	Slump (cm)
7	0.68	14	8	0.93	12	9	1.50	11
								





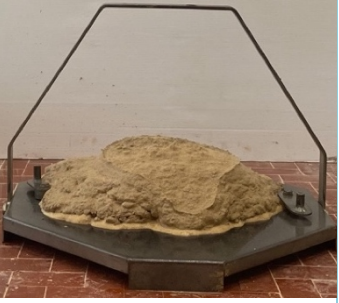

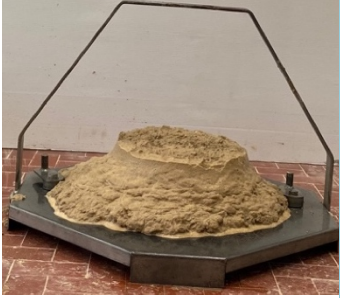


No.	Time (h)	Slump (cm)	No.	Time (h)	Slump (cm)	No.	Time (h)	Slump (cm)
10	1.83	6	11	2.08	6	12	2.50	6
								
No.	Time (h)	Slump (cm)	No.	Time (h)	Slump (cm)	No.	Time (h)	Slump (cm)
13	4.50	4	14	5.03	3	15	5.78	2
								
No.	Time (h)	Slump (cm)	No.	Time (h)	Slump (cm)			
16	6.33	1	17	7.00	1			
								



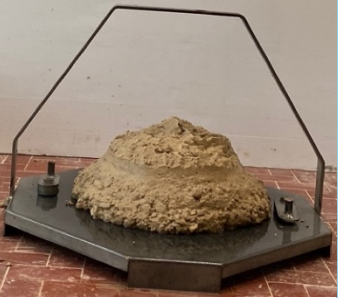
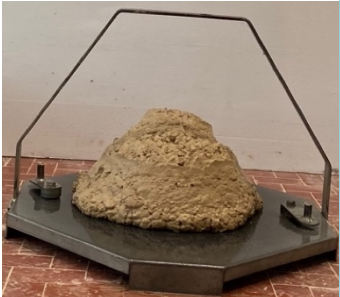
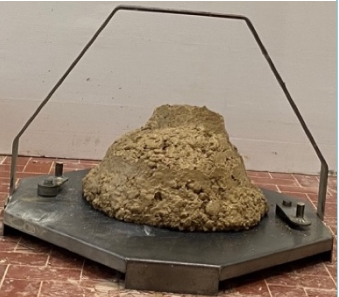




9.3 Test Campaign C

Table 9_5: Conditioning set parameters – Test campaign C


Conditioning Set Parameters		
Parameter	Value	Unit
Q	10	l/min
C_f	2.0	%
FIR	50	%
FER	8	-
W_{total}	9	%
$W_{natural}$	4.3	%
γ_s	1.912	kg/l
γ_{lg}	1	kg/l
W_s	20000	g
W_{dry}	19175.46	g
$W_{water\ added}$	901.25	g
W_{foam}	653.77	g
T_{water}	19.80	$^{\circ}C$
T_{room}	26.30	$^{\circ}C$
Humidity	71.10	%

Table 9_6: Slump test results – Test campaign C


Test Campaign C								
No.	Time (h)	Slump (cm)	No.	Time (h)	Slump (cm)	No.	Time (h)	Slump (cm)
1	0.00	24	2	0.13	22	3	0.28	21
								
No.	Time (h)	Slump (cm)	No.	Time (h)	Slump (cm)	No.	Time (h)	Slump (cm)
4	0.43	20	5	0.58	20	6	0.77	20
								
No.	Time (h)	Slump (cm)	No.	Time (h)	Slump (cm)	No.	Time (h)	Slump (cm)
7	1.08	20	8	1.42	19	9	1.70	18
								

No.	Time (h)	Slump (cm)	No.	Time (h)	Slump (cm)	No.	Time (h)	Slump (cm)
10	1.93	18	11	2.27	17	12	2.60	17
								
No.	Time (h)	Slump (cm)	No.	Time (h)	Slump (cm)	No.	Time (h)	Slump (cm)
13	2.93	16	14	4.85	15	15	5.35	14
								
No.	Time (h)	Slump (cm)	No.	Time (h)	Slump (cm)	No.	Time (h)	Slump (cm)
16	5.85	13	17	6.35	12	18	6.85	13
								

No.	Time (h)	Slump (cm)	No.	Time (h)	Slump (cm)	No.	Time (h)	Slump (cm)
19	7.35	9	20	24.02	3	21	29.02	1



No.	Time (h)	Slump (cm)
22	30.85	failed


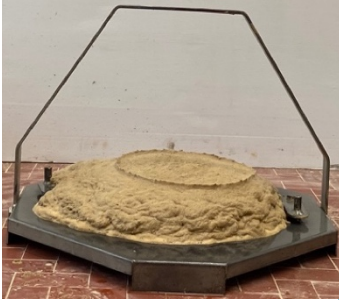
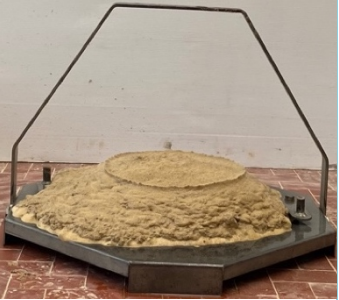

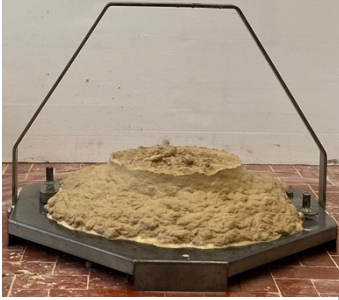
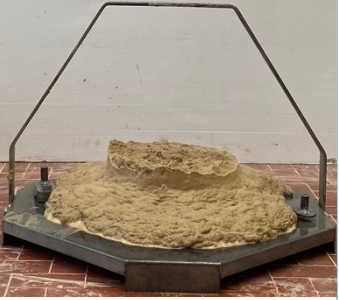
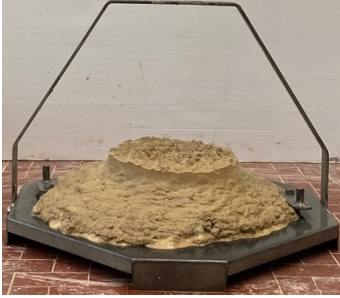
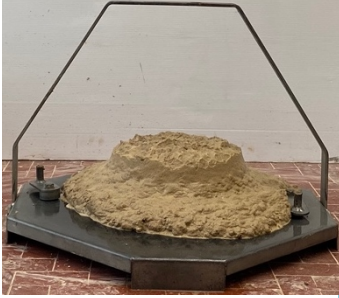






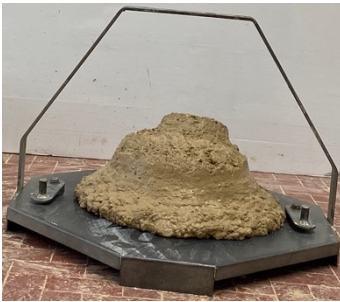


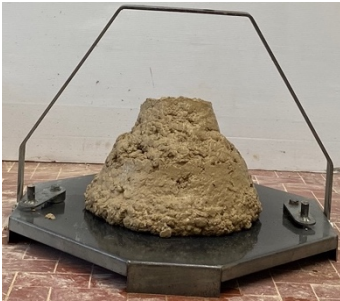


9.4 Test Campaign D

Table 9_7: Conditioning set parameters – Test campaign D

Conditioning Set Parameters		
Parameter	Value	Unit
Q	2.8	l/min
C_f	2.0	%
FIR	50	%
FER	8	-
w_{total}	9	%
$w_{natural}$	3.8	%
γ_s	1.912	kg/l
γ_{lg}	1	kg/l
W_s	20000	g
W_{dry}	19267.82	g
$W_{water\ added}$	1001.93	g
W_{foam}	653.77	g
T_{water}	20.10	$^{\circ}C$
T_{room}	26.80	$^{\circ}C$
Humidity	68.00	%

Table 9_8: Slump test results – Test campaign D

Test Campaign D								
No.	Time (h)	Slump (cm)	No.	Time (h)	Slump (cm)	No.	Time (h)	Slump (cm)
1	0.00	23	2	0.12	23	3	0.23	22
								
No.	Time (h)	Slump (cm)	No.	Time (h)	Slump (cm)	No.	Time (h)	Slump (cm)
4	0.40	22	5	0.55	21	6	0.80	21
								
No.	Time (h)	Slump (cm)	No.	Time (h)	Slump (cm)	No.	Time (h)	Slump (cm)
7	1.08	21	8	1.43	20	9	1.77	19
								

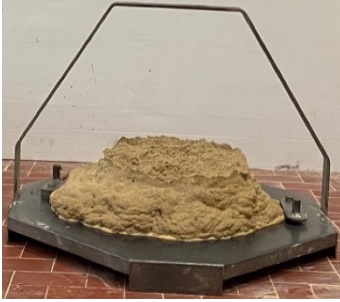


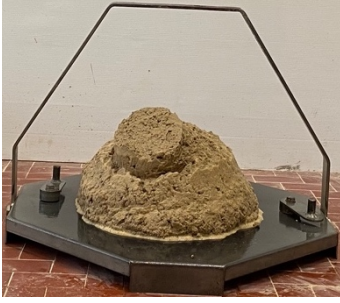




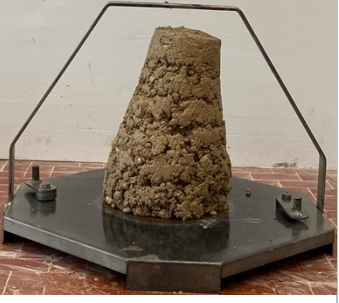
No.	Time (h)	Slump (cm)	No.	Time (h)	Slump (cm)	No.	Time (h)	Slump (cm)
10	2.13	19	11	2.43	18	12	2.85	17
								
No.	Time (h)	Slump (cm)	No.	Time (h)	Slump (cm)	No.	Time (h)	Slump (cm)
13	4.77	16	14	5.27	16	15	5.85	14
								
No.	Time (h)	Slump (cm)	No.	Time (h)	Slump (cm)	No.	Time (h)	Slump (cm)
16	6.35	13	17	6.77	12	18	23.52	8
								

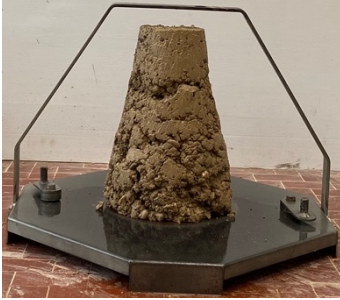




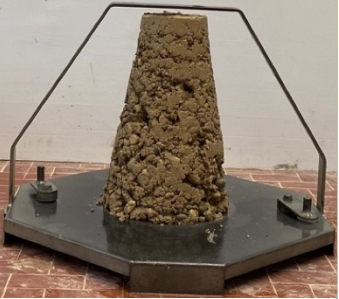

9.5 Test Campaign E

Table 9_9: Conditioning set parameters – Test campaign E

Conditioning Set Parameters		
Parameter	Value	Unit
Q	10	l/min
C_f	2.0	%
FIR	40	%
FER	15	-
w_{total}	9	%
$w_{natural}$	3.9	%
γ_s	1.912	kg/l
γ_{lg}	1	kg/l
W_s	20000	g
W_{dry}	19249.28	g
$W_{water\ added}$	981.71	g
W_{foam}	278.94	g
T_{water}	19.40	$^{\circ}C$
T_{room}	29.90	$^{\circ}C$
Humidity	62.40	%

Table 9_10: Slump test results – Test campaign E

Test Campaign E								
No.	Time (h)	Slump (cm)	No.	Time (h)	Slump (cm)	No.	Time (h)	Slump (cm)
1	0.00	21	2	0.08	20	3	0.18	16
								
No.	Time (h)	Slump (cm)	No.	Time (h)	Slump (cm)	No.	Time (h)	Slump (cm)
4	0.27	15	5	0.37	12	6	0.48	8
								
No.	Time (h)	Slump (cm)	No.	Time (h)	Slump (cm)	No.	Time (h)	Slump (cm)
7	0.57	6	8	0.70	4	9	0.90	4
								






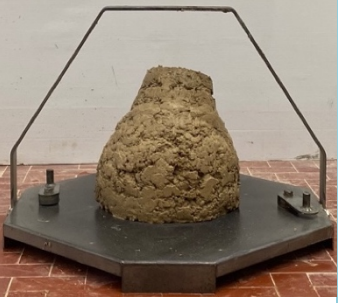

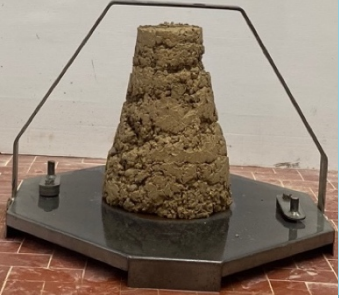

No.	Time (h)	Slump (cm)	No.	Time (h)	Slump (cm)	No.	Time (h)	Slump (cm)
10	1.17	3	11	1.68	1	12	2.18	1
								
No.	Time (h)	Slump (cm)	No.	Time (h)	Slump (cm)	No.	Time (h)	Slump (cm)
13	2.68	1	14	4.68	1	15	5.35	1
								
No.	Time (h)	Slump (cm)						
16	6.43	1						
								







9.6 Test Campaign F

Table 9_11: Conditioning set parameters – Test campaign F

Conditioning Set Parameters		
Parameter	Value	Unit
Q	2.8	l/min
C_f	2.0	%
FIR	40	%
FER	15	-
w_{total}	9	%
$w_{natural}$	4.1	%
γ_s	1.912	kg/l
γ_{lg}	1	kg/l
W_s	20000	g
W_{dry}	19212.30	g
$W_{water\ added}$	941.40	g
W_{foam}	278.94	g
T_{water}	19.00	°C
T_{room}	29.10	°C
Humidity	65.00	%

Table 9_12: Slump test results – Test campaign F

Test Campaign F								
No.	Time (h)	Slump (cm)	No.	Time (h)	Slump (cm)	No.	Time (h)	Slump (cm)
1	0.00	20	2	0.08	19	3	0.18	17
								
No.	Time (h)	Slump (cm)	No.	Time (h)	Slump (cm)	No.	Time (h)	Slump (cm)
4	0.28	14	5	0.38	11	6	0.60	10
								
No.	Time (h)	Slump (cm)	No.	Time (h)	Slump (cm)	No.	Time (h)	Slump (cm)
7	0.93	7	8	1.33	3	9	1.73	3
								








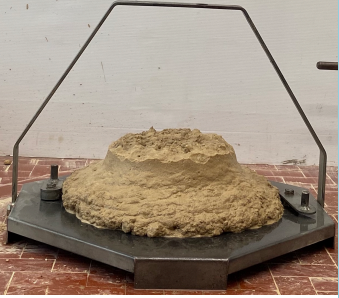

No.	Time (h)	Slump (cm)	No.	Time (h)	Slump (cm)	No.	Time (h)	Slump (cm)
10	2.20	4	11	4.45	2	12	4.95	2
								
No.	Time (h)	Slump (cm)	No.	Time (h)	Slump (cm)	No.	Time (h)	Slump (cm)
13	5.45	1	14	5.98	1	15	6.45	1
								





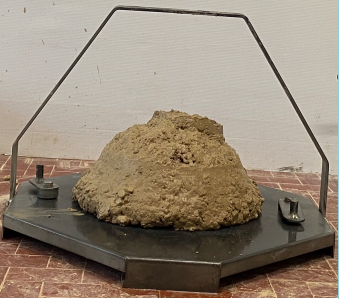




9.7 Test Campaign G

Table 9_13: Conditioning set parameters – Test campaign G

Conditioning Set Parameters		
Parameter	Value	Unit
Q	10	l/min
C_f	2.0	%
FIR	40	%
FER	8	-
w_{total}	9	%
$w_{natural}$	3.7	%
γ_s	1.912	kg/l
γ_{lg}	1	kg/l
W_s	20000	g
W_{dry}	19286.40	g
$W_{water\ added}$	1022.18	g
W_{foam}	523.01	g
T_{water}	19.00	$^{\circ}C$
T_{room}	28.80	$^{\circ}C$
Humidity	74.00	%

Table 9_14: Slump test results – Test campaign G

Test Campaign G								
No.	Time (h)	Slump (cm)	No.	Time (h)	Slump (cm)	No.	Time (h)	Slump (cm)
1	0.00	23	2	0.12	23	3	0.25	22
								
No.	Time (h)	Slump (cm)	No.	Time (h)	Slump (cm)	No.	Time (h)	Slump (cm)
4	0.45	22	5	0.75	21	6	1.02	21
								
No.	Time (h)	Slump (cm)	No.	Time (h)	Slump (cm)	No.	Time (h)	Slump (cm)
7	1.42	21	8	1.85	19	9	2.40	19
								



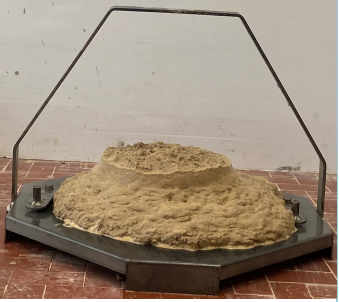






No.	Time (h)	Slump (cm)	No.	Time (h)	Slump (cm)	No.	Time (h)	Slump (cm)
10	4.60	18	11	5.18	18	12	5.73	18
								
No.	Time (h)	Slump (cm)	No.	Time (h)	Slump (cm)	No.	Time (h)	Slump (cm)
13	6.40	17	14	6.98	16	15	23.52	9
								
No.	Time (h)	Slump (cm)	No.	Time (h)	Slump (cm)	No.	Time (h)	Slump (cm)
16	25.40	7	17	29.82	4	18	31.25	2
								










9.8 Test Campaign H

Table 9_15: Conditioning set parameters – Test campaign H

Conditioning Set Parameters		
Parameter	Value	Unit
Q	2.8	l/min
C_f	2.0	%
FIR	40	%
FER	8	-
w_{total}	9	%
$w_{natural}$	4.3	%
γ_s	1.912	kg/l
γ_{lg}	1	kg/l
W_s	20000	g
W_{dry}	19175.46	g
$W_{water\ added}$	901.25	g
W_{foam}	523.01	g
T_{water}	18.60	°C
T_{room}	28.20	°C
Humidity	67.50	%

Table 9_16: Slump test results – Test campaign H

Test Campaign H								
No.	Time (h)	Slump (cm)	No.	Time (h)	Slump (cm)	No.	Time (h)	Slump (cm)
1	0.00	23	2	0.10	22	3	0.33	21
								
No.	Time (h)	Slump (cm)	No.	Time (h)	Slump (cm)	No.	Time (h)	Slump (cm)
4	0.50	22	5	0.67	22	6	0.85	20
								
No.	Time (h)	Slump (cm)	No.	Time (h)	Slump (cm)	No.	Time (h)	Slump (cm)
7	1.00	20	8	1.30	20	9	1.67	19
								

No.	Time (h)	Slump (cm)	No.	Time (h)	Slump (cm)	No.	Time (h)	Slump (cm)
10	2.05	17	11	2.45	17	12	4.78	16
								
No.	Time (h)	Slump (cm)	No.	Time (h)	Slump (cm)	No.	Time (h)	Slump (cm)
13	5.28	15	14	5.87	14	15	6.48	12
								
No.	Time (h)	Slump (cm)	No.	Time (h)	Slump (cm)	No.	Time (h)	Slump (cm)
16	6.95	11	17	23.20	6	18	25.72	3
								
No.	Time (h)	Slump (cm)						
19	29.83	2						


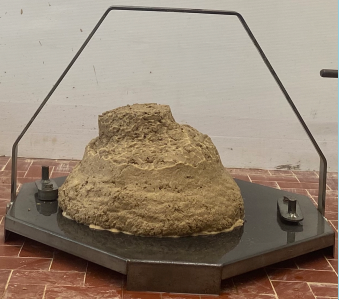
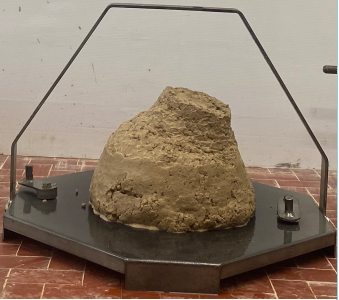


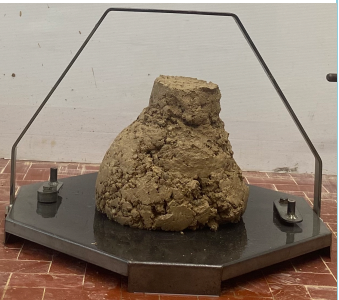





9.9 Test Campaign I


Table 9_17: Conditioning set parameters – Test campaign I

Conditioning Set Parameters		
Parameter	Value	Unit
Q	10	l/min
C_f	2.0	%
FIR	30	%
FER	15	-
W_{total}	9	%
$W_{natural}$	4.5	%
γ_s	1.912	kg/l
γ_{lg}	1	kg/l
W_s	20000	g
W_{dry}	19138.76	g
$W_{water\ added}$	861.24	g
W_{foam}	209.21	g
T_{water}	18.60	$^{\circ}C$
T_{room}	28.50	$^{\circ}C$
Humidity	77.50	%


Table 9_18: Slump test results – Test campaign I

Test Campaign I								
No.	Time (h)	Slump (cm)	No.	Time (h)	Slump (cm)	No.	Time (h)	Slump (cm)
1	0.00	18	2	0.08	16	3	0.15	13
								
No.	Time (h)	Slump (cm)	No.	Time (h)	Slump (cm)	No.	Time (h)	Slump (cm)
4	0.23	9	5	0.32	8	6	0.43	10
								
No.	Time (h)	Slump (cm)	No.	Time (h)	Slump (cm)	No.	Time (h)	Slump (cm)
7	0.57	5	8	1.07	4	9	1.50	4
								

No.	Time (h)	Slump (cm)	No.	Time (h)	Slump (cm)	No.	Time (h)	Slump (cm)
10	1.98	2	11	2.53	2	12	4.70	2



No.	Time (h)	Slump (cm)	No.	Time (h)	Slump (cm)	No.	Time (h)	Slump (cm)
13	5.43	1	14	6.02	1	15	6.82	1

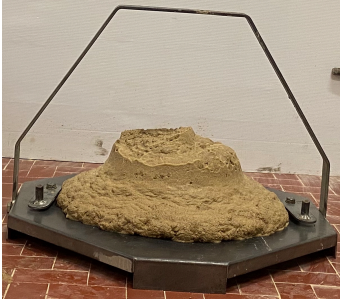
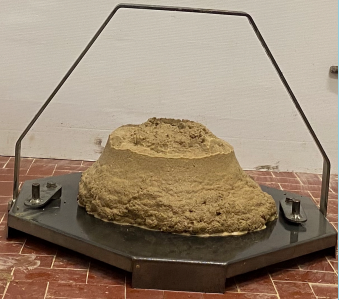
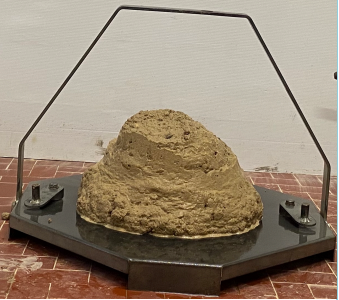












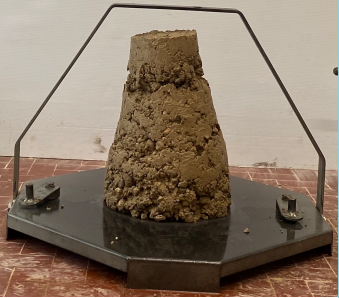




9.10 Test Campaign J

Table 9_19: Conditioning set parameters – Test campaign J

Conditioning Set Parameters		
Parameter	Value	Unit
Q	2.8	l/min
C_f	2.0	%
FIR	30	%
FER	15	-
w_{total}	9	%
$w_{natural}$	4	%
γ_s	1.912	kg/l
γ_{lg}	1	kg/l
W_s	20000	g
W_{dry}	19230.77	g
$W_{water\ added}$	961.54	g
W_{foam}	209.21	g
T_{water}	18.90	°C
T_{room}	27.20	°C
Humidity	74.70	%

Table 9_20: Slump test results – Test campaign J

Test Campaign J								
No.	Time (h)	Slump (cm)	No.	Time (h)	Slump (cm)	No.	Time (h)	Slump (cm)
1	0.00	18	2	0.08	18	3	0.18	15
								
No.	Time (h)	Slump (cm)	No.	Time (h)	Slump (cm)	No.	Time (h)	Slump (cm)
4	0.27	15	5	0.40	13	6	0.47	11
								
No.	Time (h)	Slump (cm)	No.	Time (h)	Slump (cm)	No.	Time (h)	Slump (cm)
7	0.60	11	8	0.70	9	9	0.82	9
								

No.	Time (h)	Slump (cm)	No.	Time (h)	Slump (cm)	No.	Time (h)	Slump (cm)
10	0.93	6	11	1.12	7	12	1.60	6
								
No.	Time (h)	Slump (cm)	No.	Time (h)	Slump (cm)	No.	Time (h)	Slump (cm)
13	2.15	4	14	2.65	3	15	3.13	3
								
No.	Time (h)	Slump (cm)	No.	Time (h)	Slump (cm)	No.	Time (h)	Slump (cm)
16	5.37	2	17	5.87	1	18	6.33	1
								
No.	Time (h)	Slump (cm)						
19	6.83	1						






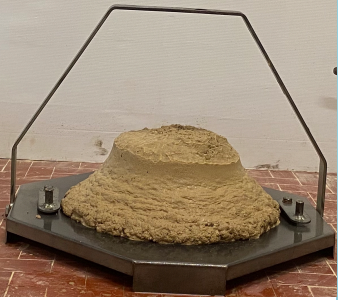
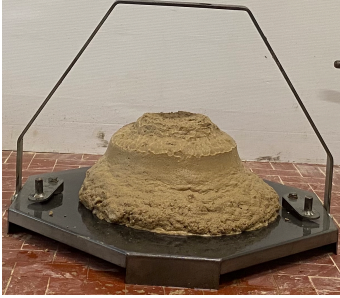
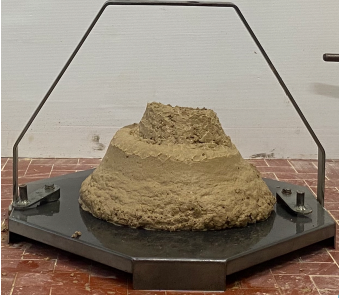



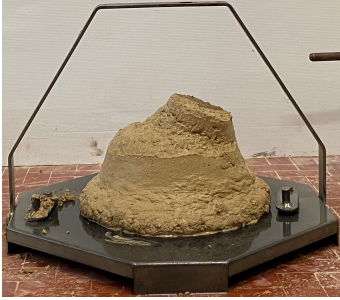




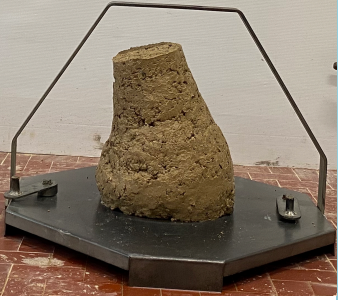


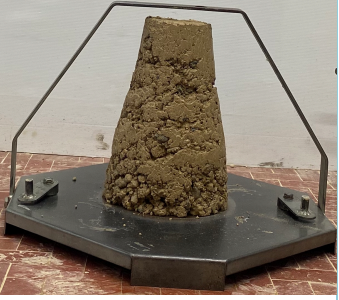
9.11 Test Campaign K

Table 9_21: Conditioning set parameters – Test campaign K

Conditioning Set Parameters		
Parameter	Value	Unit
Q	10	l/min
C_f	2.0	%
FIR	30	%
FER	8	-
w_{total}	9	%
w_{mean}	4.3	%
γ_s	1.912	kg/l
γ_{lg}	1	kg/l
W_s	20000	g
W_{dry}	19175.46	g
$W_{water\ added}$	901.25	g
W_{foam}	392.26	g
T_{water}	18.80	$^{\circ}C$
T_{room}	25.50	$^{\circ}C$
Humidity	74.00	%

Table 9_22: Slump test results – Test campaign K

Test Campaign K								
No.	Time (h)	Slump (cm)	No.	Time (h)	Slump (cm)	No.	Time (h)	Slump (cm)
1	0.00	23	2	0.08	21	3	0.20	21
								
No.	Time (h)	Slump (cm)	No.	Time (h)	Slump (cm)	No.	Time (h)	Slump (cm)
4	0.37	20	5	0.53	18	6	0.70	18
								
No.	Time (h)	Slump (cm)	No.	Time (h)	Slump (cm)	No.	Time (h)	Slump (cm)
7	0.87	17	8	1.03	15	9	1.28	15
								










No.	Time (h)	Slump (cm)	No.	Time (h)	Slump (cm)	No.	Time (h)	Slump (cm)
10	1.63	14	11	1.98	12	12	2.32	10
								
No.	Time (h)	Slump (cm)	No.	Time (h)	Slump (cm)	No.	Time (h)	Slump (cm)
13	2.65	9	14	4.73	9	15	5.18	6
								
No.	Time (h)	Slump (cm)	No.	Time (h)	Slump (cm)	No.	Time (h)	Slump (cm)
16	5.68	5	17	6.18	3	18	7.02	2
								



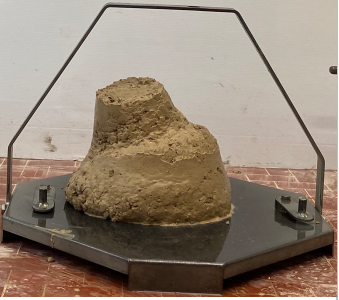



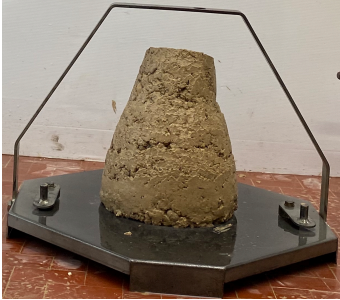


9.12 Test Campaign L

Table 9_23: Conditioning set parameters – Test campaign L

Conditioning Set Parameters		
Parameter	Value	Unit
Q	2.8	l/min
C_f	2.0	%
FIR	30	%
FER	8	-
w_{total}	9	%
w_{mean}	4.3	%
γ_s	1.912	kg/l
γ_{lg}	1	kg/l
W_s	20000	g
W_{dry}	19175.46	g
$W_{water\ added}$	901.25	g
W_{foam}	392.26	g
T_{water}	19.00	°C
T_{room}	27.10	°C
Humidity	71.70	%

Table 9_24: Slump test results – Test campaign L

Test Campaign L								
No.	Time (h)	Slump (cm)	No.	Time (h)	Slump (cm)	No.	Time (h)	Slump (cm)
1	0.00	22	2	0.08	21	3	0.22	20
								
No.	Time (h)	Slump (cm)	No.	Time (h)	Slump (cm)	No.	Time (h)	Slump (cm)
4	0.35	19	5	0.52	18	6	0.73	18
								
No.	Time (h)	Slump (cm)	No.	Time (h)	Slump (cm)	No.	Time (h)	Slump (cm)
7	0.90	17	8	1.07	15	9	1.32	15
								

No.	Time (h)	Slump (cm)	No.	Time (h)	Slump (cm)	No.	Time (h)	Slump (cm)
10	1.55	14	11	2.05	14	12	2.38	12
								
No.	Time (h)	Slump (cm)	No.	Time (h)	Slump (cm)	No.	Time (h)	Slump (cm)
13	2.62	12	14	2.98	10	15	5.10	9
								
No.	Time (h)	Slump (cm)	No.	Time (h)	Slump (cm)	No.	Time (h)	Slump (cm)
16	5.60	6	17	5.93	5	18	6.85	6
								
No.	Time (h)	Slump (cm)						
19	8.02	3						


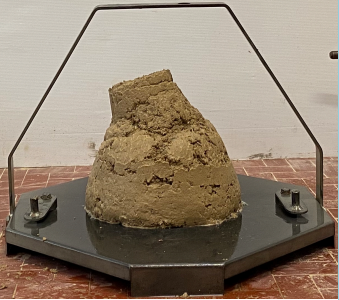



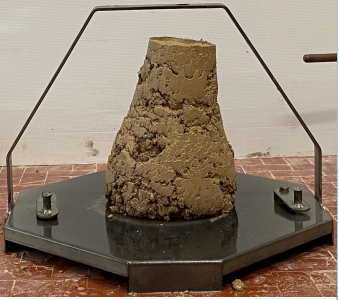





9.13 Test Campaign M


Table 9_25: Conditioning set parameters – Test campaign M

Conditioning Set Parameters		
Parameter	Value	Unit
Q	10	l/min
C_f	2.0	%
FIR	20	%
FER	15	-
w_{total}	9	%
w_{mean}	4.3	%
γ_s	1.912	kg/l
γ_{lg}	1	kg/l
W_s	20000	g
W_{dry}	19175.46	g
$W_{water\ added}$	901.25	g
W_{foam}	139.47	g
T_{water}	18.80	$^{\circ}C$
T_{room}	25.50	$^{\circ}C$
Humidity	74.00	%


Table 9_26: Slump test results – Test campaign M

Test Campaign M								
No.	Time (h)	Slump (cm)	No.	Time (h)	Slump (cm)	No.	Time (h)	Slump (cm)
1	0.00	13	2	0.08	11	3	0.17	8
								
No.	Time (h)	Slump (cm)	No.	Time (h)	Slump (cm)	No.	Time (h)	Slump (cm)
4	0.25	8	5	0.42	5	6	0.50	5
								
No.	Time (h)	Slump (cm)	No.	Time (h)	Slump (cm)	No.	Time (h)	Slump (cm)
7	0.83	3	8	1.17	2	9	3.22	2
								

No.	Time (h)	Slump (cm)	No.	Time (h)	Slump (cm)	No.	Time (h)	Slump (cm)
10	4.00	2	11	4.65	2	12	5.08	2



No.	Time (h)	Slump (cm)	No.	Time (h)	Slump (cm)
13	5.83	2	14	6.33	2





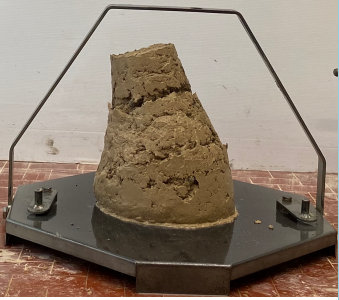
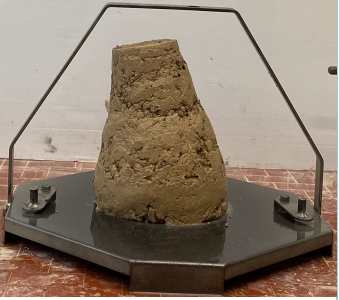

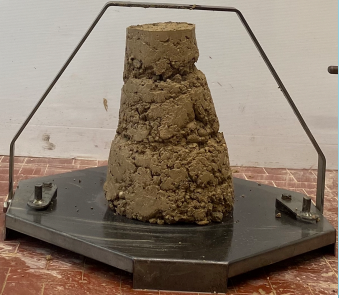
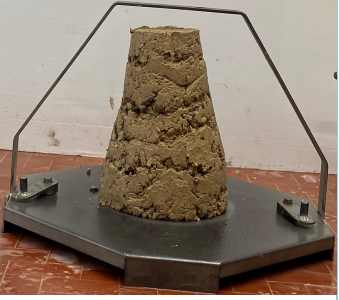


9.14 Test Campaign N


Table 9_27: Conditioning set parameters – Test campaign N

Conditioning Set Parameters		
Parameter	Value	Unit
Q	2.8	l/min
C_f	2.0	%
FIR	20	%
FER	8	-
w_{total}	9	%
w_{mean}	4.2	%
γ_s	1.912	kg/l
γ_{lg}	1	kg/l
W_s	20000	g
W_{dry}	19193.86	g
$W_{water\ added}$	921.31	g
W_{foam}	261.51	g
T_{water}	19.00	°C
T_{room}	27.10	°C
Humidity	71.70	%


Table 9_28: Slump test results – Test campaign N

Test Campaign N								
No.	Time (h)	Slump (cm)	No.	Time (h)	Slump (cm)	No.	Time (h)	Slump (cm)
1	0.00	13	2	0.08	10	3	0.17	10
								
No.	Time (h)	Slump (cm)	No.	Time (h)	Slump (cm)	No.	Time (h)	Slump (cm)
4	0.25	7	5	0.42	6	6	0.52	5
								
No.	Time (h)	Slump (cm)	No.	Time (h)	Slump (cm)	No.	Time (h)	Slump (cm)
7	0.77	5	8	1.12	2	9	3.30	3
								

No.	Time (h)	Slump (cm)	No.	Time (h)	Slump (cm)	No.	Time (h)	Slump (cm)
10	3.75	2	11	4.37	2	12	4.97	4



No.	Time (h)	Slump (cm)
13	6.05	2

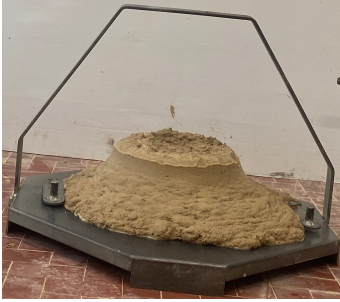
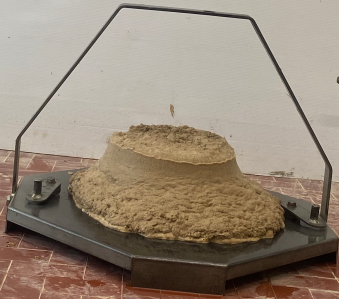

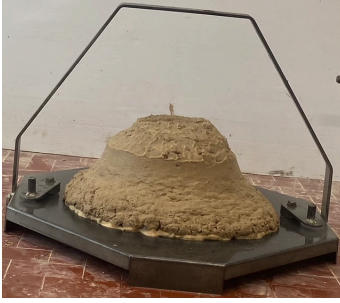







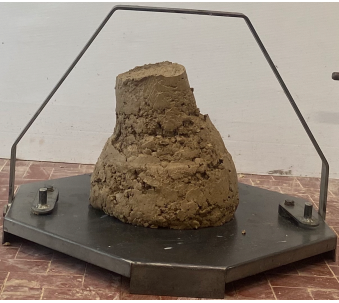




9.15 Test Campaign O

Table 9_29: Conditioning set parameters – Test campaign O

Conditioning Set Parameters		
Parameter	Value	Unit
Q	10	l/min
C_f	2.0	%
FIR	20	%
FER	8	-
w_{total}	9	%
w_{mean}	4	%
γ_s	1.912	kg/l
γ_{lg}	1	kg/l
W_s	20000	g
W_{dry}	19230.77	g
$W_{water\ added}$	961.54	g
W_{foam}	261.51	g
T_{water}	18.60	°C
T_{room}	32.10	°C
Humidity	52.40	%

Table 9_30: Slump test results – Test campaign O

Test Campaign O								
No.	Time (h)	Slump (cm)	No.	Time (h)	Slump (cm)	No.	Time (h)	Slump (cm)
1	0.00	21	2	0.10	20	3	0.22	18
								
No.	Time (h)	Slump (cm)	No.	Time (h)	Slump (cm)	No.	Time (h)	Slump (cm)
4	0.38	17	5	0.52	16	6	0.83	14
								
No.	Time (h)	Slump (cm)	No.	Time (h)	Slump (cm)	No.	Time (h)	Slump (cm)
7	1.07	14	8	1.42	12	9	1.73	10
								




No.	Time (h)	Slump (cm)	No.	Time (h)	Slump (cm)	No.	Time (h)	Slump (cm)
10	2.08	9	11	2.43	8	12	4.45	5
								
No.	Time (h)	Slump (cm)	No.	Time (h)	Slump (cm)	No.	Time (h)	Slump (cm)
13	4.95	5	14	5.45	3	15	5.95	2
								
No.	Time (h)	Slump (cm)						
16	6.50	2						
								

9.16 Test Campaign Q

Table 9_31: Conditioning set parameters – Test campaign Q

Conditioning Set Parameters		
Parameter	Value	Unit
FIR	0	%
W_{total}	9	%
W_{mean}	3.8	%
γ_s	1.912	kg/l
γ_{lg}	1	kg/l
W_s	20000	g
W_{dry}	19267.82	g
$W_{water\ added}$	1001.93	g
W_{foam}	0	g
T_{water}	19	°C
T_{room}	29.10	°C
Humidity	65.00	%

Table 9_32: Slump test results – Test campaign Q

Test Campaign Q								
No.	Time (h)	Slump (cm)	No.	Time (h)	Slump (cm)	No.	Time (h)	Slump (cm)
1	0.00	1	2	0.25	1	3	0.50	1
								

Chapter 10

References

Al Yousef, Z.A.; Almobarky, M.A.; Schechter, D.S. (2018). The effect of nanoparticle aggregation on surfactant foam stability. *J. Colloid Interface Sci.*, 511, 365–373. [[CrossRef](#)]

Anagnostou, G. and Kovári, K. (1996a). Face stability conditions with Earth Pressure Balanced Shields. *Tunnelling and Underground Space Technology*, 11(2):165–173. [[CrossRef](#)]

ASTM (2000). Standard Test Methods for Liquid Limit, Plastic Limit, and Plasticity Index of Soils. ASTM D4318-17; ASTM: West Conshohocken, PA, USA. [[CrossRef](#)]

ASTM (2009). Standard Test Methods for Particle-Size Distribution (Gradation) of Soils Using Sieve Analysis. ASTM D6913-04; ASTM: West Conshohocken, PA, USA. [[CrossRef](#)]

ASTM (2015a). Standard Test Method for Field Vane Shear Test in Cohesive Soil; ASTM D2573-01; ASTM: West Conshohocken, PA, USA. [[CrossRef](#)]

ASTM (2015b). Standard test method for slump of hydraulic-cement concrete. ASTM C143-15a, ASTM: West Conshohocken, PA, USA. [[CrossRef](#)]

ASTM (2016). Standard test methods for laboratory miniature vane shear test for saturated fine-grained clayey soil. ASTM D4648-16, ASTM: West Conshohocken, PA, USA. [[CrossRef](#)]

ASTM (2019). Standard Test Methods for Laboratory Determination of Water (Moisture) Content of Soil and Rock by Mass. ASTM D2216-19, ASTM: West Conshohocken, PA, USA. [[CrossRef](#)]

Baghali, H.; Chakeri, H.; Sharghi, M.; Dias, D. (2020). Effect of Soil Moisture and Granulometry on Soil Conditioning for EPB-TBM Tunneling: Case Study. *Journal of Testing and Evaluation*, 49(1). [[CrossRef](#)]

Bezuijen, A.; Schaminée, P. E. L.; Kleinjan, J. A. (1999). Additive testing for earth pressure balance shields. In *Geotechnical engineering for transportation infrastructure. 12th European conference on soil mechanics and geotechnical engineering, 1991–1996*. [[CrossRef](#)]

Bezuijen, A.; Schaminée, P. E. L.; Kleinjan, J. A. (1999). Additive testing for earth pressure balance shields. In *Geotechnical engineering for transportation infrastructure. 12th European conference on soil mechanics and geotechnical engineering, 1991–1996*. [[CrossRef](#)]

Boone, S.; Artigiani, E.; Shirlaw, N.; Ginanneschi, R.; Leinala, T.; Kochmanova, N. (2005). Use of ground conditioning agents for Earth Pressure Balance machine tunnelling, *Congres international de Chambéry*, 313-319. [[CrossRef](#)]

Borio, L. and Peila, D. (2011). Laboratory test for EPB tunnelling assessment: Results of test campaign on two different granular soils. *Gospodarka Surowcami Mineralnymi – Mineral Resources Management*, 27(1), 85–100. [[CrossRef](#)]

BS EN 12350-2 (2019). Testing fresh concrete Sampling and common apparatus. British Standards Institution. [[CrossRef](#)]

Carigi, A.; Luciani, A.; Todaro, C.; Martinelli, D.; Peila, D. (2020). Influence of conditioning on the behavior of alluvial soils with cobbles. *Tunnelling and Underground Space Technology*, 96, 103–225. [[CrossRef](#)]

Carigi, A.; Todaro, C.; Martinelli, D.; Amoroso, C.; Peila, D. (2020). Evaluation of the Geo-Mechanical Properties Property Recovery in Time of Conditioned Soil for EPB-TBM Tunneling. *Geosciences*, 10(11), 438. [[CrossRef](#)]

Carigi, A.; Todaro, C.; Martinelli, D.; Peila, D. (2022). A More Comprehensive Way to Analyze Foam Stability for EPB Tunnelling—Introduction of a Mathematical Characterization. *Geosciences*, 12(5), 191. [[CrossRef](#)]

EFNARC (2005). Specification and guidelines for the use of specialist products for Mechanized Tunnelling (TBM) in Soft Ground and Hard Rock, before extraction after extraction. Technical report, EFNARC: Farnham, UK. [\[CrossRef\]](#)

Elbaz, K.; Shen, S.L.; Cheng, W.C.; Arulrajah, A. (2018). Cutter-disc consumption during earth pressure balance tunnelling in mixed strata. *Geotechnical Engineering, ICE Proceedings*, 171(4), 363–376. [\[CrossRef\]](#)

Fameau, A.L.; Salonen, A. (2014). Effect of particles and aggregated structures on the foam stability and aging. *Comptes Rendus Phys.*, 15, 748–760. [\[CrossRef\]](#)

Gharahbagh, E.A.; Rostami, J.; Talebi, K. (2014). Experimental study of the effect of conditioning on abrasive wear and torque requirement of full face tunneling machines. *Tunnelling and Underground Space Technology*, 41, 127-136. [\[CrossRef\]](#)

Guglielmetti, V.; Grasso, P.; Mahtab, A.; Xu, S. (2007). Mechanized tunnelling in urban areas. Taylor & Francis group, London. 1, 528. [\[CrossRef\]](#)

Gylland A.; Emdal A.; Thakur V. (2016). Extended interpretation basis for the vane shear test. 17th Nordic Geotechnical Meeting (NGM), 233. [\[CrossRef\]](#)

Herrenknecht AG. (n.d.). EPB Shield. [\[CrossRef\]](#)

Herrenknecht, M. (1994). EPB or slurry machine: the choice. *Tunnels and Tunnelling International*, 35–36.

Herrenknecht, M.; Thewes, M.; Budach, C. (2011). The development of earth pressure shields: from the beginning to the present / Entwicklung der Erddruckschilde: Von den Anfängen bis zur Gegenwart. *Geomechanik Tunnelbau*, 4: 11-35. [\[CrossRef\]](#)

Horozov, T.S. (2008). Foams and foam films stabilized by solid particles. *Curr. Opin. Colloid Interface Sci.*, 13, 134–140. [\[CrossRef\]](#)

Jancsecz, S.; Krause, R.; Langmaack, L. (1999). Advantages of soil conditioning in shield tunnelling: experiences of LRTS Izmir. Alten et al (eds), 1999, Balkema-Rotterdam, 865-875. [\[CrossRef\]](#)

- Liu, X.; Shen, S.; Xu, Y.; Yin, Z. (2018). Analytical approach for time-dependent groundwater inflow into shield tunnel face in confined aquifer. *International Journal for Numerical and Analytical Methods in Geomechanics*, 42 (4), 655–673. [[CrossRef](#)]
- Magrabi, S.A.; Dlugogorski, B.Z.; Jameson, G.J. (1999). Bubble size distribution and coarsening of aqueous foams. *Chemical Engineering Science*, 54 (18), 4007–4022. [[CrossRef](#)]
- Maidl, B.; Herrenknecht, M.; Anheuser, L. (1995). *Mechanised Shield Tunnelling*. Ernst & Sohn, Berlin, 428. [[CrossRef](#)]
- Mair, R.J.; Merritt, A.S.; Borghi, F.X.; Yamazaki, H.; Minami, T. (2003). Soil conditioning for clay soils. *Tunnels and Tunnelling International*, 35(4), 29-32. [[CrossRef](#)]
- Martinelli, D. (2016). *Mechanical Behaviour of Conditioned Material for EPBS Tunnelling*. PhD Thesis, Politecnico di Torino, Torino, Italy. [[CrossRef](#)]
- Martinelli, D.; Peila, D.; Campa, E. (2015). Feasibility study of tar sands conditioning for earth pressure balance tunnelling. *Journal of Rock Mechanics and Geotechnical Engineering*, 7(6), 684-690. [[CrossRef](#)]
- Martinelli, D.; Todaro, C.; Luciani, A.; Peila, D. (2019). Use of a large triaxial cell for testing conditioned soil for EPBS tunnelling. *Tunnelling and Underground Space Technology*, 94, 103–126. [[CrossRef](#)]
- Martinelli, D.; Winderholler, R.; Peila, D. (2017). Undrained behaviour of granular soils conditioned for EPB tunnelling—A new experimental procedure tunnelling. *Geomechanick und Tunnelbau*, 10, 81–89. [[CrossRef](#)]
- Merritt, A. and Mair, R.J. (2006). Mechanics of tunnelling machine screw conveyor: model tests. *Geotechnique*, 56(9), 605-615. [[CrossRef](#)]
- Moll, P.; Grossmann, L.; Kutzli, I.; Weiss, J. (2019). Influence of energy density and viscosity on foam stability - A study with pea protein (*Pisum sativum* L.). *Journal of Dispersion Science and Technology*, 41(12), 1789–1796. [[CrossRef](#)]

Mooney, M.A.; Parikh, D.; Mori, L.; Wu, Y. (2018). EPB granular soil conditioning under pressure. *Geotechnical Aspects of Underground Construction in Soft Ground*. Taylor & Francis group, London, 33-46. [\[CrossRef\]](#)

Pamukcu, S. and Suhayda, J. (1988). Low-Strain Shear Measurement Using a Triaxial Vane Device. *Vane shear strength testing in soils: Field and laboratory studies*, ASTM STP 1014, 193-208. [\[CrossRef\]](#)

Peila, D.; Martinelli, D.; Todaro, C.; Luciani, A. (2019). Soil conditioning in EPB shield tunnelling – An overview of laboratory tests. *Geomechanics and Tunnelling*, 12(5), 491-498. [\[CrossRef\]](#)

Peila, D.; Oggeri, C.; Borio, L. (2008). Influence of granulometry, time and temperature on soil conditioning for EPBS applications. In *Proceedings World Tunnel Congress*. 22-24. [\[CrossRef\]](#)

Peila, D.; Oggeri, C.; Borio, L. (2009). Using the slump test to assess the behavior of conditioned soil for EPB tunnelling. *Environ. Eng. Geosci.*, 15, 167–174. [\[CrossRef\]](#)

Peila, D.; Picchio, A.; Martinelli, D., Dal Negro, E. (2016). Laboratory tests on soil conditioning of clayey soil. *Acta Geotecnica*, 11(5), 1062–1074. [\[CrossRef\]](#)

Pellet, A.L. and Kastner, R. (1998). Comparison of microtunnel jacking force theoretical calculation and experimental data. *Tunnels and Metropolises'*, Negro J. & Ferreira (eds), Balkema, 2, 733-738. [\[CrossRef\]](#)

Psomas, S. (2001). Properties of foam/sand mixtures for tunneling applications. *Master's Thesis*, Oxford University, Oxford, UK. [\[CrossRef\]](#)

Quebaud, S.; Sibai, M.; Henry, J.P. (1998). Use of chemical foam for improvements in drilling by earth pressure balanced shields in granular soils. *Tunnelling and Underground Space Technology*, 13 (2), 173-180. [\[CrossRef\]](#)

Salazar, C.G.O.; Gabriela, C.; Todaro, C.; Bosio, F.; Emilio, B.; Peila, D. (2018). A new test device for the study of metal wear in conditioned granular soil used in EPB shield tunneling. *Tunnelling and Underground Space Technology*, 73, 212-221. [\[CrossRef\]](#)

Salazar, C.G.O.; Martinelli, D.; Todaro, C.; Luciani, A.; Boscaro, A.; Peila, D. (2016). Preliminary study of wear induced by granular soil on metallic parts of EPB tunnelling machines. *GEAM: Geingegneria Ambientale e Mineraria*, 2, 67-70. [[CrossRef](#)]

Schramm, L.L. and Wassmuth, F. (1994). *Foams: Basic Principles*. American Chemical Society, 242(1):3-45. [[CrossRef](#)]

Sebastiani, D.; Vilardi, D.; Bavasso, I.; Di Palma, L.; Miliziano, S. (2019). Classification of foam and foaming products for EPB mechanized tunnelling based on half-life time. *Tunnelling and Underground Space Technology*, 92, 103044. [[CrossRef](#)]

Shin, Y.J.; Kang, S.W.; Lee, J.W.; Kim, D.Y. (2021). Challenges of EPB TBM in Pressurized Mixed Grounds under Hangang River: Effect of Clogging. *Advances in Structural Engineering and Mechanics (ASEM21)*. GECE. [[CrossRef](#)]

Tao, L.; Chen, Z.; Cui, J.; Wang, H.; Fang, Y. (2019). Experimental methods to assess the effectiveness of soil conditioning with foam in fully weathered granite. *Advances in Materials Science and Engineering*, 2019, 1-12. [[CrossRef](#)]

Thewes, M. and Budach, C.; Bezuijen, A. (2012). Foam conditioning in EPB tunnelling. *Geotechnical Aspects of Underground Construction in Soft Ground*, CRC Press, 127–135. [[CrossRef](#)]

Todaro, C. (2016). Analysis on the penetration of foams in the excavation with EPB. *GEAM: Geingegneria Ambientale e Mineraria*, 147, 49–52. [[CrossRef](#)]

Todaro, C.; Carigi, A.; Peila, L.; Martinelli, D.; Peila, D. (2021). Soil conditioning tests of clay for EPB tunnelling. *Underground Space*, 7(4), 483-497. [[CrossRef](#)]

United Nations Department of Economic and Social Affairs, Population Division (2022). *World Population Prospects 2022: Summary of Results*. UN DESA/POP/2022/TR/NO. 3. [[CrossRef](#)]

Vinai, R. (2006). A contribution to the study of soil conditioning techniques for EPB-TBM applications in cohesionless soils. PhD Thesis, Politecnico di Torino.

Vinai, R.; Oggeri, C.; Peila, D. (2008). Soil conditioning of sand for EPB applications: A laboratory research. *Tunnelling and Underground Space Technology*, 23(3), 308-317. [\[CrossRef\]](#)

Wang, S.; Ni, Z.; Qu, T.; Wang, H.; Pan, Q. (2022). A Novel Index to Evaluate the Workability of Conditioned Coarse-Grained Soil for EPB Shield Tunnelling. *Journal of Construction Engineering and Management*, 148(6). [\[CrossRef\]](#)

Williamson, G.E.; Traylor, M.T.; Higuchi, M. (1999). Soil conditioning for EPB shield tunneling on the South Bay Ocean Outfall, RETC proceedings, 51, 897-925.

Wu, Y.; Mooney, M.A.; Cha, M. (2018). An experimental examination of foam stability under pressure for EPB TBM tunneling. *Tunnelling and Underground Space Technology*, 77, 80–93. [\[CrossRef\]](#)

Wu, Y.; Nazem, A.; Meng, F.; Mooney, M.A. (2020). Experimental study on the stability of foam-conditioned sand under pressure in the EPBM chamber. *Tunnelling and Underground Space Technology*, 106. [\[CrossRef\]](#)

Xu, Q.; Zhang, L.; Zhu, H.; Gong, Z.; Liu, J.; Zhu, Y. (2020). Laboratory tests on conditioning the sandy cobble soil for EPB shield tunnelling and its field application. *Tunnelling and Underground Space Technology*, 105. [\[CrossRef\]](#)

Ye, X.; Wang, S.; Yang, J.; Sheng, D.; Xiao, C. (2017). Soil conditioning for EPB shield tunneling in argillaceous siltstone with high content of clay minerals: Case study. *International Journal of Geomechanics*, 17(4). [\[CrossRef\]](#)

Yoshikawa, T. (1996). Soil pressure drop at the screw conveyor for shielded machines. *Transactions of the Japan Society of Mechanical Engineers Serie C*, 62 (595), 1197-1203. [\[CrossRef\]](#)

Zhang, N.; Shen, S.; Zhou, A.; Lyu, H. (2020). Challenges of earth-pressure-balance tunnelling in weathered granite with boulders. *Geotechnical Engineering, ICE Proceedings*, 174(4), 372-389. [\[CrossRef\]](#)

Zhang, Y.; Chang, Z.; Luo, W.; Gu, S.; Li, W.; An, J. (2015). Effect of starch particles on foam stability and dilational viscoelasticity of aqueous-foam. *Chinese Journal of Chemical Engineering*, 23(1), 276–280. [\[CrossRef\]](#)

Zhao, B.Y.; Liu, D.Y.; Jiang, B. (2018). Soil Conditioning of Waterless Sand–Pebble Stratum in EPB Tunnel Construction. *Geotechnical and Geological Engineering*, 36(4), 2495–2504. [[CrossRef](#)]

Zheng, D.; Bezujen, A.; Thewes, M. (2021). An experimental study on foam infiltration into saturated sand and its consequence for EPB shield tunneling. *Tunnelling and Underground Space Technology*, 111. [[CrossRef](#)]

Zheng, D.; Bezujen, A.; Thewes, M. (2022). Modelling the infiltration behaviour of foam into saturated sand considering capillary resistance for EPB shield tunnelling. *Géotechnique*, 1-11. [[CrossRef](#)]

Zhou, X. and Yang, Y. (2020). Effect of Foam Parameters on Cohesionless Soil Permeability and Its Application to Prevent the Water Spewing. *Applied Sciences*, 10(5):1787. [[CrossRef](#)]